## ABSTRACT

# AXISYMMETRIC VIBRATIONS OF HOMOGENEOUS AND SANDWICH SPHERICAL SHELLS WITH A HOLE AT THE CENTER

**by**
**Wai-Kwong Wong**

Based on Hamilton's principle and the theory of elasticity, both linear and nonlinear governing equations of motion are derived for elastic spherical shells. Most of the analysis is focused on the free axisymmetric vibrations of homogeneous and sandwich shallow spherical shells. The nonlinear behavior, which allows for small deflections, is also discussed.

The linear vibrations of homogeneous and sandwich shallow spherical shells with a hole at the center are investigated with emphasis placed on the effect of thickness-shear deformation and rotatory inertia. The effects of curvature and the size of the central hole are studied for free axisymmetric motions of spherical shells with various types of edge conditions. Two tracers are introduced to identify the transverse-shear deformation and rotatory inertia terms in the homogeneous shell and in the core of the sandwich shell. The refined model is derived which includes these two effects while the classical model is formulated by setting the tracers equal to zero. The face layers of the sandwich shell are taken to be membranes. Equations governing the axisymmetric motion of shallow shells are deduced yielding a system of three second-order differential equations in terms of the displacements and time. The numerical solution of the governing equations is obtained by using the *Shooting Method*, in which the natural frequency is assumed to be the same in all

displacements. By introducing dimensionless ratios related to the elastic and geometric properties of the shell, the equations appear in a form which is readily adaptable for solutions of homogeneous and sandwich shallow spherical shells as well as circular plates.

Numerical results for the linear vibrations of a sandwich shell reveal that the effect of thickness-shear deformation and rotatory inertia must be considered in calculating the natural frequencies. For both homogeneous and sandwich shells, the curvature has a dramatic effect on the increase of the fundamental frequencies. The fundamental frequencies increase with the increase of the size of the central hole for all of the boundary conditions investigated for the refined model. For the classical model, the frequency increase with size of hole is limited to the case of the clamped outer boundary conditions.

Numerical results show that for the nonlinear vibrations of the homogeneous shell with relatively small curvature, the magnitude of the deflection should be small in order to get the natural frequency.

On the other hand, the *Finite Difference Method*, which is employed to solve both the linear and nonlinear cases, shows that the natural frequency may not be the same for all displacements.

# AXISYMMETRIC VIBRATIONS OF HOMOGENEOUS AND SANDWICH SPHERICAL SHELLS WITH A HOLE AT THE CENTER

by
Wai-Kwong Wong

A Dissertation
Submitted to the Faculty of
New Jersey Institute of Technology
in Partial Fulfillment of Requirements for Degree of
Doctor of Philosophy in Mechanical Engineering

Department of Mechanical Engineering

August 2000

**APPROVAL PAGE**

**AXISYMMETRIC VIBRATIONS OF HOMOGENEOUS AND SANDWICH SPHERICAL SHELLS WITH A HOLE AT THE CENTER**

**Wai-Kwong Wong**

Dr. Bernard Koplik, Dissertation Advisor — Date
Professor of Mechanical Engineering, NJIT

Dr. Rong-Yaw Chen, Committee Member — Date
Professor of Mechanical Engineering, NJIT

Dr. Benedict C. Sun, Committee Member — Date
Associate Professor of Mechanical Engineering Technology, NJIT

Dr. John Tavantzis, Committee Member — Date
Professor of Mathematics, NJIT

Dr. Ansel C. Ugural, Committee Member — Date
Research Professor of Mechanical Engineering, NJIT

## BIOGRAPHICAL SKETCH

**Author:** Wai-Kwong Wong

**Degree:** Doctor of Philosophy in Mechanical Engineering

**Date:** August 2000

**Undergraduate and Graduate Education:**

Doctor of Philosophy in Mechanical Engineering
New Jersey Institute of Technology, Newark, NJ, 2000

Bachelor of Science in Mechanical Engineering,
Rutgers University, College of Engineering, New Brunswick, NJ, 1995

**Major:** Mechanical Engineering

To my beloved wife, Debbie

## ACKNOWLEDGEMENT

I would like to express my appreciation to my research advisor, Dr. Bernard Koplik, for his supervision, suggestions and encouragement throughout this research. It has been my great pleasure to work with Professor Koplik and to become his Ph.D. student.

I am grateful to Dr. John Tavantzis who taught me valuable mathematical approaches for this research. I would like to thank Professor Tavantzis for his patient guidance and constant support throughout the four years of my Ph.D. studies. I am also thankful to Dr. Rong-Yaw Chen who gave me guidance in taking the courses and arranged for my financial support from the Mechanical Engineering Department at the New Jersey Institute of Technology. I also express my special thanks to Dr. Benedict C. Sun and Dr. Ansel C. Ugural for their suggestions to improve this dissertation.

Specially, I want to thank my wife, Debbie, for her patience, comfort and support. I also would like to thank my mom and my family for their support throughout my life.

Finally, I extend my thanks to my Lord, who has provided me extra strength and wisdom throughout this research.

## TABLE OF CONTENTS

## TABLE OF CONTENTS
## (Continued)

**Chapter** **Page**

## TABLE OF CONTENTS
## (Continued)

**Chapter** **Page**

## LIST OF TABLES

**Table** **Page**

## LIST OF TABLES
## (Continued)

**Table** **Page**

## LIST OF TABLES
## (Continued)

**Table** **Page**

## LIST OF TABLES
## (Continued)

**Table** **Page**

## LIST OF FIGURES

**Figure** **Page**

## LIST OF FIGURES
## (Continued)

**Figure** **Page**

## LIST OF FIGURES
## (Continued)

**Figure** **Page**

## LIST OF SYMBOLS

| | |
|---|---|
| $U_\phi, U_\theta, U_z$ | Displacements in $\phi, \theta$, z directions |
| $u, \beta, w$ | Shallow shell displacements |
| $R$ | Radius of curvature of middle surface of shell |
| $H$ | Rise from reference plane to the highest point in the middle surface of the shell |
| $a$ | Projected radius of the shell on the reference plane |
| $h$ | Total half-thickness of sandwich |
| $h_1$ | Half-thickness of core |
| $h_2$ | Half-thickness of each face |
| $\upsilon$ | Poisson's ratio |
| E | Young's modulus |
| $\rho$ | Density |
| $N_{rr}, N_{\theta\theta}$ | Membrane forces |
| $M_{rr}, M_{\theta\theta}$ | Bending Moments |
| $Q_{rz}$ | Transverse shear force |
| $\sigma_{ij}$ | Stress components |
| $e_{ij}$ | Strain components |
| $\omega$ | Fundamental frequency |
| $k_s$ | Tracer for transverse shear deformation |
| $k_g$ | Tracer for rotatory inertia |
| $k_t$ | Tracer for the effect of transverse shear force on member force |

# CHAPTER 1

# INTRODUCTION

## 1.1 Research Objectives

The problem of vibrations of both homogeneous and sandwich spherical shells has been investigated extensively because of the important applications of such structures in different fields of aerospace and mechanical engineering. Since sandwich structures possess good heat insulating properties, their shell configurations find wide applications in various modern and sophisticated components such as space vehicles, domes, nuclear reactors, and pressure vessels.

Time-dependent vibratory motions are set up in a spherical shell whenever it is disturbed from a position of stable equilibrium. If these motions occur in the absence of external loads, they are classified as *free vibrations*. If these motions are set up by time-dependent external loads, they are referred to as *forced vibrations*. A spherical shell, since it is assumed to be an elastic body, is composed of an infinite number of mass particles. As a consequence, when it is set into motion it possesses an infinite number of degrees of freedom. Its response to a disturbance may thus be analyzed into an infinite number of periodic motions which are referred to as its normal modes of free vibration. Each of theses normal modes has an associated natural frequency of free vibration.

A knowledge of the free-vibration characteristics of elastic shells is important both to our general understanding of the fundamentals of the behavior of a shell and to the industrial application of spherical shell structures. In connection with the latter, the natural frequencies of the spherical shells must be known in order to avoid the destructive effect of resonance with nearby rotating or oscillating equipment.

The objective of this investigation is to study linear axisymmetric free vibrations of homogeneous and sandwich shallow spherical shells with a circular hole at its center, in which various types of edge conditions are employed. The curvature of the shell and the size of the central hole are varied to investigate the free natural frequencies by using the Shooting Method. Emphasis is on the transition from the vibrations of a circular flat plate to those of a spherical shell. The effects of transverse shear deformation and rotatory inertia are included in the analysis.

On the other hand, there are many situations such as seismic tests or nuclear explosions, in which these structures are subjected to transient loads and large amplitudes of motion may occur. If the amplitude of motion is of the same order as the thickness of the shell, then for the mathematical description of the motion the linear theory of shells is inadequate and the use of nonlinear theory of shells is necessary. This will take into account the large deformation with higher order bending and stretching effects.

The further work of this investigation on nonlinear behavior of the free vibration of homogeneous spherical shells will be discussed because it is necessary to employ nonlinear theories which allow for finite deflections, since the solutions predicted by the linear theory are valid only for small displacements. The nonlinear behavior assumes the angles of rotation are large compared to the linear strain components and small compared to unity, thus leading to nonlinear strain-displacement relations. It follows that the problem becomes geometrically nonlinear but remains linear in material properties.

## 1.2 Literature Survey

By using a generalized Hamilton's principle in derivation of the equations of motion, Koplik [1] and Grossman [2] investigated the vibrations of both linear and nonlinear spherical shells without a central hole, respectively.

Simplified nonlinear elasticity theory, referred to as the case of small deformations and small rotations [3], has been applied by many authors in considering the finite displacements of thin elastic bodies such as plates and shells. Yu [4] introduced a generalized variational equation of motion in nonlinear elasticity theory in which displacements and strains are expressed in powers of the thickness coordinate and stresses are integrated over the thickness to yield shell-stresses. Carrying out the variational approximation in the thickness direction yields the generalized variational equation of motion for the shell, with Euler equations yielding the complete system of stress equations of motion, boundary conditions, and stress-strain-displacement relations. Koplik [1] derived a complete and consistent system of first-order dynamic equations for both thin homogeneous spherical shells and thin sandwich spherical shells, by adopting the linearized version of the generalized Hamilton's principle.

To simplify the nonlinear theory, small deformations and small rotations are applied, in which the angles of rotation are large compared to the linear strain components and small compared to unity, thus leading to nonlinear strain-displacement relations. However, the strains still maintain their linear relationship with the stresses, with the result that the problem becomes geometrically nonlinear but remains linear in material properties. For such simplified nonlinear strains, Yu [5] made use of the ordinary variational equation of motion to derive the nonlinear equations of motion and

boundary conditions for cylindrical shells. Grossman [2] derived a complete and consistent system of nonlinear dynamic equations for thin homogeneous spherical shells by adopting the generalized variational equation of motion.

Recently, Xu and Chia [6] employed the Marguerre-type shallow-shell theory to study dynamics of shallow spherical shells with a circular opening at the apex. However, in spite of the importance of their research, their work received little attention. Hence, in this dissertation, we will derive the linear dynamic equations for both the thin homogeneous and sandwich spherical shells with a hole at the center. Also, we will show the nonlinear dynamic equations for thin homogeneous spherical shells with holes at the center. The derivation is based on the work done in [1, 2, 4, 5] and Hamilton's principle [7, 8]. The texts by Leissa [9, 10] include a very well-prepared bibliography, covering the literature in spherical shell and circular plates. The books by Wang [11] and Sokolnikoff [12] explain the background of the theory of elasticity.

### 1.3 Present Work

In Chapter 2 of this dissertation, the linearized stress equations of motion for both thin homogeneous shallow spherical shells and thin sandwich shallow spherical shells are derived for axisymmetric vibrations. Two tracers are introduced to identify the effects of transverse shear deformation and rotatory inertia terms in the homogeneous shell and in the core of the sandwich shell. The face layers of the sandwich shell are taken to be membranes. The governing differential equations of the refined model which includes these two effects are deduced yielding a system of three second-order differential equations in terms of the displacements. The governing differential equations of the

classical model are formulated by neglecting the two effects by setting the tracers equal to zero.

Chapter 3 of this investigation, the nonlinear axisymmetric vibrations for thin homogeneous spherical shells are derived for both the refined and classical models.

In Chapter 4, the Shooting Method [13, 14, 15] is employed to solve for the natural frequencies of the linear axisymmetric vibrations of homogeneous and sandwich spherical shells for both models. The analysis is applied for varied curvature and the size of the central hole of the shells with various edge conditions.

Finally in Chapter 5, the Finite Difference Method [16, 17, 18] is applied to analyze the transition from linear axisymmetric vibrations to nonlinear axisymmetric vibrations for the classical model.

# CHAPTER 2

# EQUATIONS FOR HOMOGENOUS AND SANDWICH SPHERICAL SHELLS

## 2.1 Spherical Shell Coordinates

In this thesis, the basic assumptions are that the spherical shells are thin and elastic. Generally, if the shell is composed of a single homogeneous material, the middle surface is selected as the reference surface. If the shell is of layered construction, it is more convenient to use, as the reference surface, or so-called neutral surface that is analogous to the neutral axis of a beam.

In order to understand the sandwich spherical shell coordinates, it is advisable as a first step to present a single-layered homogeneous spherical shell. The spherical coordinates for the homogeneous case, $\phi$, $\theta$, and $R+z$ are chosen so that $z=0$ designates the middle surface whose radius is $R$ and $z=\pm h$ designates the outer and inner surfaces.

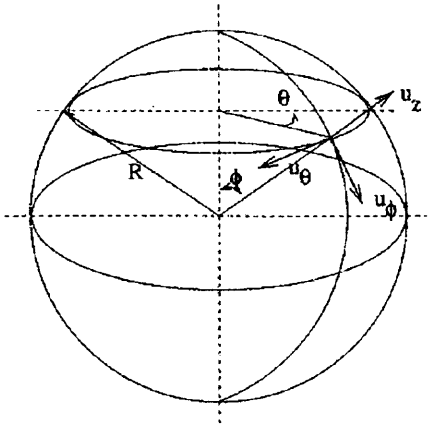


**Figure 1.1** Spherical Coordinates

As shown in Figure 1.1, $\phi$ is the angle between the normal to the middle surface and the $z$ axis in the horizontal plane. The coordinates $\phi$ and $\theta$ are sufficient to locate a particular point on the middle surface.

In treating problems with spherical sandwich shells, $\phi$, $\theta$, $z_i$ are employed with the three spherical middle surfaces of the layers as the reference surfaces for measurements in the thickness direction, the subscript $i=1,2$, or 3 referring to the core, inner or outer face layers of the sandwich.

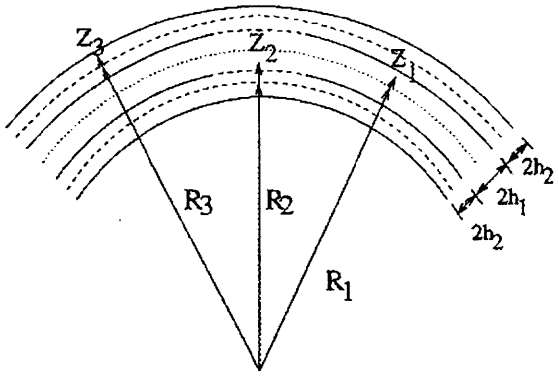


**Figure 1.2** Cross-section of Sandwich Spherical Shell

As shown in Figure 1.2, this coordinate system requires the use of the three radii, $R_i$. Based on the assumption from [1], the two face layers are chosen to have the same thickness and to be of the same material. The core has a thickness $2h_1$, each of the two face layers a thickness $2h_2$, and the total thickness of the shell is $2h$.

Due to the assumption that the face layers are membranes with $\frac{h_2}{h_1} \le \frac{1}{20}$, it is reasonable to set the three radii, $R_i$ approximately equal to $R$, so as to offer the

convenience of symmetrical integration in the derivation. In this manner, the stress-strain-displacement relations, introduced later, can be deduced most easily from those of the homogeneous spherical shell. Of course, both the $z$ and $z_i$ coordinates can be used interchangeably for homogeneous and sandwich problems.

To employ the thin shell assumption the following is taken as,

$$(R+z) = R(1+\frac{z}{R}) \approx R \tag{2.1}$$

due to $\frac{z}{R} << 1$.

Further, by assuming $\phi$ to be much smaller than unity, the corresponding equations can be reduced to those for shallow spherical shells. For such shells this assumption leads to the following reductions,

$$\sin\phi \approx \phi, \quad \cot\phi \approx \frac{1}{\phi}, \quad R\phi = r, \quad \frac{1}{R}\frac{\partial}{\partial\phi} \approx \frac{\partial}{\partial r}. \tag{2.2}$$

By means of these relations the $\phi$, $\theta$, $z$ coordinates are then replaced by the $r$, $\theta$, $z$ coordinates, respectively.

The criterion for shallowness accepted in [1] as well as by most authors is adopted as follows,

$$\frac{H}{a} = \frac{H}{2h}\frac{2h}{a} \leq \frac{1}{4} \tag{2.3}$$

where $H$ is the rise from the reference plane to the highest point in the middle surface of the shell and $a$ is the projected radius of the shell on the reference plane, as shown in Figure 1.3. If the equation of a meridian of a spherical shell is taken in the form,

$$R^2 = (R-H)^2 + a^2$$

then, $R^2 = R^2 - 2HR + H^2 + a^2$

For a shallow spherical shell, the $H^2$ term is taken to be zero, resulting in,

$$a^2 \cong 2HR. \tag{2.4}$$

The shallow shell equations can then be further reduced by restricting the analysis to that of axisymmetric (torsionless) motion. This is accomplished by setting $u_\theta = 0$, $\beta_\theta = 0$ and independence of $\theta$.

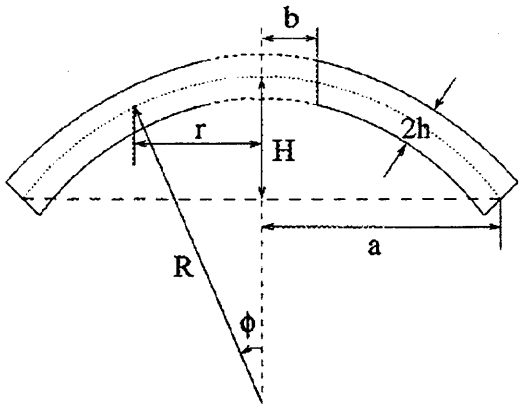


**Figure 1.3** Homogeneous Shallow Spherical Shell

## 2.2 Displacement Form

For a moderately thin shallow spherical shell of uniform thickness $2h$ with coordinates $r$, $\theta$ in the middle surface and its faces at $z = \pm h$, the displacements are assumed to be of the following form:

$$\begin{aligned} U_r(r,\theta,z,t) &= u_r(r,\theta,t) + z\beta_r(r,\theta,t), \\ U_\theta(r,\theta,z,t) &= u_\theta(r,\theta,t) + z\beta_\theta(r,\theta,t), \\ U_z(r,\theta,z,t) &= w(r,\theta,t), \end{aligned} \tag{2.5}$$

where the quantities $u_r$, $u_\theta, \beta_r, \beta_\theta$ and $w$ are the shell-displacements and all are functions of $r$, $\theta$ and time, $t$ only. Whereas $u_r$, $u_\theta$, and $w$ are displacements at the middle surface of the shell in the $r$, $\theta$ and thickness direction $z$, the variables $\beta_r$ and $\beta_\theta$ are the angular displacements of the normal to the middle surface of the shell in the $r$ and $\theta$ directions.

By taking the axisymmetric (torsionless) assumptions, the displacement form is further reduced to,

$$U_r(r,\theta,z,t) = u(r,t) + z\beta(r,t),$$

$$U_\theta = 0, \tag{2.6}$$

$$U_z(r,\theta,z,t) = w(r,t).$$

It should be noted that the assumed displacements are the truncated forms of the infinite expansion series for displacements given by Cauchy and Poisson for plates [1]. Since a plate is a special case of a spherical shell with an infinite radius of curvature, these displacements are assumed in [1] to obtain axisymmetric and shallow spherical shell equations for infinitesimal displacements.

To present a unified approach for the sandwich spherical shells, $r$, $\theta$, $z_i$ coordinate system is adopted, where the subscript $i = 1,2$, or 3 referring to the core, inner or outer face layers of the sandwich respectively.

By taking the axisymmetric (torsionless) and shallow shell assumptions and the face layers to be membranes and therefore neglecting their flexural rigidities, the resulting displacements are in the form:

$$
\begin{aligned}
&U_\theta^{(1)}(r,\theta,z_1,t) = U_\theta^{(2)}(r,\theta,z_2,t) = U_\theta^{(3)}(r,\theta,z_3,t) = 0,\\
&U_r^{(1)}(r,\theta,z_1,t) = u(r,t) + z_1\beta(r,t),\\
&U_r^{(2)}(r,\theta,z_2,t) = u(r,t) - h_1\beta(r,t),\\
&U_r^{(3)}(r,\theta,z_3,t) = u(r,t) + h_1\beta(r,t),\\
&U_z^{(1)}(r,\theta,z_1,t) = U_z^{(2)}(r,\theta,z_2,t) = U_z^{(3)}(r,\theta,z_3,t) = w(r,t).
\end{aligned}
\tag{2.7}
$$

The superscript ($i$) =1,2 or 3 designates the core, inner or outer face layer of the sandwich and $z_i$ is measured from the middle surface of each layer.

The quantities $u, \beta$ and $w$ are the shell-displacements and all are functions of $r$ and time, $t$ only. Whereas $u$ and $w$ are displacements at the middle surface of the core in the $r$ and $z$ directions, respectively. The variable $\beta$ is the angular displacement of the normal to the middle surface of the core in the $r$ direction.

With the shell-displacements chosen in this form it can be seen that the displacements are continuous at the interfaces between the core and faces of the sandwich shallow spherical shell. Furthermore, with independence of $\beta$ and $w$, the thickness-shear deformation of the core can be included in the analysis, although no account is taken of this effect in the faces.

## 2.3 Hamilton's Principle

Of the many procedures that are available to derive the equations of motion for the thin elastic spherical shell, Hamilton's principle is employed on account of its simplicity and elegance and because, at the same time, the natural boundary conditions that are to be derived. Hamilton's principle is an extension of the principle of virtual work from statics

to dynamics. It can be formulated for either a rigid or deformable body by invoking D'Alembert's principle to accommodate inertia forces. Integration with respect to time is carried out between fixed initial and final instants of time $t_0$ and $t_1$, under the constraint that the virtual displacement is required to vanish at $t_0$ and $t_1$. In the case of a deformable body, the virtual displacement must also vanish at those parts of the boundary on which displacement are prescribed.

Hence, the Hamilton's principle is given as,

$$\delta \int_{t_0}^{t_1} (\mathrm{K} - \mathrm{U} + \mathrm{W}) dt = 0, \tag{2.8a}$$

where U is the strain energy and K is the kinetic energy, and W is the work potential. However, W is set to be zero for the free vibration analysis, hence,

$$\delta \int_{t_0}^{t_1} (\mathrm{K} - \mathrm{U}) dt = 0. \tag{2.8b}$$

The times $t_0$ and $t_1$ are arbitrary. The symbol $\delta$ is the variational symbol and is treated mathematically like a differential symbol. Variational displacements are arbitrary. Since the strain energy involves the stress and strain terms, with both related to the displacements, the next section is to show the stress-strain-displacement relations.

## 2.4 Stress-Strain-Displacement Relations

### 2.4.1 Strain-Displacement Relations

The theory of elasticity is employed to derive the strain-displacement relations for the homogeneous spherical shell, in which the derivation is shown in Appendix A. Then the strain – displacement relations for the sandwich spherical shells become,

$$e_{rr}^{(1)} = \frac{\partial U_r^{(1)}}{\partial r} + \frac{U_z^{(1)}}{R} = \frac{\partial u}{\partial r} + \frac{w}{R} + z_1 \frac{\partial \beta}{\partial r}, \qquad e_{\theta\theta}^{(1)} = \frac{U_r^{(1)}}{r} + \frac{U_z^{(1)}}{R} = \frac{u}{r} + \frac{w}{R} + z_1 \frac{\beta}{r},$$

$$e_{rz}^{(1)} = \frac{\partial U_r^{(1)}}{\partial z_1} - \frac{U_r^{(1)}}{R} + \frac{\partial U_z^{(1)}}{\partial r} \approx \frac{\partial w}{\partial r} + \beta, \qquad e_{rr}^{(2)} = \frac{\partial U_r^{(2)}}{\partial r} + \frac{U_z^{(2)}}{R} = \frac{\partial u}{\partial r} + \frac{w}{R} - h_1 \frac{\partial \beta}{\partial r},$$

$$e_{\theta\theta}^{(2)} = \frac{U_r^{(2)}}{r} + \frac{U_z^{(2)}}{R} = \frac{u}{r} + \frac{w}{R} - h_1 \frac{\beta}{r}, \qquad e_{rr}^{(3)} = \frac{\partial U_r^{(3)}}{\partial r} + \frac{U_z^{(3)}}{R} = \frac{\partial u}{\partial r} + \frac{w}{R} + h_1 \frac{\partial \beta}{\partial r},$$

$$e_{\theta\theta}^{(3)} = \frac{U_r^{(3)}}{r} + \frac{U_z^{(3)}}{R} = \frac{u}{r} + \frac{w}{R} + h_1 \frac{\beta}{r}, \qquad e_{rz}^{(2)} = e_{rz}^{(3)} = 0, \tag{2.9}$$

where the superscript $(i)$ =1,2 or 3 designates the core, inner or outer face layer of the sandwich, respectively. It should be noted that due to the assumption that the face layers are membranes, the transverse shearing shell-stresses in the faces are equal to zero, so that,

$$e_{rz}^{(2)} = e_{rz}^{(3)} = 0. \tag{2.10}$$

While $e_{\theta z}^{(i)}$ and $e_{r\theta}^{(i)}$ are zero because of the axisymmetric assumption, which is shown in the Appendix A.

### 2.4.2 Stress-Strain Relations

With the assumption of the shell to be elastic, generalized Hooke's law [7] can be applied to the shells that are made of elastic materials. The following shows the stress-strain relations,

$$\sigma_{rr}^{(i)} = \frac{\mathrm{E}_i}{1-\upsilon_i^2}\left(e_{rr}^{(i)} + \upsilon_i e_{\theta\theta}^{(i)}\right), \tag{2.11a}$$

$$\sigma_{\theta\theta}^{(i)} = \frac{\mathrm{E}_i}{1-\upsilon_i^2}\left(e_{\theta\theta}^{(i)} + \upsilon_i e_{rr}^{(i)}\right), \tag{2.11b}$$

$$\sigma_{rz}^{(i)} = \frac{\mathrm{E}_i k_H}{2(1+\upsilon_i)} e_{rz}^{(i)}, \tag{2.11c}$$

where $i$ =1, 2 or 3, $\mathrm{E}_3 = \mathrm{E}_2$ , $\upsilon_3 = \upsilon_2$ and $h_3 = h_2$ due to the same face layers thickness

$k_H$ is the correction factor having the value $\frac{\pi^2}{12}$ as in [1] for the purpose of adjusting the simple thickness-shear frequency of a homogeneous plate to its exact value. $k_H$ is taken equal to unity for the sandwich spherical shell.

It should be noted that due to the membrane face layers assumption, we get,

$$\sigma_{rz}^{(2)} = \sigma_{rz}^{(3)} = 0. \tag{2.12a}$$

The normal stress $\sigma_{zz}^{(i)}$, which acts in normal direction to the neutral surface, is neglected,

$$\sigma_{zz}^{(i)} = 0. \tag{2.12b}$$

This is based on the argument that on an unloaded outer shell surface it is zero, or if a load acts on the shell, it is equivalent in magnitude to the external load on the shell, which is a relatively small value in most cases.

Furthermore, since $e_{\theta z}^{(i)}$ and $e_{r\theta}^{(i)}$ are zero, we have,

$$\sigma_{\theta z}^{(i)} = \sigma_{r\theta}^{(i)} = 0. \tag{2.12c}$$

### 2.4.3 Stress Resultant-Displacement Relations

Since the strains, and therefore the stresses, have been shown to be linear across the thickness of a thin elastic spherical shell, it is convenient to integrate the stress distributions through the thickness of the shell and to replace the usual consideration of stresses by a consideration of statically equivalent force resultants, $N_{rr}^{(i)}$, $N_{\theta\theta}^{(i)}$, $Q_{rz}^{(1)}$ and bending moments resultants, $M_{rr}^{(1)}, M_{\theta\theta}^{(1)}$. In the following, all the stresses will be integrated in which they act on a shell element whose dimensions are infinitesimal in the r and $\theta$ directions and equal to the shell thickness in the normal direction, $z_i$.

Hence the corresponding resultants are,

$$\text{Membrane forces: } N_{jj}^{(i)} = \int_{-h_i}^{h_i} \sigma_{jj}^{(i)} dz_i , \tag{2.13a}$$

$$\text{Bending moments: } M_{jj}^{(i)} = \int_{-h_i}^{h_i} z_i \sigma_{jj}^{(i)} dz_i , \tag{2.13b}$$

$$\text{Transverse shear force: } Q_{rz}^{(1)} = \int_{-h_1}^{h_1} \sigma_{rz}^{(1)} dz_1 , \tag{2.13c}$$

where $i = 1, 2$ or 3, $jj = rr$ or $\theta\theta$, $h_3 = h_2$ due to the same face layers thickness

It should be noted that the following integral equations are for the integration of the stresses across the thickness:

$$\int_{-h_i}^{h_i} dz_i = 2h_i , \qquad \int_{-h_i}^{h_i} z_i dz_i = 0 , \qquad \int_{-h_i}^{h_i} z_i^2 dz_i = \frac{2h_i^3}{3}. \tag{2.14}$$

The membrane force $N_{rr}^{(1)}$, is obtained by substituting (2.11a) into (2.13a) giving the force-strain relation,

$$N_{rr}^{(1)} = \int_{-h_1}^{h_1} \sigma_{rr}^{(1)} dz_1 = \frac{E_1}{1-\upsilon_1^2} \int_{-h_1}^{h_1} \left(e_{rr}^{(1)} + \upsilon_1 e_{\theta\theta}^{(1)}\right) dz_1 .$$

The force-displacement relation is now obtained by substituting (2.9) into the above equation,

$$N_{rr}^{(1)} = \frac{E_1}{1-\upsilon_1^2} \int_{-h_1}^{h_1} \left\{ \left[ \frac{\partial u}{\partial r} + \frac{w}{R} + z_1 \frac{\partial \beta}{\partial r} \right] + \upsilon_1 \left[ \frac{u}{r} + \frac{w}{R} + z_1 \frac{\beta}{r} \right] \right\} dz_1 ,$$

or

$$N_{rr}^{(1)} = \frac{2E_1 h_1}{1-\upsilon_1^2} \left[ \frac{\partial u}{\partial r} + \upsilon_1 \frac{u}{r} + (1+\upsilon_1) \frac{w}{R} \right]. \tag{2.15a}$$

For the membrane force $N_{rr}^{(2)}$, the force-strain relation is,

$$N_{rr}^{(2)} = \int_{-h_2}^{h_2} \sigma_{rr}^{(2)} dz_2 = \frac{E_2}{1-\upsilon_2^2} \int_{-h_2}^{h_2} \left(e_{rr}^{(2)} + \upsilon_2 e_{\theta\theta}^{(2)}\right) dz_2 .$$

Then the force-displacement relation is,

$$N_{rr}^{(2)} = \frac{E_2}{1-\upsilon_2^2} \int_{-h_2}^{h_2} \left\{ \left[ \frac{\partial u}{\partial r} + \frac{w}{R} - h_1 \frac{\partial \beta}{\partial r} \right] + \upsilon_2 \left[ \frac{u}{r} + \frac{w}{R} - h_1 \frac{\beta}{r} \right] \right\} dz_2 ,$$

or

$$N_{rr}^{(2)} = \frac{2E_2 h_2}{1-\upsilon_2^2} \left[ \frac{\partial u}{\partial r} + \upsilon_2 \frac{u}{r} + (1+\upsilon_2) \frac{w}{R} - h_1 \frac{\partial \beta}{\partial r} - \upsilon_2 h_1 \frac{\beta}{r} \right], \tag{2.15b}$$

similarly

$$N_{rr}^{(3)} = \frac{2E_2 h_2}{1-\upsilon_2^2} \left[ \frac{\partial u}{\partial r} + \upsilon_2 \frac{u}{r} + (1+\upsilon_2) \frac{w}{R} + h_1 \frac{\partial \beta}{\partial r} + \upsilon_2 h_1 \frac{\beta}{r} \right]. \tag{2.15c}$$

By the same substitution process with (2.9), (2.11b), (2.13a) and (2.14), the membrane forces $N_{\theta\theta}^{(i)}$ are obtained as follows,

$$N_{\theta\theta}^{(1)} = \frac{2E_1 h_1}{1-\upsilon_1^2} \left[ \upsilon_1 \frac{\partial u}{\partial r} + \frac{u}{r} + (1+\upsilon_1) \frac{w}{R} \right], \tag{2.16a}$$

$$N_{\theta\theta}^{(2)} = \frac{2E_2 h_2}{1-\upsilon_2^2}\left[\upsilon_2 \frac{\partial u}{\partial r} + \frac{u}{r} + (1+\upsilon_2)\frac{w}{R} - \upsilon_2 h_1 \frac{\partial \beta}{\partial r} - h_1 \frac{\beta}{r}\right], \tag{2.16b}$$

$$N_{\theta\theta}^{(3)} = \frac{2E_2 h_2}{1-\upsilon_2^2}\left[\upsilon_2 \frac{\partial u}{\partial r} + \frac{u}{r} + (1+\upsilon_2)\frac{w}{R} + \upsilon_2 h_1 \frac{\partial \beta}{\partial r} + h_1 \frac{\beta}{r}\right]. \tag{2.16c}$$

To obtain the bending moment $M_{rr}^{(1)}$, (2.11a) is substituted into (2.13b) giving the moment-strain relation,

$$M_{rr}^{(1)} = \int_{-h_1}^{h_1} z_1 \sigma_{rr}^{(1)} dz_1 = \frac{E_1}{1-\upsilon_1^2}\int_{-h_1}^{h_1} z_1 \left(e_{rr}^{(1)} + \upsilon_1 e_{\theta\theta}^{(1)}\right) dz_1 .$$

The moment-displacement relation is now obtained by substituting (2.9) into the above equation,

$$M_{rr}^{(1)} = \frac{E_1}{1-\upsilon_1^2}\int_{-h_1}^{h_1}\left\{z_1\left[\frac{\partial u}{\partial r} + \frac{w}{R} + z_1\frac{\partial \beta}{\partial r}\right] + \upsilon_1 z_1\left[\frac{u}{r} + \frac{w}{R} + z_1\frac{\beta}{r}\right]\right\} dz_1 .$$

therefore $$M_{rr}^{(1)} = \frac{2E_1 h_1^3}{3(1-\upsilon_1^2)}\left[\frac{\partial \beta}{\partial r} + \upsilon_1 \frac{\beta}{r}\right], \tag{2.17a}$$

similarly $$M_{\theta\theta}^{(1)} = \int_{-h_1}^{h_1} z_1 \sigma_{\theta\theta}^{(1)} dz_1 = \frac{E_1}{1-\upsilon_1^2}\int_{-h_1}^{h_1} z_1 \left(e_{\theta\theta}^{(1)} + \upsilon_1 e_{rr}^{(1)}\right) dz_1 ,$$

or $$M_{\theta\theta}^{(1)} = \frac{2E_1 h_1^3}{3(1-\upsilon_1^2)}\left[\upsilon_1 \frac{\partial \beta}{\partial r} + \frac{\beta}{r}\right]. \tag{2.17b}$$

By the same substitution process utilizing (2.9), (2.11a), (2.11b), (2.13a) and (2.14), the bending moments $M_{rr}^{(2)}$, $M_{rr}^{(3)}$, $M_{\theta\theta}^{(2)}$ and $M_{\theta\theta}^{(2)}$ are all equal to zero because all the terms in the integration involve $\int_{-h_i}^{h_i} z_i dz_i$, which is equal to zero.

To obtain the transverse shear force $Q_{rz}^{(1)}$, we substitute (2.11c) into (2.13c) giving the force-strain relation,

$$Q_{rz}^{(1)} = \int_{-h_1}^{h_1} \sigma_{rz}^{(1)} dz_1 = \frac{E_1}{2k_s(1+\upsilon_1)} \int_{-h_1}^{h_1} e_{rz}^{(1)} dz_1 .$$

The force-displacement relation is now obtained by substituting (2.9) into the above equation,

$$Q_{rz}^{(1)} = \frac{E_1}{2k_s(1+\upsilon_1)} \int_{-h_1}^{h_1} \left[ \frac{\partial w}{\partial r} + \beta \right] dz_1 ,$$

therefore $$Q_{rz}^{(1)} = \frac{E_1 h_1}{k_s(1+\upsilon_1)} \left[ \frac{\partial w}{\partial r} + \beta \right] = \frac{E_1 h_1}{k_s(1+\upsilon_1)} \left[ \frac{\partial w}{\partial r} + \beta \right], \qquad (2.18)$$

where $k_s \left(= \frac{1}{k_H}\right)$ is a tracer for transverse shear deformation.

From (2.12a) and (2.12c), all the other transverse shear forces are equal to zero due to their related zero stresses.

Since the normal stresses are assumed to be zero in (2.12b), normal forces $N_{zz}^{(i)}$ are equal to zero.

## 2.5 Stress Equations of Motion

In this section, the stress equations of motion for the homogeneous and sandwich spherical shells are derived by using Hamilton's principle, introduced in Section 2.3.

Refer to (2.8b), $\delta\int_{t_0}^{t_1}(\mathrm{K}-\mathrm{U})dt=0$, the kinetic energy K and the strain energy U are shown as the following:

The kinetic energy of an infinitesimal element is given by,

$$\mathrm{dK}=\frac{1}{2}\rho_1[(\dot{U}_r^{(1)})^2+(\dot{U}_z^{(1)})^2]dV_1+\frac{1}{2}\rho_2[(\dot{U}_r^{(2)})^2+(\dot{U}_z^{(2)})^2]dV_2$$

$$+\frac{1}{2}\rho_2[(\dot{U}_r^{(3)})^2+(\dot{U}_z^{(3)})^2]dV_3, \qquad (2.19)$$

where the dot indicates a time derivative, $dV_i = rdrd\theta dz_i$ is the infinitesimal volume, $i$=1,2 or 3 , and $\rho_i$ is the density, where $\rho_3 = \rho_2$.

Substituting (2.7) into (2.19) gives,

$$\mathrm{K}=\frac{\rho_1}{2}\int_\theta\int_r\int_{-h_1}^{h_1}[(\dot{u}+z_1\dot{\beta})^2+\dot{w}^2]dz_1rdrd\theta+\frac{\rho_2}{2}\int_\theta\int_r\int_{-h_2}^{h_2}[(\dot{u}-h_1\dot{\beta})^2+\dot{w}^2]dz_2rdrd\theta$$

$$+\frac{\rho_2}{2}\int_\theta\int_r\int_{-h_2}^{h_2}[(\dot{u}+h_1\dot{\beta})^2+\dot{w}^2]dz_3rdrd\theta.$$

Since the displacements are independent of $\theta$, measured from 0 to $2\pi$ , then

$$\mathrm{K}=2\pi\frac{\rho_1}{2}\int_r\int_{-h_1}^{h_1}[\dot{u}^2+2z_1\dot{u}\dot{\beta}+z_1^2\dot{\beta}^2+\dot{w}^2]dz_1rdr$$

$$+2\pi\frac{\rho_2}{2}\int_r\int_{-h_2}^{h_2}[\dot{u}^2-2h_1\dot{u}\dot{\beta}+h_1^2\dot{\beta}^2+\dot{w}^2]dz_2rdr$$

$$+2\pi\frac{\rho_2}{2}\int_r\int_{-h_2}^{h_2}[\dot{u}^2+2h_1\dot{u}\dot{\beta}+h_1^2\dot{\beta}^2+\dot{w}^2]dz_3rdr\,.$$

Integrating over the thickness of the shell gives,

$$\mathrm{K}=2\pi\rho_1h_1\int_r[\dot{u}^2+\dot{w}^2]rdr+2\pi\frac{\rho_1h_1^3}{3}\int_r\dot{\beta}^2rdr$$

$$+4\pi\rho_2h_2\int_r[\dot{u}^2+\dot{w}^2]rdr+4\pi\rho_2h_1^2h_2\int_r\dot{\beta}^2rdr\,.$$

Taking the variations for the displacements and applying Hamilton's principle yields,

$$\int_{t_0}^{t_1}\delta\mathrm{K}dt=2\pi\int_{t_0}^{t_1}\int_r[-(2\rho_1h_1+4\rho_2h_2)\ddot{u}\delta u-(2\rho_1h_1+4\rho_2h_2)\ddot{w}\delta w$$

$$-(\frac{2\rho_1h_1^3}{3}+4\rho_2h_1^2h_2)\ddot{\beta}\delta\beta]rdrdt\,. \qquad (2.20)$$

Since from integrating by parts, for instance,

$$\delta\int_{t_0}^{t_1}\dot{u}^2dt=\int_{t_0}^{t_1}2\dot{u}\delta\dot{u}dt=2[\dot{u}\delta u]_{t_0}^{t_1}-2\int_{t_0}^{t_1}\ddot{u}\delta udt=-2\int_{t_0}^{t_1}\ddot{u}\delta udt\,,$$

while $[\dot{u}\delta u]_{t_o}^{t_1}=0$ because the virtual displacement or the velocity is zero at $t=t_0$ and $t=t_1$.

In the following the strain energy is determined by using Hamilton's principle.

The strain energy of one infinitesimal element is given by,

$$\mathrm{dU}=\sum_{i=1}^{3}\frac{1}{2}(\sigma_{rr}^{(i)}e_{rr}^{(i)}+\sigma_{\theta\theta}^{(i)}e_{\theta\theta}^{(i)}+\sigma_{rz}^{(i)}e_{rz}^{(i)})dV_i\,. \qquad (2.21)$$

Integrating over the volume of the shell we have,

$$\mathrm{U}=\sum_{i=1}^{3}\frac{1}{2}\int_\theta\int_r\int_{-h_i}^{h_i}[\sigma_{rr}^{(i)}e_{rr}^{(i)}+\sigma_{\theta\theta}^{(i)}e_{\theta\theta}^{(i)}+\sigma_{rz}^{(i)}e_{rz}^{(i)}]dz_irdrd\theta\,.$$

To apply Hamilton's principle of strain energy yields,

$$\int_{t_0}^{t_1}\delta U dt = \sum_{i=1}^{3}\frac{1}{2}\int_{t_0}^{t_1}\int_{\theta}\int_{r}\int_{-h_i}^{h_i}[\delta\sigma_{rr}^{(i)}e_{rr}^{(i)}+\sigma_{rr}^{(i)}\delta e_{rr}^{(i)}+\delta\sigma_{\theta\theta}^{(i)}e_{\theta\theta}^{(i)}+\sigma_{\theta\theta}^{(i)}\delta e_{\theta\theta}^{(i)}$$

$$\delta\sigma_{rz}^{(i)}e_{rz}^{(i)}+\sigma_{rz}^{(i)}\delta e_{rz}^{(i)}]dz_i r dr d\theta dt .$$

By substituting (2.11a), (2.11b) and (2.11c) into the equation we obtain,

$$\int_{t_0}^{t_1}\delta U dt = \sum_{i=1}^{3}\frac{1}{2}\int_{t_0}^{t_1}\int_{\theta}\int_{r}\int_{-h_i}^{h_i}[\frac{E_i}{1-\upsilon_i^2}(\delta e_{rr}^{(i)}+\upsilon_i\delta e_{\theta\theta}^{(i)})e_{rr}^{(i)}+\frac{E_i}{1-\upsilon_i^2}(e_{rr}^{(i)}+\upsilon_i e_{\theta\theta}^{(i)})\delta e_{rr}^{(i)}$$

$$+\frac{E_i}{1-\upsilon_i^2}(\delta e_{\theta\theta}^{(i)}+\upsilon_i\delta e_{rr}^{(i)})e_{\theta\theta}^{(i)}+\frac{E_i}{1-\upsilon_i^2}(e_{\theta\theta}^{(i)}+\upsilon_i e_{rr}^{(i)})\delta e_{\theta\theta}^{(i)}$$

$$+\frac{E_i k_H}{2(1+\upsilon_i)}\delta e_{rz}^{(i)}e_{rz}^{(i)}+\frac{E_i k_H}{2(1+\upsilon_i)}e_{rz}^{(i)}\delta e_{rz}^{(i)}]dz_i r dr d\theta dt .$$

Collecting the terms of variational strain gives,

$$\int_{t_0}^{t_1}\delta U dt = \sum_{i=1}^{3}\frac{1}{2}\int_{t_0}^{t_1}\int_{\theta}\int_{r}\int_{-h_i}^{h_i}[\frac{2E_i}{1-\upsilon_i^2}(e_{rr}^{(i)}+\upsilon_i e_{\theta\theta}^{(i)})\delta e_{rr}^{(i)}+\frac{2E_i}{1-\upsilon_i^2}(e_{\theta\theta}^{(i)}+\upsilon_i e_{rr}^{(i)})\delta e_{\theta\theta}^{(i)}$$

$$+\frac{E_i k_H}{1+\upsilon_i}e_{rz}^{(i)}\delta e_{rz}^{(i)}]dz_i r dr d\theta dt .$$

By using stress-strain relations from (2.11a), (2.11b) and (2.11c) yields,

$$\int_{t_0}^{t_1}\delta U dt = \sum_{i=1}^{3}\int_{t_0}^{t_1}\int_{\theta}\int_{r}\int_{-h_i}^{h_i}[\sigma_{rr}^{(i)}\delta e_{rr}^{(i)}+\sigma_{\theta\theta}^{(i)}\delta e_{\theta\theta}^{(i)}+\sigma_{rz}^{(i)}\delta e_{rz}^{(i)}]dz_i r dr d\theta dt . \qquad (2.22)$$

By substituting (2.9), (2.10) and (2.12a) into (2.22) and integrating the $\theta$ from 0 to $2\pi$,

$$\int_{t_0}^{t_1}\delta U dt = 2\pi\int_{t_0}^{t_1}\int_{r}\int_{-h_1}^{h_1}\{\sigma_{rr}^{(1)}[\frac{\partial(\delta u)}{\partial r}+\frac{\delta w}{R}+z_1\frac{\partial(\delta\beta)}{\partial r}]+\sigma_{\theta\theta}^{(1)}[\frac{\delta u}{r}+\frac{\delta w}{R}+z_1\frac{\delta\beta}{r}]$$

$$+\sigma_{rz}^{(1)}[\frac{\partial(\delta w)}{\partial r}+\delta\beta]\}dz_1 rdrdt$$

$$+2\pi\int_{t_0}^{t_1}\int_{r}\int_{-h_2}^{h_2}\{\sigma_{rr}^{(2)}[\frac{\partial(\delta u)}{\partial r}+\frac{\delta w}{R}-h_1\frac{\partial(\delta\beta)}{\partial r}]+\sigma_{\theta\theta}^{(2)}[\frac{\delta u}{r}+\frac{\delta w}{R}-h_1\frac{\delta\beta}{r}]\}dz_2 rdrdt$$

$$+2\pi\int_{t_0}^{t_1}\int_{r}\int_{-h_2}^{h_2}\{\sigma_{rr}^{(3)}[\frac{\partial(\delta u)}{\partial r}+\frac{\delta w}{R}+h_1\frac{\partial(\delta\beta)}{\partial r}]+\sigma_{\theta\theta}^{(3)}[\frac{\delta u}{r}+\frac{\delta w}{R}+h_1\frac{\delta\beta}{r}]\}dz_3 rdrdt\,.$$

Substituting (2.13) into the above equation yields,

$$\int_{t_0}^{t_1}\delta U dt = 2\pi\int_{t_0}^{t_1}\int_{r}\{[N_{rr}^{(1)}+N_{rr}^{(2)}+N_{rr}^{(3)}][\frac{\partial(\delta u)}{\partial r}+\frac{\delta w}{R}]+[N_{\theta\theta}^{(1)}+N_{\theta\theta}^{(2)}+N_{\theta\theta}^{(3)}][\frac{\delta u}{r}+\frac{\delta w}{R}]$$

$$+[M_{rr}^{(1)}-h_1N_{rr}^{(2)}+h_1N_{rr}^{(3)}]\frac{\partial(\delta\beta)}{\partial r}+[M_{\theta\theta}^{(1)}-h_1N_{\theta\theta}^{(2)}+h_1N_{\theta\theta}^{(3)}]\frac{\delta\beta}{r}$$

$$+Q_{rz}^{(1)}[\frac{\partial(\delta w)}{\partial r}+\delta\beta]\}rdrdt\,,$$

or

$$\int_{t_0}^{t_1}\delta U dt = 2\pi\int_{t_0}^{t_1}\int_{r}\{[-\frac{1}{r}\frac{\partial(rN_{rr}^{(1)})}{\partial r}-\frac{1}{r}\frac{\partial(rN_{rr}^{(2)})}{\partial r}-\frac{1}{r}\frac{\partial(rN_{rr}^{(3)})}{\partial r}+\frac{N_{\theta\theta}^{(1)}}{r}+\frac{N_{\theta\theta}^{(2)}}{r}+\frac{N_{\theta\theta}^{(3)}}{r}]\delta u$$

$$+[-\frac{1}{r}\frac{\partial(rM_{rr}^{(1)})}{\partial r}+\frac{1}{r}h_1\frac{\partial(rN_{rr}^{(2)})}{\partial r}-\frac{1}{r}h_1\frac{\partial(rN_{rr}^{(3)})}{\partial r}+\frac{M_{\theta\theta}^{(1)}}{r}-h_1\frac{N_{\theta\theta}^{(2)}}{r}+h_1\frac{N_{\theta\theta}^{(3)}}{r}+Q_{rz}^{(1)}]\delta\beta$$

$$+[-\frac{1}{r}\frac{\partial(rQ_{rz}^{(1)})}{\partial r}+\frac{(N_{rr}^{(1)}+N_{rr}^{(2)}+N_{rr}^{(3)})}{R}+\frac{(N_{\theta\theta}^{(1)}+N_{\theta\theta}^{(2)}+N_{\theta\theta}^{(3)})}{R}]\delta w\}rdrdt$$

$$+2\pi\int_{t_0}^{t_1}[(rN_{rr}^{(1)}+rN_{rr}^{(2)}+rN_{rr}^{(3)})\delta u+(rM_{rr}^{(1)}-rh_1N_{rr}^{(2)}+rh_1N_{rr}^{(3)})\delta\beta+(rQ_{rz}^{(1)})\delta w]_{r_0}^{r_1}dt\,.$$

(2.23)

From integration by parts, we have for the first terms as an example,

$$\int_{t_0}^{t_1}\int_{r} N_{rr}\frac{\partial(\delta u)}{\partial r} r dr dt = \int_{t_0}^{t_1}[rN_{rr}\delta u]_{r_0}^{r_1} dt - \int_{t_0}^{t_1}\int_{r}[\frac{1}{r}\frac{\partial(rN_{rr})}{\partial r}\delta u] r dr dt ,$$

Applying Hamilton's principle (2.8b), $\delta\int_{t_0}^{t_1}(\mathrm{K}-\mathrm{U})dt = \int_{t_0}^{t_1}(\delta\mathrm{K}-\delta\mathrm{U})dt = 0$, and by using (2.20) and (2.23),we obtain,

$$2\pi\int_{t_0}^{t_1}\int_{r}\{[\frac{\partial N_{rr}^{(1)}}{\partial r}+\frac{\partial N_{rr}^{(2)}}{\partial r}+\frac{\partial N_{rr}^{(3)}}{\partial r}+(\frac{N_{rr}^{(1)}+N_{rr}^{(2)}+N_{rr}^{(3)}}{r})-(\frac{N_{\theta\theta}^{(1)}+N_{\theta\theta}^{(2)}+N_{\theta\theta}^{(3)}}{r})$$

$$-(2\rho_1 h_1+4\rho_2 h_2)\ddot{u}]\delta u$$

$$+[\frac{\partial M_{rr}^{(1)}}{\partial r}-h_1\frac{\partial N_{rr}^{(2)}}{\partial r}+h_1\frac{\partial N_{rr}^{(3)}}{\partial r}+\frac{M_{rr}^{(1)}}{r}-h_1\frac{N_{rr}^{(2)}}{r}+h_1\frac{N_{rr}^{(3)}}{r}$$

$$-\frac{M_{\theta\theta}^{(1)}}{r}+h_1\frac{N_{\theta\theta}^{(2)}}{r}-h_1\frac{N_{\theta\theta}^{(3)}}{r}-Q_{rz}^{(1)}-(\frac{2\rho_1 h_1^3}{3}+4\rho_2 h_1^2 h_2)\ddot{\beta}]\delta\beta$$

$$+[\frac{\partial Q_{rz}^{(1)}}{\partial r}+\frac{Q_{rz}^{(1)}}{r}-\frac{(N_{rr}^{(1)}+N_{rr}^{(2)}+N_{rr}^{(3)})}{R}-\frac{(N_{\theta\theta}^{(1)}+N_{\theta\theta}^{(2)}+N_{\theta\theta}^{(3)})}{R}$$

$$-(2\rho_1 h_1+4\rho_2 h_2)\ddot{w}]\delta w\}r dr dt$$

$$-2\pi\int_{t_0}^{t_1}[(rN_{rr}^{(1)}+rN_{rr}^{(2)}+rN_{rr}^{(3)})\delta u+(rM_{rr}^{(1)}-rh_1N_{rr}^{(2)}+rh_1N_{rr}^{(3)})_{r_0}^{r_1}\delta\beta+(rQ_{rz}^{(1)})\delta w]_{r_0}^{r_1} dt \;=0.$$

(2.24)

The equation (2.24) can only be satisfied if each of the double and single integral parts is zero individually. Moreover, since the variational displacements are arbitrary, each integral equation can only be satisfied if the coefficients of the variational displacements are zero. Thus, the coefficients of the double integral set to zero give the following three *Stress Equations of Motion*:

$$(\frac{\partial N_{rr}^{(1)}}{\partial r}+\frac{\partial N_{rr}^{(2)}}{\partial r}+\frac{\partial N_{rr}^{(3)}}{\partial r})+(\frac{N_{rr}^{(1)}+N_{rr}^{(2)}+N_{rr}^{(3)}}{r})-(\frac{N_{\theta\theta}^{(1)}+N_{\theta\theta}^{(2)}+N_{\theta\theta}^{(3)}}{r})$$

$$-(2\rho_1 h_1+4\rho_2 h_2)\ddot{u}=0, \qquad (2.25a)$$

$$(\frac{\partial M_{rr}^{(1)}}{\partial r}-h_1\frac{\partial N_{rr}^{(2)}}{\partial r}+h_1\frac{\partial N_{rr}^{(3)}}{\partial r})+(\frac{M_{rr}^{(1)}}{r}-h_1\frac{N_{rr}^{(2)}}{r}+h_1\frac{N_{rr}^{(3)}}{r})-(\frac{M_{\theta\theta}^{(1)}}{r}-h_1\frac{N_{\theta\theta}^{(2)}}{r}+h_1\frac{N_{\theta\theta}^{(3)}}{r})$$

$$-Q_{rz}^{(1)}-k_g(\frac{2\rho_1 h_1^3}{3}+4\rho_2 h_1^2 h_2)\ddot{\beta}=0, \qquad (2.25b)$$

$$(\frac{\partial Q_{rz}^{(1)}}{\partial r}+\frac{Q_{rz}^{(1)}}{r})-\frac{(N_{rr}^{(1)}+N_{\theta\theta}^{(1)})}{R}-\frac{(N_{rr}^{(2)}+N_{\theta\theta}^{(2)})}{R}-\frac{(N_{rr}^{(3)}+N_{\theta\theta}^{(3)})}{R}$$

$$-(2\rho_1 h_1+4\rho_2 h_2)\ddot{w}=0, \qquad (2.25c)$$

where $k_g$ is a tracer for rotatory inertia.

## 2.6 Boundary Conditions

For the single integral part of (2.24) to be zero, the coefficients of the virtual displacements or the virtual displacements are set to be zero. Since virtual displacements are only zero at all times when the boundary displacements are prescribed, this translates into the following possible boundary conditions for $r_o$ and $r_1$,

$$[rN_{rr}^{(1)}+rN_{rr}^{(2)}+rN_{rr}^{(3)}]_{r_0}^{r_1}=0 \quad \text{or} \quad [\delta u]_{r_0}^{r_1}=0 \qquad (2.26a)$$

$$[rM_{rr}^{(1)}-rh_1N_{rr}^{(2)}+rh_1N_{rr}^{(3)}]_{r_0}^{r_1}=0 \quad \text{or} \quad [\delta\beta]_{r_0}^{r_1}=0 \qquad (2.26b)$$

$$[rQ_{rz}^{(1)}]_{r_0}^{r_1}=0 \quad \text{or} \quad [\delta w]_{r_0}^{r_1}=0 \qquad (2.26c)$$

## 2.7 Displacement Equations of Motion

This section derives the displacement equations of motion for the homogeneous and sandwich spherical shell. Two models will be presented. Since the equations include the effects of rotatory inertia $\ddot{\beta}$ and transverse shear $Q_{rz}^{(1)}$, the model is called the *Refined Model*. To obtain results for this model, calculations are made with the tracers $k_s = k_g = 1$ for the sandwich case and $k_s = \frac{12}{\pi^2}$ and $k_g = 1$ for the homogeneous case. The second model, called the *Classical Model* is obtained by setting $k_s = k_g = 0$, in which rotatory inertia and transverse shear effects are neglected.

### 2.7.1 Refined Model

Substituting the stress resultant-displacements relations from (2.15) to (2.18) into the stress equation of motion (2.25) results in the following three *Displacement Equations of Motion*.

The first one in the $u$-direction is obtained by substituting (2.15) and (2.16) into (2.25a):

$$\frac{2E_1h_1}{1-\upsilon_1^2}\left[\frac{\partial^2 u}{\partial r^2}+\upsilon_1\frac{\partial}{\partial r}\left(\frac{u}{r}\right)+\frac{(1+\upsilon_1)}{R}\frac{\partial w}{\partial r}\right]$$

$$+\frac{2E_2h_2}{1-\upsilon_2^2}\left[\frac{\partial^2 u}{\partial r^2}+\upsilon_2\frac{\partial}{\partial r}\left(\frac{u}{r}\right)+\frac{(1+\upsilon_2)}{R}\frac{\partial w}{\partial r}-h_1\frac{\partial^2\beta}{\partial r^2}-\upsilon_2h_1\frac{\partial}{\partial r}\left(\frac{\beta}{r}\right)\right]$$

$$+\frac{2E_2h_2}{1-\upsilon_2^2}\left[\frac{\partial^2 u}{\partial r^2}+\upsilon_2\frac{\partial}{\partial r}\left(\frac{u}{r}\right)+\frac{(1+\upsilon_2)}{R}\frac{\partial w}{\partial r}+h_1\frac{\partial^2\beta}{\partial r^2}+\upsilon_2h_1\frac{\partial}{\partial r}\left(\frac{\beta}{r}\right)\right]$$

$$+\frac{2E_1h_1}{1-\upsilon_1^2}\left(\frac{1}{r}\right)\left[\frac{\partial u}{\partial r}+\upsilon_1\frac{u}{r}+(1+\upsilon_1)\frac{w}{R}\right]$$

$$+\frac{2E_2h_2}{1-\upsilon_2^2}(\frac{1}{r})\left[\frac{\partial u}{\partial r}+\upsilon_2\frac{u}{r}+(1+\upsilon_2)\frac{w}{R}-h_1\frac{\partial\beta}{\partial r}-\upsilon_2h_1\frac{\beta}{r}\right]$$

$$+\frac{2E_2h_2}{1-\upsilon_2^2}(\frac{1}{r})\left[\frac{\partial u}{\partial r}+\upsilon_2\frac{u}{r}+(1+\upsilon_2)\frac{w}{R}+h_1\frac{\partial\beta}{\partial r}+\upsilon_2h_1\frac{\beta}{r}\right]$$

$$-\frac{2E_1h_1}{1-\upsilon_1^2}(\frac{1}{r})\left[\upsilon_1\frac{\partial u}{\partial r}+\frac{u}{r}+(1+\upsilon_1)\frac{w}{R}\right]$$

$$-\frac{2E_2h_2}{1-\upsilon_2^2}(\frac{1}{r})\left[\upsilon_2\frac{\partial u}{\partial r}+\frac{u}{r}+(1+\upsilon_2)\frac{w}{R}-\upsilon_2h_1\frac{\partial\beta}{\partial r}-h_1\frac{\beta}{r}\right]$$

$$-\frac{2E_2h_2}{1-\upsilon_2^2}(\frac{1}{r})\left[\upsilon_2\frac{\partial u}{\partial r}+\frac{u}{r}+(1+\upsilon_2)\frac{w}{R}+\upsilon_2h_1\frac{\partial\beta}{\partial r}+h_1\frac{\beta}{r}\right]$$

$$-(2\rho_1h_1+4\rho_2h_2)\ddot{u}=0.$$

By expanding and collecting the terms with the same coefficients yields,

$$\frac{2E_1h_1}{1-\upsilon_1^2}[\frac{\partial^2u}{\partial r^2}+\frac{\upsilon_1}{r}\frac{\partial u}{\partial r}-\frac{\upsilon_1}{r^2}u+\frac{(1+\upsilon_1)}{R}\frac{\partial w}{\partial r}$$

$$+\frac{1}{r}\frac{\partial u}{\partial r}+\frac{\upsilon_1}{r^2}u+\frac{(1+\upsilon_1)}{r}\frac{w}{R}-\frac{\upsilon_1}{r}\frac{\partial u}{\partial r}-\frac{1}{r^2}u-\frac{(1+\upsilon_1)}{r}\frac{w}{R}]$$

$$+\frac{4E_2h_2}{1-\upsilon_2^2}[\frac{\partial^2u}{\partial r^2}+\frac{\upsilon_2}{r}\frac{\partial u}{\partial r}-\frac{\upsilon_2}{r^2}u+\frac{(1+\upsilon_2)}{R}\frac{\partial w}{\partial r}$$

$$+\frac{1}{r}\frac{\partial u}{\partial r}+\frac{\upsilon_2}{r^2}u+\frac{(1+\upsilon_2)}{r}\frac{w}{R}-\frac{\upsilon_2}{r}\frac{\partial u}{\partial r}-\frac{1}{r^2}u-\frac{(1+\upsilon_2)}{r}\frac{w}{R}]$$

$$-(2\rho_1h_1+4\rho_2h_2)\ddot{u}=0,$$

or,
$$[\frac{2E_1h_1}{1-\upsilon_1^2}+\frac{4E_2h_2}{1-\upsilon_2^2}][\frac{\partial^2u}{\partial r^2}+\frac{1}{r}\frac{\partial u}{\partial r}-\frac{1}{r^2}u]+[\frac{2E_1h_1(1+\upsilon_1)}{R(1-\upsilon_1^2)}+\frac{4E_2h_2(1+\upsilon_2)}{R(1-\upsilon_2^2)}]\frac{\partial w}{\partial r}$$

$$-(2\rho_1h_1+4\rho_2h_2)\ddot{u}=0.$$

(2.27a)

The second equation in the $\beta$-direction is obtained by substituting (2.15) to (2.18) into (2.25b),

$$\frac{2E_1h_1^3}{3(1-\upsilon_1^2)}\left[\frac{\partial^2\beta}{\partial r^2}+\upsilon_1\frac{\partial}{\partial r}(\frac{\beta}{r})\right]$$

$$-\frac{2E_2h_1h_2}{1-\upsilon_2^2}\left[\frac{\partial^2 u}{\partial r^2}+\upsilon_2\frac{\partial}{\partial r}(\frac{u}{r})+\frac{(1+\upsilon_2)}{R}\frac{\partial w}{\partial r}-h_1\frac{\partial^2\beta}{\partial r^2}-\upsilon_2h_1\frac{\partial}{\partial r}(\frac{\beta}{r})\right]$$

$$+\frac{2E_2h_1h_2}{1-\upsilon_2^2}\left[\frac{\partial^2 u}{\partial r^2}+\upsilon_2\frac{\partial}{\partial r}(\frac{u}{r})+\frac{(1+\upsilon_2)}{R}\frac{\partial w}{\partial r}+h_1\frac{\partial^2\beta}{\partial r^2}+\upsilon_2h_1\frac{\partial}{\partial r}(\frac{\beta}{r})\right]$$

$$+\frac{2E_1h_1^3}{3(1-\upsilon_1^2)}(\frac{1}{r})\left[\frac{\partial\beta}{\partial r}+\upsilon_1\frac{\beta}{r}\right]$$

$$-\frac{2E_2h_1h_2}{1-\upsilon_2^2}(\frac{1}{r})\left[\frac{\partial u}{\partial r}+\upsilon_2\frac{u}{r}+(1+\upsilon_2)\frac{w}{R}-h_1\frac{\partial\beta}{\partial r}-\upsilon_2h_1\frac{\beta}{r}\right]$$

$$+\frac{2E_2h_1h_2}{1-\upsilon_2^2}(\frac{1}{r})\left[\frac{\partial u}{\partial r}+\upsilon_2\frac{u}{r}+(1+\upsilon_2)\frac{w}{R}+h_1\frac{\partial\beta}{\partial r}+\upsilon_2h_1\frac{\beta}{r}\right]$$

$$-\frac{2E_1h_1^3}{3(1-\upsilon_1^2)}(\frac{1}{r})\left[\upsilon_1\frac{\partial\beta}{\partial r}+\frac{\beta}{r}\right]$$

$$+\frac{2E_2h_1h_2}{1-\upsilon_2^2}(\frac{1}{r})\left[\upsilon_2\frac{\partial u}{\partial r}+\frac{u}{r}+(1+\upsilon_2)\frac{w}{R}-\upsilon_2h_1\frac{\partial\beta}{\partial r}-h_1\frac{\beta}{r}\right]$$

$$-\frac{2E_2h_1h_2}{1-\upsilon_2^2}(\frac{1}{r})\left[\upsilon_2\frac{\partial u}{\partial r}+\frac{u}{r}+(1+\upsilon_2)\frac{w}{R}+\upsilon_2h_1\frac{\partial\beta}{\partial r}+h_1\frac{\beta}{r}\right]$$

$$-\frac{E_1h_1}{k_s(1+\upsilon_1)}\left[\frac{\partial w}{\partial r}+\beta\right]$$

$$-k_g(\frac{2\rho_1h_1^3}{3}+4\rho_2h_1^2h_2)\ddot{\beta}=0.$$

Collecting terms with the same coefficients:

$$\frac{2E_1h_1^3}{3(1-\upsilon_1^2)}[\frac{\partial^2\beta}{\partial r^2}+\frac{\upsilon_1}{r}\frac{\partial\beta}{\partial r}-\frac{\upsilon_1}{r^2}\beta+\frac{1}{r}\frac{\partial\beta}{\partial r}+\frac{\upsilon_1}{r^2}\beta-\frac{\upsilon_1}{r}\frac{\partial\beta}{\partial r}-\frac{1}{r^2}\beta]$$

$$+\frac{4E_2h_1^2h_2}{1-\upsilon_2^2}[\frac{\partial^2\beta}{\partial r^2}+\frac{\upsilon_2}{r}\frac{\partial\beta}{\partial r}-\frac{\upsilon_2}{r^2}\beta+\frac{1}{r}\frac{\partial\beta}{\partial r}+\frac{\upsilon_2}{r^2}\beta-\frac{\upsilon_2}{r}\frac{\partial\beta}{\partial r}-\frac{1}{r^2}\beta]$$

$$-\frac{E_1h_1}{k_s(1+\upsilon_1)}\left[\frac{\partial w}{\partial r}+\beta\right]-k_g(\frac{2\rho_1h_1^3}{3}+4\rho_2h_1^2h_2)\ddot{\beta}=0,$$

therefore,

$$[\frac{2E_1h_1^3}{3(1-\upsilon_1^2)}+\frac{4E_2h_1^2h_2}{1-\upsilon_2^2}][\frac{\partial^2\beta}{\partial r^2}+\frac{1}{r}\frac{\partial\beta}{\partial r}-\frac{1}{r^2}\beta]-\frac{E_1h_1}{k_s(1+\upsilon_1)}[\frac{\partial w}{\partial r}+\beta]$$

$$-k_g(\frac{2\rho_1h_1^3}{3}+4\rho_2h_1^2h_2)\ddot{\beta}=0. \qquad (2.27b)$$

The third equation in the *w*-direction is obtained by substituting (2.15), (2.16) and (2.18) into (2.25c),

$$\frac{E_1h_1}{k_s(1+\upsilon_1)}\left[\frac{\partial^2w}{\partial r^2}+\frac{\partial\beta}{\partial r}+\frac{1}{r}\frac{\partial w}{\partial r}+\frac{\beta}{r}\right]$$

$$-\frac{2E_1h_1}{1-\upsilon_1^2}(\frac{1}{R})\left[(1+\upsilon_1)\frac{\partial u}{\partial r}+(1+\upsilon_1)\frac{u}{r}+(1+\upsilon_1)\frac{2w}{R}\right]$$

$$-\frac{2E_2h_2}{1-\upsilon_2^2}(\frac{1}{R})\left[(1+\upsilon_2)\frac{\partial u}{\partial r}+(1+\upsilon_2)\frac{u}{r}+(1+\upsilon_2)\frac{2w}{R}-(1+\upsilon_2)h_1\frac{\partial\beta}{\partial r}-(1+\upsilon_2)h_1\frac{\beta}{r}\right]$$

$$-\frac{2E_2h_2}{1-\upsilon_2^2}(\frac{1}{R})\left[(1+\upsilon_2)\frac{\partial u}{\partial r}+(1+\upsilon_2)\frac{u}{r}+(1+\upsilon_2)\frac{2w}{R}+(1+\upsilon_2)h_1\frac{\partial\beta}{\partial r}+(1+\upsilon_2)h_1\frac{\beta}{r}\right]$$

$$-(2\rho_1h_1+4\rho_2h_2)\ddot{w}=0,$$

or,

$$\frac{E_1 h_1}{k_s(1+\upsilon_1)}\left[\frac{\partial^2 w}{\partial r^2}+\frac{1}{r}\frac{\partial w}{\partial r}+\frac{\partial \beta}{\partial r}+\frac{\beta}{r}\right]-\left[\frac{2E_1 h_1(1+\upsilon_1)}{R(1-\upsilon_1^2)}+\frac{4E_2 h_2(1+\upsilon_2)}{R(1-\upsilon_2^2)}\right]\left[\frac{\partial u}{\partial r}+\frac{u}{r}+\frac{2w}{R}\right]$$

$$-(2\rho_1 h_1+4\rho_2 h_2)\ddot{w}=0. \tag{2.27c}$$

Hence, equations (2.27a) through (2.27c) for the *Refined Model* yields the *Linear Axisymmetric Displacement Equations of Homogeneous and Sandwich Spherical Shells as follows,*

$$C_1\left(\frac{\partial^2 u}{\partial r^2}+\frac{1}{r}\frac{\partial u}{\partial r}-\frac{1}{r^2}u\right)+C_2\frac{\partial w}{\partial r}-C_3\ddot{u}=0, \tag{2.28a}$$

$$C_4\left(\frac{\partial^2 \beta}{\partial r^2}+\frac{1}{r}\frac{\partial \beta}{\partial r}-\frac{1}{r^2}\beta\right)-C_5\left(\frac{\partial w}{\partial r}+\beta\right)-C_6\ddot{\beta}=0, \tag{2.28b}$$

$$C_5\left(\frac{\partial^2 w}{\partial r^2}+\frac{1}{r}\frac{\partial w}{\partial r}+\frac{\partial \beta}{\partial r}+\frac{\beta}{r}\right)-C_2\left(\frac{\partial u}{\partial r}+\frac{u}{r}+\frac{2w}{R}\right)-C_3\ddot{w}=0, \tag{2.28c}$$

where

$$C_1=\frac{2E_1 h_1}{1-\upsilon_1^2}+\frac{4E_2 h_2}{1-\upsilon_2^2}, \qquad C_2=\frac{2E_1 h_1(1+\upsilon_1)}{R(1-\upsilon_1^2)}+\frac{4E_2 h_2(1+\upsilon_2)}{R(1-\upsilon_2^2)},$$

$$C_3=2\rho_1 h_1+4\rho_2 h_2, \qquad C_4=\frac{2E_1 h_1^3}{3(1-\upsilon_1^2)}+\frac{4E_2 h_1^2 h_2}{1-\upsilon_2^2},$$

$$C_5=\frac{E_1 h_1}{k_s(1+\upsilon_1)}, \qquad C_6=k_g\left(\frac{2\rho_1 h_1^3}{3}+4\rho_2 h_1^2 h_2\right), \tag{2.29}$$

for the sandwich case $k_s=1$, for the homogeneous case $k_s=\frac{12}{\pi^2}$ while $k_g=1$.

### 2.7.2 Classical Model

The *Classical Model* for the *Displacement Equations of Homogeneous and Sandwich Spherical Shell* is formulated by neglecting the effects of both transverse shear deformation and rotatory inertia by setting $k_s = k_g = 0$.

Letting $k_g = 0$ in (2.25b) gives,

$$Q_{rz}^{(1)} = \left(\frac{\partial M_{rr}^{(1)}}{\partial r} - h_1 \frac{\partial N_{rr}^{(2)}}{\partial r} + h_1 \frac{\partial N_{rr}^{(3)}}{\partial r}\right) + \left(\frac{M_{rr}^{(1)}}{r} - h_1 \frac{N_{rr}^{(2)}}{r} + h_1 \frac{N_{rr}^{(3)}}{r}\right)$$
$$- \left(\frac{M_{\theta\theta}^{(1)}}{r} - h_1 \frac{N_{\theta\theta}^{(2)}}{r} + h_1 \frac{N_{\theta\theta}^{(3)}}{r}\right).$$

Substituting the above equation into (2.25c) yields,

$$\left(\frac{\partial}{\partial r} + \frac{1}{r}\right)\left[\left(\frac{\partial M_{rr}^{(1)}}{\partial r} - h_1 \frac{\partial N_{rr}^{(2)}}{\partial r} + h_1 \frac{\partial N_{rr}^{(3)}}{\partial r}\right) + \left(\frac{M_{rr}^{(1)}}{r} - h_1 \frac{N_{rr}^{(2)}}{r} + h_1 \frac{N_{rr}^{(3)}}{r}\right)\right.$$
$$\left. - \left(\frac{M_{\theta\theta}^{(1)}}{r} - h_1 \frac{N_{\theta\theta}^{(2)}}{r} + h_1 \frac{N_{\theta\theta}^{(3)}}{r}\right)\right]$$
$$- \frac{(N_{rr}^{(1)} + N_{\theta\theta}^{(1)})}{R} - \frac{(N_{rr}^{(2)} + N_{\theta\theta}^{(2)})}{R} - \frac{(N_{rr}^{(3)} + N_{\theta\theta}^{(3)})}{R} - (2\rho_1 h_1 + 4\rho_2 h_2)\ddot{w} = 0. \tag{2.25d}$$

By setting $k_s = 0$ in (2.18), leads to $\beta$ being neglected and in terms of $w$,

$$\beta = -\frac{\partial w}{\partial r}. \tag{2.25e}$$

By substituting the stress resultant-displacements relations from (2.15) to (2.17) into the stress equation of motion (2.25) gives the following two Displacement Equations of Motion.

The first one in the $u$-direction is obtained by substituting (2.15) and (2.16) into (2.25a), which is the same as the refined model,

$$[\frac{2E_1h_1}{1-\upsilon_1^2}+\frac{4E_2h_2}{1-\upsilon_2^2}][\frac{\partial^2 u}{\partial r^2}+\frac{1}{r}\frac{\partial u}{\partial r}-\frac{1}{r^2}u]+[\frac{2E_1h_1(1+\upsilon_1)}{R(1-\upsilon_1^2)}+\frac{4E_2h_2(1+\upsilon_2)}{R(1-\upsilon_2^2)}]\frac{\partial w}{\partial r}$$

$$-(2\rho_1h_1+4\rho_2h_2)\ddot{u}=0.$$

The second equation in the $w$-direction is obtained by substituting (2.15) to (2.17) into (2.25d),

$$\frac{2E_1h_1^3}{3(1-\upsilon_1^2)}(\frac{\partial}{\partial r}+\frac{1}{r})\left[\frac{\partial^2\beta}{\partial r^2}+\upsilon_1\frac{\partial}{\partial r}(\frac{\beta}{r})\right]$$

$$-\frac{2E_2h_1h_2}{1-\upsilon_2^2}(\frac{\partial}{\partial r}+\frac{1}{r})\left[\frac{\partial^2 u}{\partial r^2}+\upsilon_2\frac{\partial}{\partial r}(\frac{u}{r})+\frac{(1+\upsilon_2)}{R}\frac{\partial w}{\partial r}-h_1\frac{\partial^2\beta}{\partial r^2}-\upsilon_2h_1\frac{\partial}{\partial r}(\frac{\beta}{r})\right]$$

$$+\frac{2E_2h_1h_2}{1-\upsilon_2^2}(\frac{\partial}{\partial r}+\frac{1}{r})\left[\frac{\partial^2 u}{\partial r^2}+\upsilon_2\frac{\partial}{\partial r}(\frac{u}{r})+\frac{(1+\upsilon_2)}{R}\frac{\partial w}{\partial r}+h_1\frac{\partial^2\beta}{\partial r^2}+\upsilon_2h_1\frac{\partial}{\partial r}(\frac{\beta}{r})\right]$$

$$+\frac{2E_1h_1^3}{3(1-\upsilon_1^2)}(\frac{\partial}{\partial r}+\frac{1}{r})\left[\frac{1}{r}\frac{\partial\beta}{\partial r}+\upsilon_1\frac{\beta}{r^2}\right]$$

$$-\frac{2E_2h_1h_2}{1-\upsilon_2^2}(\frac{\partial}{\partial r}+\frac{1}{r})\left[\frac{1}{r}\frac{\partial u}{\partial r}+\upsilon_2\frac{u}{r^2}+\frac{(1+\upsilon_2)}{r}\frac{w}{R}-h_1\frac{1}{r}\frac{\partial\beta}{\partial r}-\upsilon_2h_1\frac{\beta}{r^2}\right]$$

$$+\frac{2E_2h_1h_2}{1-\upsilon_2^2}(\frac{\partial}{\partial r}+\frac{1}{r})\left[\frac{1}{r}\frac{\partial u}{\partial r}+\upsilon_2\frac{u}{r^2}+\frac{(1+\upsilon_2)}{r}\frac{w}{R}+h_1\frac{1}{r}\frac{\partial\beta}{\partial r}+\upsilon_2h_1\frac{\beta}{r^2}\right]$$

$$-\frac{2E_1h_1^3}{3(1-\upsilon_1^2)}(\frac{\partial}{\partial r}+\frac{1}{r})\left[\upsilon_1\frac{1}{r}\frac{\partial\beta}{\partial r}+\frac{\beta}{r^2}\right]$$

$$+\frac{2E_2h_1h_2}{1-\upsilon_2^2}(\frac{\partial}{\partial r}+\frac{1}{r})\left[\upsilon_2\frac{1}{r}\frac{\partial u}{\partial r}+\frac{u}{r^2}+\frac{(1+\upsilon_2)}{r}\frac{w}{R}-\upsilon_2h_1\frac{1}{r}\frac{\partial\beta}{\partial r}-h_1\frac{\beta}{r^2}\right]$$

$$-\frac{2E_2h_1h_2}{1-\upsilon_2^2}(\frac{\partial}{\partial r}+\frac{1}{r})\left[\upsilon_2\frac{1}{r}\frac{\partial u}{\partial r}+\frac{u}{r^2}+\frac{(1+\upsilon_2)}{r}\frac{w}{R}+\upsilon_2h_1\frac{1}{r}\frac{\partial\beta}{\partial r}+h_1\frac{\beta}{r^2}\right]$$

$$-\frac{2E_1h_1}{1-\upsilon_1^2}(\frac{1}{R})\left[(1+\upsilon_1)\frac{\partial u}{\partial r}+(1+\upsilon_1)\frac{u}{r}+(1+\upsilon_1)\frac{2w}{R}\right]$$

$$-\frac{2E_2h_2}{1-\upsilon_2^2}(\frac{1}{R})\left[(1+\upsilon_2)\frac{\partial u}{\partial r}+(1+\upsilon_2)\frac{u}{r}+(1+\upsilon_2)\frac{2w}{R}-(1+\upsilon_2)h_1\frac{\partial\beta}{\partial r}-(1+\upsilon_2)h_1\frac{\beta}{r}\right]$$

$$-\frac{2E_2h_2}{1-\upsilon_2^2}(\frac{1}{R})\left[(1+\upsilon_2)\frac{\partial u}{\partial r}+(1+\upsilon_2)\frac{u}{r}+(1+\upsilon_2)\frac{2w}{R}+(1+\upsilon_2)h_1\frac{\partial\beta}{\partial r}+(1+\upsilon_2)h_1\frac{\beta}{r}\right]$$

$$-(2\rho_1h_1+4\rho_2h_2)\ddot{w}=0.$$

Expanding and collecting the terms with the same coefficients yields:

$$\frac{2E_1h_1^3}{3(1-\upsilon_1^2)}(\frac{\partial}{\partial r}+\frac{1}{r})[\frac{\partial^2\beta}{\partial r^2}+\frac{\upsilon_1}{r}\frac{\partial\beta}{\partial r}-\frac{\upsilon_1}{r^2}\beta+\frac{1}{r}\frac{\partial\beta}{\partial r}+\frac{\upsilon_1}{r^2}\beta-\frac{\upsilon_1}{r}\frac{\partial\beta}{\partial r}-\frac{1}{r^2}\beta]$$

$$+\frac{4E_2h_1^2h_2}{1-\upsilon_2^2}(\frac{\partial}{\partial r}+\frac{1}{r})[\frac{\partial^2\beta}{\partial r^2}+\frac{\upsilon_2}{r}\frac{\partial\beta}{\partial r}-\frac{\upsilon_2}{r^2}\beta+\frac{1}{r}\frac{\partial\beta}{\partial r}+\frac{\upsilon_2}{r^2}\beta-\frac{\upsilon_2}{r}\frac{\partial\beta}{\partial r}-\frac{1}{r^2}\beta]$$

$$-[\frac{2E_1h_1(1+\upsilon_1)}{R(1-\upsilon_1^2)}+\frac{4E_2h_2(1+\upsilon_2)}{R(1-\upsilon_2^2)}][\frac{\partial u}{\partial r}+\frac{u}{r}+\frac{2w}{R}]-(2\rho_1h_1+4\rho_2h_2)\ddot{w}=0.$$

After simplifying we obtain,

$$[\frac{2E_1h_1^3}{3(1-\upsilon_1^2)}+\frac{4E_2h_1^2h_2}{1-\upsilon_2^2}](\frac{\partial}{\partial r}+\frac{1}{r})[\frac{\partial^2\beta}{\partial r^2}+\frac{1}{r}\frac{\partial\beta}{\partial r}-\frac{1}{r^2}\beta]$$

$$-[\frac{2E_1h_1(1+\upsilon_1)}{R(1-\upsilon_1^2)}+\frac{4E_2h_2(1+\upsilon_2)}{R(1-\upsilon_2^2)}][\frac{\partial u}{\partial r}+\frac{u}{r}+\frac{2w}{R}]-(2\rho_1h_1+4\rho_2h_2)\ddot{w}=0.$$

By taking the coefficients $C_2, C_3$ *and* $C_4$ from (2.29) and expanding out $\beta$ gives:

$$C_4(\frac{\partial^3\beta}{\partial r^3}+\frac{1}{r}\frac{\partial^2\beta}{\partial r^2}-\frac{1}{r^2}\frac{\partial\beta}{\partial r}-\frac{1}{r^2}\frac{\partial\beta}{\partial r}+\frac{2}{r^3}\beta+\frac{1}{r}\frac{\partial^2\beta}{\partial r^2}+\frac{1}{r^2}\frac{\partial\beta}{\partial r}-\frac{1}{r^3}\beta)$$

$$-C_2(\frac{\partial u}{\partial r}+\frac{u}{r}+\frac{2w}{R})-C_3\ddot{w}=0,$$

or

$$C_4(\frac{\partial^3\beta}{\partial r^3}+\frac{2}{r}\frac{\partial^2\beta}{\partial r^2}-\frac{1}{r^2}\frac{\partial\beta}{\partial r}+\frac{1}{r^3}\beta)-C_2(\frac{\partial u}{\partial r}+\frac{u}{r}+\frac{2w}{R})-C_3\ddot{w}=0.$$

By substituting (2.25e) into the above equation yields,

$$C_4(\frac{\partial^4 w}{\partial r^4}+\frac{2}{r}\frac{\partial^3 w}{\partial r^3}-\frac{1}{r^2}\frac{\partial^2 w}{\partial r^2}+\frac{1}{r^3}\frac{\partial w}{\partial r})+C_2(\frac{\partial u}{\partial r}+\frac{u}{r}+\frac{2w}{R})+C_3\ddot{w}=0.$$

Hence, the *Classical Model* for the *Linear Axisymmetric Displacement Equations of Homogeneous and Sandwich Spherical Shells become*:

$$C_1(\frac{\partial^2 u}{\partial r^2}+\frac{1}{r}\frac{\partial u}{\partial r}-\frac{1}{r^2}u)+C_2\frac{\partial w}{\partial r}-C_3\ddot{u}=0 \tag{2.30a}$$

$$C_4(\frac{\partial^4 w}{\partial r^4}+\frac{2}{r}\frac{\partial^3 w}{\partial r^3}-\frac{1}{r^2}\frac{\partial^2 w}{\partial r^2}+\frac{1}{r^3}\frac{\partial w}{\partial r})+C_2(\frac{\partial u}{\partial r}+\frac{u}{r}+\frac{2w}{R})+C_3\ddot{w}=0 \tag{2.30b}$$

where

$$C_1=\frac{2E_1h_1}{1-\upsilon_1^2}+\frac{4E_2h_2}{1-\upsilon_2^2}, \qquad C_2=\frac{2E_1h_1(1+\upsilon_1)}{R(1-\upsilon_1^2)}+\frac{4E_2h_2(1+\upsilon_2)}{R(1-\upsilon_2^2)},$$

$$C_3=2\rho_1h_1+4\rho_2h_2, \qquad C_4=\frac{2E_1h_1^3}{3(1-\upsilon_1^2)}+\frac{4E_2h_1^2h_2}{1-\upsilon_2^2}. \tag{2.31}$$

# CHAPTER 3

# EQUATIONS FOR THE NONLINEAR VIBRATIONS OF HOMOGENEOUS SPHERICAL SHELLS

## 3.1 Introduction

In order to study the nonlinear free vibration problem, the nonlinear elasticity theory [2] is employed to derive the nonlinear governing equations for the homogeneous spherical shell. Since nonlinear equations represent a logical extension of their linear counterpart, the derivation in this chapter is similar to that of the linear case presented in Chapter 2. Therefore, the homogeneous spherical shell is assumed to be thin and elastic. Hence, the spherical shell coordinates, $\phi$, $\theta$, and $R + z$ are chosen so that $z = 0$ designates the middle surface whose radius is $R$ and $z = \pm h$ designates the outer and inner surfaces. Furthermore, the shell is taken to be shallow and vibrates axisymmetrically (torsionless motion). Then from (2.6), the displacement form is:

$$\begin{aligned} U_r(r,\theta,z,t) &= u(r,t) + z\beta(r,t), \\ U_\theta &= 0, \\ U_z(r,\theta,z,t) &= w(r,t). \end{aligned} \tag{3.1}$$

The governing equations can also be formulated by using the Hamilton's principle, introduced in section three of Chapter 2, by (2.8b),

$$\delta \int_{t_0}^{t_1} (\mathrm{K} - \mathrm{U}) dt = 0 \tag{3.2}$$

where U is the strain energy and K is the kinetic energy. W is the work potential which is equal to zero for free vibration.

The times $t_0$ and $t_1$ are arbitrary. The symbol $\delta$ is the variational symbol and is treated mathematically like a differential symbol. Variational displacements are arbitrary. Since the strain energy involves the stress and strain terms, both relating to the displacements, we obtain the stress-strain-displacement relations in the next section.

## 3.2 Nonlinear Stress-Strain-Displacement Relations

### 3.2.1 Nonlinear Strain-Displacement Relations

The nonlinear theory of elasticity [2] is employed to derive the strain-displacement relations for the homogeneous spherical shell, the derivation work is presented in Appendix B. The following is the nonlinear strain-displacement relations for the homogeneous shells,

$$e_{rr} = \frac{\partial u}{\partial r} + \frac{w}{R} + z\frac{\partial \beta}{\partial r} + \frac{1}{2}\omega_\theta^2, \tag{3.3a}$$

$$e_{\theta\theta} = \frac{u}{r} + \frac{w}{R} + z\frac{\beta}{r}, \tag{3.3b}$$

$$e_{rz} = \frac{\partial w}{\partial r} + \beta, \tag{3.3c}$$

where the rotation, $\omega_\theta = \frac{1}{2}(\beta - \frac{\partial w}{\partial r})$. (3.3d)

### 3.2.2 Nonlinear Stress-Strain Relations

The following shows the nonlinear stress-strain relations,

$$\sigma_{rr} = \frac{\mathrm{E}}{1-\upsilon^2}(e_{rr} + \upsilon\, e_{\theta\theta}), \tag{3.4a}$$

$$\sigma_{\theta\theta} = \frac{\mathrm{E}}{1-\upsilon^2}(e_{\theta\theta} + \upsilon\, e_{rr}), \tag{3.4b}$$

$$\sigma_{rz} = \frac{E}{2(1+\upsilon)} e_{rz} . \tag{3.4c}$$

It should be noted that the normal stress $\sigma_{zz}$, which acts in the normal direction to the neutral surface, is assumed to be zero.

### 3.2.3 Nonlinear Stress Resultant-Displacement Relations

Similar to the linear case, it is convenient to integrate the stress distributions through the thickness of the shell and to replace the stresses by the stress resultants. All the stresses will be integrated over the region they act on a shell element whose dimensions are infinitesimal in the r and $\theta$ directions and equal to shell thickness in the normal direction, $z$,

$$\text{Membrane forces: } N_{ii} = \int_{-h}^{h} \sigma_{ii} dz , \tag{3.5a}$$

$$\text{Bending moments: } M_{ii} = \int_{-h}^{h} z\sigma_{ii} dz , \tag{3.5b}$$

$$\text{Transverse shear force: } Q_{rz} = \int_{-h}^{h} (\sigma_{rz} - \sigma_{rr}\omega_{\theta}) dz , \tag{3.5c}$$

where $ii = rr$ or $\theta\theta$.

Equations (2.14) give the following equations for the integration of the stresses across the thickness,

$$\int_{-h}^{h} dz = 2h , \qquad \int_{-h}^{h} z dz = 0 , \qquad \int_{-h}^{h} z^2 dz = \frac{2h^3}{3} . \tag{3.6}$$

Membrane force $N_{rr}$ can be obtained by substituting (3.4a) into (3.5a),

$$N_{rr} = \int_{-h}^{h} \sigma_{rr} dz = \frac{E}{1-\upsilon^2} \int_{-h}^{h} (e_{rr} + \upsilon e_{\theta\theta}) dz .$$

The nonlinear force-displacement relation is now obtained by substituting (3.3) into the above equation,

$$N_{rr} = \frac{\mathrm{E}}{1-\upsilon^2}\int_{-h}^{h}\left\{\left[\frac{\partial u}{\partial r}+\frac{w}{R}+z\frac{\partial \beta}{\partial r}+\frac{1}{2}\omega_\theta^2\right]+\upsilon\left[\frac{u}{r}+\frac{w}{R}+z\frac{\beta}{r}\right]\right\}dz,$$

therefore $$N_{rr} = \frac{2\mathrm{E}h}{1-\upsilon^2}\left[\frac{\partial u}{\partial r}+\upsilon\frac{u}{r}+(1+\upsilon)\frac{w}{R}+\frac{1}{2}\omega_\theta^2\right]. \tag{3.7a}$$

By the same substituting process with (3.3), (3.4b), (3.5a) and (3.6), the nonlinear membrane force $N_{\theta\theta}$ is,

$$N_{\theta\theta} = \int_{-h}^{h}\sigma_{\theta\theta}dz = \frac{\mathrm{E}}{1-\upsilon^2}\int_{-h}^{h}(e_{\theta\theta}+\upsilon\, e_{rr})dz$$

$$= \frac{\mathrm{E}}{1-\upsilon^2}\int_{-h}^{h}\left\{\left[\frac{u}{r}+\frac{w}{R}+z\frac{\beta}{r}\right]+\upsilon\left[\frac{\partial u}{\partial r}+\frac{w}{R}+z\frac{\partial \beta}{\partial r}+\frac{1}{2}\omega_\theta^2\right]\right\}dz,$$

or $$N_{\theta\theta} = \frac{2\mathrm{E}h}{1-\upsilon^2}\left[\upsilon\frac{\partial u}{\partial r}+\frac{u}{r}+(1+\upsilon)\frac{w}{R}+\frac{\upsilon}{2}\omega_\theta^2\right]. \tag{3.7b}$$

To get the bending moment $M_{rr}$, we substitute (3.4a) into (3.5b) giving us the moment-strain relation,

$$M_{rr} = \int_{-h}^{h} z\sigma_{rr}dz = \frac{\mathrm{E}}{1-\upsilon^2}\int_{-h}^{h} z(e_{rr}+\upsilon\, e_{\theta\theta})dz.$$

The nonlinear moment-displacement relation is now obtained by substituting (3.3) into the above equation,

$$M_{rr} = \frac{\mathrm{E}}{1-\upsilon^2}\int_{-h}^{h}\left\{z\left[\frac{\partial u}{\partial r}+\frac{w}{R}+z\frac{\partial \beta}{\partial r}+\frac{1}{2}\omega_\theta^2\right]+\upsilon z\left[\frac{u}{r}+\frac{w}{R}+z\frac{\beta}{r}\right]\right\}dz,$$

therefore $$M_{rr} = \frac{2\mathrm{E}h^3}{3(1-\upsilon^2)}\left[\frac{\partial \beta}{\partial r}+\upsilon\frac{\beta}{r}\right], \tag{3.7c}$$

Similarly for $M_{\theta\theta}$,

$$M_{\theta\theta} = \int_{-h}^{h} z\sigma_{\theta\theta}\,dz = \frac{\mathrm{E}}{1-\upsilon^2}\int_{-h}^{h} z\left(e_{\theta\theta} + \upsilon\, e_{rr}\right)dz$$

$$= \frac{\mathrm{E}}{1-\upsilon^2}\int_{-h}^{h}\left\{z\left[\frac{u}{r} + \frac{w}{R} + z\frac{\beta}{r}\right] + \upsilon z\left[\frac{\partial u}{\partial r} + \frac{w}{R} + z\frac{\partial \beta}{\partial r} + \frac{1}{2}\omega_\theta^2\right]\right\}dz,$$

or $$M_{\theta\theta} = \frac{2\mathrm{E}h^3}{3(1-\upsilon^2)}\left[\upsilon\frac{\partial \beta}{\partial r} + \frac{\beta}{r}\right]. \tag{3.7d}$$

The nonlinear transverse shear force $Q_{rz}$ is obtained by substituting (3.4a) and (3.4c) into (3.5c),

$$Q_{rz} = \int_{-h}^{h}(\sigma_{rz} - \sigma_{rr}\omega_\theta)dz = \frac{\mathrm{E}}{2(1+\upsilon)}\int_{-h}^{h} e_{rz}dz - \frac{\mathrm{E}}{1-\upsilon^2}\int_{-h}^{h}\left(e_{rr} + \upsilon\, e_{\theta\theta}\right)\omega_\theta dz.$$

The nonlinear force-displacement relation is obtained by substituting (3.3) into the above equation,

$$Q_{rz} = \frac{\mathrm{E}}{2(1+\upsilon)}\int_{-h}^{h}\left[\frac{\partial w}{\partial r} + \beta\right]dz - \frac{\mathrm{E}}{1-\upsilon^2}\int_{-h}^{h}\left\{\left[\frac{\partial u}{\partial r} + \frac{w}{R} + z\frac{\partial \beta}{\partial r} + \frac{1}{2}\omega_\theta^2\right] + \upsilon\left[\frac{u}{r} + \frac{w}{R} + z\frac{\beta}{r}\right]\right\}\omega_\theta dz$$

therefore,

$$Q_{rz} = \frac{\mathrm{E}h}{k_s(1+\upsilon)}\left[\frac{\partial w}{\partial r} + \beta\right] - k_t\frac{2\mathrm{E}h}{1-\upsilon^2}\left[\frac{\partial u}{\partial r} + \upsilon\frac{u}{r} + (1+\upsilon)\frac{w}{R} + \frac{1}{2}\omega_\theta^2\right]\omega_\theta$$

$$= \frac{\mathrm{E}h}{k_s(1+\upsilon)}\left[\frac{\partial w}{\partial r} + \beta\right] - k_t N_{rr}\omega_\theta, \tag{3.7e}$$

where $k_s$ is a tracer for transverse shear deformation, and $k_t$ is a tracer for the effect of transverse shear force on membrane force.

### 3.3 Nonlinear Stress Equations of Motion

In this section, we derive the nonlinear stress equations of motion for the homogeneous spherical shell by using Hamilton's principle which is given by equation (3.2),

$\delta\int_{t_0}^{t_1}(\mathrm{K}-\mathrm{U})dt=0$, where K is the kinetic energy and U is the strain energy.

The kinetic energy of one infinitesimal element is given by,

$$\mathrm{dK}=\frac{1}{2}\rho(\dot{U}_r^2+\dot{U}_z^2)dV, \tag{3.8}$$

where the dot indicates time derivatives, $dV = rdrd\theta dz$ is the infinitesimal volume, and $\rho$ is the density.

Substituting (3.1) into (3.8) yields,

$$\mathrm{K}=\frac{\rho}{2}\int_{\theta}\int_{r}\int_{-h}^{h}[(\dot{u}+z\dot{\beta})^2+\dot{w}^2]dzrdrd\theta$$

$$=\frac{\rho}{2}\int_{\theta}\int_{r}\int_{-h}^{h}[\dot{u}^2+2z\dot{u}\dot{\beta}+z^2\dot{\beta}^2+\dot{w}^2]dzrdrd\theta.$$

Integrating over the thickness of the shell and over $\theta$, measured form 0 to $2\pi$ gives,

$$\mathrm{K}=2\pi\rho h\int_{r}[\dot{u}^2+\dot{w}^2]rdr+2\pi\frac{\rho h^3}{3}\int_{r}\dot{\beta}^2rdr.$$

Taking the variations for the displacements and applying Hamilton's principle,

$$\int_{t_0}^{t_1}\delta\mathrm{K}dt=2\pi\int_{t_0}^{t_1}\int_{r}[-2\rho h\ddot{u}\delta u-\frac{2\rho h^3}{3}\ddot{\beta}\delta\beta-2\rho h\ddot{w}\delta w]rdrdt. \tag{3.9}$$

Integrating the first term by parts, we have,

$$\int_{t_0}^{t_1}\delta\dot{u}^2dt=\int_{t_0}^{t_1}2\dot{u}\delta\dot{u}dt=2[\dot{u}\delta u]_{t_0}^{t_1}-2\int_{t_0}^{t_1}\ddot{u}\delta udt=-2\int_{t_0}^{t_1}\ddot{u}\delta udt$$

where $[\dot{u}\delta u]_{t_0}^{t_1} = 0$ since the virtual displacement is zero at $t = t_0$ and $t = t_1$.

On the other hand, the strain energy of an infinitesimal element is given by,

$$\mathrm{dU} = \frac{1}{2}(\sigma_{rr}e_{rr} + \sigma_{\theta\theta}e_{\theta\theta} + \sigma_{rz}e_{rz})dV . \tag{3.10}$$

Integrating over the volume of the shell, we have,

$$\mathrm{U} = \frac{1}{2}\int_{\theta}\int_{r}\int_{-h}^{h}[\sigma_{rr}e_{rr} + \sigma_{\theta\theta}e_{\theta\theta} + \sigma_{rz}e_{rz}]dzrdrd\theta .$$

Applying Hamilton's principle we get,

$$\int_{t_0}^{t_1}\delta \mathrm{U}dt = \frac{1}{2}\int_{t_0}^{t_1}\int_{\theta}\int_{r}\int_{-h}^{h}[\delta\sigma_{rr}e_{rr} + \sigma_{rr}\delta e_{rr} + \delta\sigma_{\theta\theta}e_{\theta\theta} + \sigma_{\theta\theta}\delta e_{\theta\theta} + \delta\sigma_{rz}e_{rz} + \sigma_{rz}\delta e_{rz}]dzrdrd\theta dt .$$

Substituting (3.4) yields,

$$\begin{aligned}\int_{t_0}^{t_1}\delta \mathrm{U}dt = \frac{1}{2}\int_{t_0}^{t_1}\int_{\theta}\int_{r}\int_{-h}^{h}[&\frac{\mathrm{E}}{1-\upsilon^2}(\delta e_{rr} + \upsilon\delta e_{\theta\theta})e_{rr} + \frac{\mathrm{E}}{1-\upsilon^2}(e_{rr} + \upsilon e_{\theta\theta})\delta e_{rr} \\ &+ \frac{\mathrm{E}}{1-\upsilon^2}(\delta e_{\theta\theta} + \upsilon\delta e_{rr})e_{\theta\theta} + \frac{\mathrm{E}}{1-\upsilon^2}(e_{\theta\theta} + \upsilon e_{rr})\delta e_{\theta\theta} \\ &+ \frac{\mathrm{E}}{2(1+\upsilon)}\delta e_{rz}e_{rz} + \frac{\mathrm{E}}{2(1+\upsilon)}e_{rz}\delta e_{rz}]dzrdrd\theta dt .\end{aligned}$$

Collecting the terms of variational strain gives,

$$\begin{aligned}\int_{t_0}^{t_1}\delta \mathrm{U}dt = \frac{1}{2}\int_{t_0}^{t_1}\int_{\theta}\int_{r}\int_{-h}^{h}[&\frac{2\mathrm{E}}{1-\upsilon^2}(e_{rr} + \upsilon e_{\theta\theta})\delta e_{rr} + \frac{2\mathrm{E}}{1-\upsilon^2}(e_{\theta\theta} + \upsilon e_{rr})\delta e_{\theta\theta} \\ &+ \frac{\mathrm{E}}{1+\upsilon}e_{rz}\delta e_{rz}]dzrdrd\theta dt ,\end{aligned}$$

therefore

$$\int_{t_0}^{t_1}\delta \mathrm{U}dt = \int_{t_0}^{t_1}\int_{\theta}\int_{r}\int_{-h}^{h}[\sigma_{rr}\delta e_{rr} + \sigma_{\theta\theta}\delta e_{\theta\theta} + \sigma_{rz}\delta e_{rz}]dzrdrd\theta dt .$$

To include the effect of transverse shear force on membrane force by (3.5c), we have an additional term,

$$\int_{t_0}^{t_1}\delta U dt=\int_{t_0}^{t_1}\int_{\theta}\int_{r}\int_{-h}^{h}[\sigma_{rr}\delta e_{rr}+\sigma_{\theta\theta}\delta e_{\theta\theta}+(\sigma_{rz}-\sigma_{rr}\omega_{\theta})\delta e_{rz}]dzrdrd\theta dt. \tag{3.11}$$

By substituting (3.3) into (3.11) and integrating $\theta$ from 0 to $2\pi$,

$$\int_{t_0}^{t_1}\delta U dt= 2\pi\int_{t_0}^{t_1}\int_{r}\int_{-h}^{h}\{\sigma_{rr}[\frac{\delta w}{R}+\frac{\partial(\delta u)}{\partial r}+z\frac{\partial(\delta\beta)}{\partial r}]+\sigma_{\theta\theta}[\frac{\delta w}{R}+\frac{\delta u}{r}+z\frac{\delta\beta}{r}]$$

$$+(\sigma_{rz}-\sigma_{rr}\omega_{\theta})[\frac{\partial(\delta w)}{\partial r}+\delta\beta]\}dzrdrdt.$$

By using (3.5) we have,

$$\int_{t_0}^{t_1}\delta U dt = 2\pi\int_{t_0}^{t_1}\int_{r}\{N_{rr}[\frac{\delta w}{R}+\frac{\partial(\delta u)}{\partial r}]+M_{rr}\frac{\partial(\delta\beta)}{\partial r}+N_{\theta\theta}[\frac{\delta w}{R}+\frac{\delta u}{r}]+M_{\theta\theta}\frac{\delta\beta}{r}$$

$$+Q_{rz}[\frac{\partial(\delta w)}{\partial r}+\delta\beta]\}rdrdt,$$

hence,

$$\int_{t_0}^{t_1}\delta U dt = 2\pi\int_{t_0}^{t_1}\int_{r}\{[-\frac{1}{r}\frac{\partial(rN_{rr})}{\partial r}+\frac{N_{\theta\theta}}{r}]\delta u\ [-\frac{1}{r}\frac{\partial(rM_{rr})}{\partial r}+\frac{M_{\theta\theta}}{r}+Q_{rz}]\delta\beta$$

$$+[-\frac{1}{r}\frac{\partial(rQ_{rz})}{\partial r}+\frac{N_{rr}}{R}+\frac{N_{\theta\theta}}{R}]\delta w\}rdrdt$$

$$+\ 2\pi\int_{t_0}^{t_1}[rN_{rr}\delta u+rM_{rr}\delta\beta+rQ_{rz}\delta w]_{r_0}^{r_1}dt. \tag{3.12}$$

Integrating the first term by parts gives,

$$\int_{t_0}^{t_1}\int_{r}N_{rr}\frac{\partial(\delta u)}{\partial r}rdrdt=\int_{t_0}^{t_1}[rN_{rr}\delta u]_{r_0}^{r_1}dt-\int_{t_0}^{t_1}\int_{r}[\frac{1}{r}\frac{\partial(rN_{rr})}{\partial r}\delta u]rdrdt,$$

Applying Hamilton's principle (3.2), $\delta\int_{t_0}^{t_1}(\mathrm{K}-\mathrm{U})dt=\int_{t_0}^{t_1}(\delta\mathrm{K}-\delta\mathrm{U})dt=0$ together with (3.9) and (3.12) gives,

$$2\pi\int_{t_0}^{t_1}\int_{r}\{[\frac{1}{r}\frac{\partial(rN_{rr})}{\partial r}-\frac{N_{\theta\theta}}{r}-2\rho h\ddot{u}]\delta u+[\frac{1}{r}\frac{\partial(rM_{rr})}{\partial r}-\frac{M_{\theta\theta}}{r}-Q_{rz}-\frac{2\rho h^3}{3}\ddot{\beta}]\delta\beta$$

$$+[\frac{1}{r}\frac{\partial(rQ_{rz})}{\partial r}-\frac{1}{R}(N_{rr}+N_{\theta\theta})-2\rho h\ddot{w}]\delta w\}rdrd\theta dt$$

$$-2\pi\int_{t_0}^{t_1}[rN_{rr}\delta u+rM_{rr}\delta\beta+rQ_{rz}\delta w]_{r_0}^{r_1}dt=0. \qquad (3.13)$$

Equation (3.13) can only be satisfied if each of the double and single integral parts is zero individually. Moreover, since the variational displacements are arbitrary, each integral equation can only be satisfied if the coefficients of the variational displacements are zero. Thus, the coefficients of the double integral are set to zero giving the following three *Nonlinear Stress Equations of Motion*:

$$\frac{\partial N_{rr}}{\partial r}+\frac{N_{rr}}{r}-\frac{N_{\theta\theta}}{r}-2\rho h\ddot{u}=0, \qquad (3.14a)$$

$$\frac{\partial M_{rr}}{\partial r}+\frac{M_{rr}}{r}-\frac{M_{\theta\theta}}{r}-Q_{rz}-\frac{2k_g\rho h^3}{3}\ddot{\beta}=0, \qquad (3.14b)$$

$$\frac{\partial Q_{rz}}{\partial r}+\frac{Q_{rz}}{r}-\frac{1}{R}(N_{rr}+N_{\theta\theta})-2\rho h\ddot{w}=0, \qquad (3.14c)$$

where $k_g$ is a tracer for rotatory inertia.

It should be noted [2] that by $Q_{rz}=\frac{\mathrm{E}h}{k_s(1+\upsilon)}\left[\frac{\partial w}{\partial r}+\beta\right]$ in (3.14b) by setting $k_t=0$ in (3.7e), and $Q_{rz}=\frac{\mathrm{E}h}{k_s(1+\upsilon)}\left[\frac{\partial w}{\partial r}+\beta\right]-k_tN_{rr}\omega_\theta$ in (3.14c) by setting $k_t=1$ in (3.7e).

For the single integral part of (3.13) to be zero, the coefficients of the virtual displacements or the virtual displacements are set equal to zero. Since virtual displacements are only zero at all times when the boundary displacements are prescribed, this translates into the following possible *boundary conditions* for $r_o$ and $r_1$,

$$[rN_{rr}]_{r_0}^{r_1} = 0 \quad \text{or} \quad [\delta u]_{r_0}^{r_1} = 0 \tag{3.15a}$$

$$[rM_{rr}]_{r_0}^{r_1} = 0 \quad \text{or} \quad [\delta\beta]_{r_0}^{r_1} = 0 \tag{3.15b}$$

$$[rQ_{rz}]_{r_0}^{r_1} = 0 \quad \text{or} \quad [\delta w]_{r_0}^{r_1} = 0 \tag{3.15c}$$

Hence the following gives the boundary conditions for the free vibration of spherical shells:

- *Free edge condition at* $r_o$

$$u(r_o) = 0, \qquad M_{rr}(r_o) = 0, \qquad Q_{rz}(r_o) = 0. \tag{3.16a}$$

- *Clamped edge condition at* $r_1$

$$u(r_1) = 0, \qquad \beta(r_1) = 0, \qquad w(r_1) = 0. \tag{3.16b}$$

- *Simple Supported edge condition at* $r_1$

$$u(r_1) = 0, \qquad M_{rr}(r_1) = 0, \qquad w(r_1) = 0. \tag{3.16c}$$

- *Free edge condition at* $r_1$

$$u(r_1) = 0, \qquad M_{rr}(r_1) = 0, \qquad Q_{rz}(r_1) = 0. \tag{3.16d}$$

### 3.4 Nonlinear Displacement Equations of Motion

In this section we derive the nonlinear displacement equations of motion for the homogeneous spherical shell. Two models will be presented. When the equations include the effects of rotatory inertia $\ddot{\beta}$ and transverse shear $Q_{r\bar{z}}$, the model is called the *Refined Model.* To obtain results for this model, calculations are made with the tracers $k_s = \frac{12}{\pi^2}$ and $k_g = 1$ for the homogeneous case. The second model, called the *Classical Model* is obtained by setting $k_s = k_g = 0$, which neglects the rotatory inertia and transverse shear effects.

#### 3.4.1 Nonlinear Refined Model

By substituting the nonlinear stress resultant-displacement relations from (3.7) into the nonlinear stress equation of motion (3.14), we obtain the following three *nonlinear displacement equations of motion of homogeneous spherical shells.*

The first one, in the u-direction, is obtained by substituting (3.7a) and (3.7b) into (3.14a),

$$\frac{2Eh}{1-\upsilon^2}\left[\frac{\partial^2 u}{\partial r^2}+\upsilon\frac{\partial}{\partial r}(\frac{u}{r})+(1+\upsilon)\frac{\partial}{\partial r}(\frac{w}{R})+\frac{1}{2}\frac{\partial\omega_\theta^2}{\partial r}\right]$$

$$+\frac{2Eh}{1-\upsilon^2}(\frac{1}{r})\left[\frac{\partial u}{\partial r}+\upsilon\frac{u}{r}+(1+\upsilon)\frac{w}{R}+\frac{1}{2}\omega_\theta^2\right]$$

$$-\frac{2Eh}{1-\upsilon^2}(\frac{1}{r})\left[\upsilon\frac{\partial u}{\partial r}+\frac{u}{r}+(1+\upsilon)\frac{w}{R}+\frac{\upsilon}{2}\omega_\theta^2\right]$$

$$-2\rho h u = 0.$$

By expanding and collecting the terms with the same coefficients we get,

$$\frac{2Eh}{1-\upsilon^2}[\frac{\partial^2 u}{\partial r^2}+\frac{\upsilon}{r}\frac{\partial u}{\partial r}-\frac{\upsilon}{r^2}u+\frac{(1+\upsilon)}{R}\frac{\partial w}{\partial r}+\frac{1}{2}(\frac{\partial}{\partial r}+\frac{1-\upsilon}{r})\omega_\theta^2$$

$$+\frac{1}{r}\frac{\partial u}{\partial r}+\frac{\upsilon}{r^2}u-\frac{\upsilon}{r}\frac{\partial u}{\partial r}-\frac{1}{r^2}u]-2\rho h\ddot{u}=0,$$

therefore,

$$\frac{2Eh}{1-\upsilon^2}[\frac{\partial^2 u}{\partial r^2}+\frac{1}{r}\frac{\partial u}{\partial r}-\frac{1}{r^2}u]+\frac{2Eh(1+\upsilon)}{R(1-\upsilon^2)}\frac{\partial w}{\partial r}+\frac{1}{2}(\frac{2Eh}{1-\upsilon^2})(\frac{\partial}{\partial r}+\frac{1-\upsilon}{r})\omega_\theta^2-2\rho h\ddot{u}=0.$$

(3.17a)

The second equation in the $\beta$-direction is obtained by substituting (3.7c), (3.7d) and (3.7e) with $k_t=0$ into (3.14b),

$$\frac{2Eh^3}{3(1-\upsilon^2)}\left[\frac{\partial^2\beta}{\partial r^2}+\upsilon\frac{\partial}{\partial r}(\frac{\beta}{r})\right]+\frac{2Eh^3}{3(1-\upsilon^2)}(\frac{1}{r})\left[\frac{\partial\beta}{\partial r}+\upsilon\frac{\beta}{r}\right]-\frac{2Eh^3}{3(1-\upsilon^2)}(\frac{1}{r})\left[\upsilon\frac{\partial\beta}{\partial r}+\frac{\beta}{r}\right]$$

$$-\frac{Eh}{k_s(1+\upsilon)}\left[\frac{\partial w}{\partial r}+\beta\right]-\frac{2k_g\rho h^3}{3}\ddot{\beta}=0.$$

Simplifying we have,

$$\frac{2Eh^3}{3(1-\upsilon^2)}[\frac{\partial^2\beta}{\partial r^2}+\frac{\upsilon}{r}\frac{\partial\beta}{\partial r}-\frac{\upsilon}{r^2}\beta+\frac{1}{r}\frac{\partial\beta}{\partial r}+\frac{\upsilon}{r^2}\beta-\frac{\upsilon}{r}\frac{\partial\beta}{\partial r}-\frac{1}{r^2}\beta]$$

$$-\frac{Eh}{k_s(1+\upsilon)}[\frac{\partial w}{\partial r}+\beta]-\frac{2k_g\rho h^3}{3}\ddot{\beta}=0,$$

thus,

$$\frac{2Eh^3}{3(1-\upsilon^2)}[\frac{\partial^2\beta}{\partial r^2}+\frac{1}{r}\frac{\partial\beta}{\partial r}-\frac{1}{r^2}\beta]-\frac{Eh}{k_s(1+\upsilon)}[\frac{\partial w}{\partial r}+\beta]-\frac{2k_g\rho h^3}{3}\ddot{\beta}=0. \quad (3.17b)$$

The third equation in w-direction is obtained by substituting (3.7a), (3.7b) and (3.7e) with $k_t=1$ into (3.14c),

$$\frac{Eh}{k_s(1+\upsilon)}[\frac{\partial^2 w}{\partial r^2}+\frac{\partial\beta}{\partial r}+\frac{1}{r}\frac{\partial w}{\partial r}+\frac{\beta}{r}]$$

$$-\frac{2Eh}{1-\upsilon^2}(\frac{\partial}{\partial r}+\frac{1}{r})[\omega_\theta(\frac{\partial}{\partial r}+\frac{\upsilon}{r})u+\omega_\theta\frac{(1+\upsilon)}{R}w+\frac{1}{2}\omega_\theta^3]$$

$$-\frac{2Eh}{1-\upsilon^2}(\frac{1}{R})[(1+\upsilon)\frac{\partial u}{\partial r}+(1+\upsilon)\frac{u}{r}+(1+\upsilon)\frac{2w}{R}+\frac{1}{2}(1+\upsilon)\omega_\theta^2]$$

$$-2\rho h\ddot{w}=0,$$

or,

$$\frac{Eh}{k_s(1+\upsilon)}[\frac{\partial^2 w}{\partial r^2}+\frac{1}{r}\frac{\partial w}{\partial r}+\frac{\partial\beta}{\partial r}+\frac{\beta}{r}]-\frac{2Eh(1+\upsilon)}{R(1-\upsilon^2)}[\frac{\partial u}{\partial r}+\frac{u}{r}+\frac{2w}{R}]-\frac{1}{2}\frac{2Eh(1+\upsilon)}{R(1-\upsilon^2)}\omega_\theta^2$$

$$-\frac{2Eh}{1-\upsilon^2}(\frac{\partial}{\partial r}+\frac{1}{r})[\omega_\theta(\frac{\partial}{\partial r}+\frac{\upsilon}{r})u+\omega_\theta\frac{(1+\upsilon)}{R}w+\frac{1}{2}\omega_\theta^3]-2\rho h\ddot{w}=0. \tag{3.17c}$$

Hence, the *Refined Model* for the *Nonlinear Axisymmetric Displacements Equations of Homogeneous Spherical Shells* is given by,

$$c_1(\frac{\partial^2 u}{\partial r^2}+\frac{1}{r}\frac{\partial u}{\partial r}-\frac{1}{r^2}u)+c_2\frac{\partial w}{\partial r}+\frac{c_1}{2}(\frac{\partial}{\partial r}+\frac{1-\upsilon}{r})\omega_\theta^2-c_3\ddot{u}=0, \tag{3.18a}$$

$$c_4(\frac{\partial^2\beta}{\partial r^2}+\frac{1}{r}\frac{\partial\beta}{\partial r}-\frac{1}{r^2}\beta)-c_5(\frac{\partial w}{\partial r}+\beta)-c_6\ddot{\beta}=0, \tag{3.18b}$$

$$c_5(\frac{\partial^2 w}{\partial r^2}+\frac{1}{r}\frac{\partial w}{\partial r}+\frac{\partial\beta}{\partial r}+\frac{\beta}{r})-c_2(\frac{\partial u}{\partial r}+\frac{u}{r}+\frac{2w}{R})-\frac{c_2}{2}\omega_\theta^2$$

$$-c_1(\frac{\partial}{\partial r}+\frac{1}{r})[\omega_\theta(\frac{\partial}{\partial r}+\frac{\upsilon}{r})u+\omega_\theta\frac{(1+\upsilon)}{R}w+\frac{1}{2}\omega_\theta^3]-c_3\ddot{w}=0, \tag{3.18c}$$

where,

$$c_1=\frac{2Eh}{1-\upsilon^2}, \qquad c_2=\frac{2Eh(1+\upsilon)}{R(1-\upsilon^2)}, \qquad c_3=2\rho h,$$

$$c_4 = \frac{2Eh^3}{3(1-\upsilon^2)}, \qquad c_5 = \frac{Eh}{k_s(1+\upsilon)}, \qquad c_6 = \frac{2k_g \rho h^3}{3}, \tag{3.19}$$

where $k_s$ is a tracer for transverse shear deformation and $k_g$ is a tracer for rotatory inertia.

### 3.4.2 Nonlinear Classical Model

The *Classical Model* for the *Nonlinear Axisymmetric Displacement Equations of Homogeneous Spherical Shell* is formulated by neglecting the effects of both transverse shear deformation and rotatory inertia, i.e. setting $k_s = k_g = 0$.

By setting $k_g = 0$ in equation (3.14b) with $k_t = 0$ we have,

$$Q_{rz} = \frac{\partial M_{rr}}{\partial r} + \frac{M_{rr}}{r} - \frac{M_{\theta\theta}}{r}.$$

Substituting the above equation into (3.14c) with $k_t = 1$ yields,

$$(\frac{\partial}{\partial r} + \frac{1}{r})[\frac{\partial M_{rr}}{\partial r} + \frac{M_{rr}}{r} - \frac{M_{\theta\theta}}{r} - N_{rr}\omega_\theta] - \frac{1}{R}(N_{rr} + N_{\theta\theta}) - 2\rho h\ddot{w} = 0. \tag{3.14d}$$

By setting $k_s = 0$ and $k_t = 0$ for equation (3.7e), in which $\beta$ is neglected,

$$\beta = -\frac{\partial w}{\partial r}. \tag{3.14e}$$

Then Substituting (3.14e) into (3.3d) yields,

$$\omega_\theta = -\frac{\partial w}{\partial r}. \tag{3.14f}$$

Substituting the nonlinear stress resultant-displacements (3.7) into the nonlinear stress equations of motion (3.14a) and (3.14d) gives the following two nonlinear axisymmetric displacement equations of motion:

The first equation in the $u$-direction is obtained by substituting (3.7a), (3.7b) and (3.14f) into (3.14a), which is the same as the refined model,

$$\frac{2Eh}{1-\upsilon^2}[\frac{\partial^2 u}{\partial r^2}+\frac{1}{r}\frac{\partial u}{\partial r}-\frac{1}{r^2}u]+\frac{2Eh(1+\upsilon)}{R(1-\upsilon^2)}\frac{\partial w}{\partial r}+\frac{1}{2}(\frac{2Eh}{1-\upsilon^2})(\frac{\partial}{\partial r}+\frac{1-\upsilon}{r})\omega_\theta^2-2\rho h\ddot{u}=0.$$

The second equation in the $w$-direction is obtained by substituting (3.14f), (3.7a) to (3.7d) into (3.14d) giving,

$$\frac{2Eh^3}{3(1-\upsilon^2)}(\frac{\partial}{\partial r}+\frac{1}{r})\left[\frac{\partial^2\beta}{\partial r^2}+\upsilon\frac{\partial}{\partial r}(\frac{\beta}{r})\right]$$

$$+\frac{2Eh^3}{3(1-\upsilon^2)}(\frac{\partial}{\partial r}+\frac{1}{r})\left[\frac{1}{r}\frac{\partial\beta}{\partial r}+\upsilon\frac{\beta}{r^2}\right]$$

$$-\frac{2Eh^3}{3(1-\upsilon^2)}(\frac{\partial}{\partial r}+\frac{1}{r})\left[\upsilon\frac{1}{r}\frac{\partial\beta}{\partial r}+\frac{\beta}{r^2}\right]$$

$$+\frac{2Eh}{1-\upsilon^2}(\frac{\partial}{\partial r}+\frac{1}{r})[\frac{\partial w}{\partial r}(\frac{\partial}{\partial r}+\frac{\upsilon}{r})u+\frac{(1+\upsilon)}{R}\frac{\partial w}{\partial r}w+\frac{1}{2}(\frac{\partial w}{\partial r})^3]$$

$$-\frac{2Eh}{1-\upsilon^2}(\frac{1}{R})[(1+\upsilon)\frac{\partial u}{\partial r}+(1+\upsilon)\frac{u}{r}+(1+\upsilon)\frac{2w}{R}+\frac{1}{2}(1+\upsilon)(\frac{\partial w}{\partial r})^2]$$

$$-2\rho h\ddot{w}=0.$$

By expanding and collecting the terms with the same coefficients we have,

$$\frac{2Eh^3}{3(1-\upsilon^2)}(\frac{\partial}{\partial r}+\frac{1}{r})[\frac{\partial^2\beta}{\partial r^2}+\frac{\upsilon}{r}\frac{\partial\beta}{\partial r}-\frac{\upsilon}{r^2}\beta+\frac{1}{r}\frac{\partial\beta}{\partial r}+\frac{\upsilon}{r^2}\beta-\frac{\upsilon}{r}\frac{\partial\beta}{\partial r}-\frac{1}{r^2}\beta]$$

$$+\frac{2Eh}{1-\upsilon^2}(\frac{\partial}{\partial r}+\frac{1}{r})[\frac{\partial w}{\partial r}(\frac{\partial}{\partial r}+\frac{\upsilon}{r})u+\frac{(1+\upsilon)}{R}\frac{\partial w}{\partial r}w+\frac{1}{2}(\frac{\partial w}{\partial r})^3]$$

$$-\frac{2Eh(1+\upsilon)}{R(1-\upsilon^2)}[\frac{\partial u}{\partial r}+\frac{u}{r}+\frac{2w}{R}]-\frac{1}{2}\frac{2Eh(1+\upsilon)}{R(1-\upsilon^2)}(\frac{\partial w}{\partial r})^2-2\rho h\ddot{w}=0.$$

After simplifying we have,

$$(\frac{2Eh^3}{3(1-\upsilon^2)})(\frac{\partial}{\partial r}+\frac{1}{r})[\frac{\partial^2\beta}{\partial r^2}+\frac{1}{r}\frac{\partial\beta}{\partial r}-\frac{1}{r^2}\beta]$$

$$+\frac{2Eh}{1-\upsilon^2}(\frac{\partial}{\partial r}+\frac{1}{r})[\frac{\partial w}{\partial r}(\frac{\partial}{\partial r}+\frac{\upsilon}{r})u+\frac{(1+\upsilon)}{R}\frac{\partial w}{\partial r}w+\frac{1}{2}(\frac{\partial w}{\partial r})^3]$$

$$-\frac{2Eh(1+\upsilon)}{R(1-\upsilon^2)}[\frac{\partial u}{\partial r}+\frac{u}{r}+\frac{2w}{R}]-\frac{1}{2}\frac{2Eh(1+\upsilon)}{R(1-\upsilon^2)}(\frac{\partial w}{\partial r})^2-2\rho h\ddot{w}=0.$$

By taking the coefficients $c_2$, $c_3$ and $c_4$ from (3.19) and expanding out $\beta$ leads to,

$$c_4(\frac{\partial^3\beta}{\partial r^3}+\frac{1}{r}\frac{\partial^2\beta}{\partial r^2}-\frac{1}{r^2}\frac{\partial\beta}{\partial r}-\frac{1}{r^2}\frac{\partial\beta}{\partial r}+\frac{2}{r^3}\beta+\frac{1}{r}\frac{\partial^2\beta}{\partial r^2}+\frac{1}{r^2}\frac{\partial\beta}{\partial r}-\frac{1}{r^3}\beta)$$

$$+c_1(\frac{\partial}{\partial r}+\frac{1}{r})[\frac{\partial w}{\partial r}(\frac{\partial}{\partial r}+\frac{\upsilon}{r})u+\frac{(1+\upsilon)}{R}\frac{\partial w}{\partial r}w+\frac{1}{2}(\frac{\partial w}{\partial r})^3]$$

$$-c_2(\frac{\partial u}{\partial r}+\frac{u}{r}+\frac{2w}{R})-\frac{c_2}{2}(\frac{\partial w}{\partial r})^2-c_3\ddot{w}=0,$$

therefore,

$$c_4(\frac{\partial^3\beta}{\partial r^3}+\frac{2}{r}\frac{\partial^2\beta}{\partial r^2}-\frac{1}{r^2}\frac{\partial\beta}{\partial r}+\frac{1}{r^3}\beta)+c_1(\frac{\partial}{\partial r}+\frac{1}{r})[\frac{\partial w}{\partial r}(\frac{\partial}{\partial r}+\frac{\upsilon}{r})u+\frac{(1+\upsilon)}{R}\frac{\partial w}{\partial r}w+\frac{1}{2}(\frac{\partial w}{\partial r})^3]$$

$$-c_2(\frac{\partial u}{\partial r}+\frac{u}{r}+\frac{2w}{R})-\frac{c_2}{2}(\frac{\partial w}{\partial r})^2-c_3\ddot{w}=0.$$

By substituting (3.14e) into the above equation yields,

$$c_4(\frac{\partial^4 w}{\partial r^4}+\frac{2}{r}\frac{\partial^3 w}{\partial r^3}-\frac{1}{r^2}\frac{\partial^2 w}{\partial r^2}+\frac{1}{r^3}\frac{\partial w}{\partial r})+c_2(\frac{\partial u}{\partial r}+\frac{u}{r}+\frac{2w}{R})+\frac{c_2}{2}(\frac{\partial w}{\partial r})^2$$

$$-c_1(\frac{\partial}{\partial r}+\frac{1}{r})[\frac{\partial w}{\partial r}(\frac{\partial}{\partial r}+\frac{\upsilon}{r})u+\frac{(1+\upsilon)}{R}\frac{\partial w}{\partial r}w+\frac{1}{2}(\frac{\partial w}{\partial r})^3]+c_3\ddot{w}=0.$$

Hence, we have the *Classical Model* for the *Nonlinear Axisymmetric Displacement Equations of Homogeneous Spherical Shell*:

$$c_1\left(\frac{\partial^2 u}{\partial r^2}+\frac{1}{r}\frac{\partial u}{\partial r}-\frac{1}{r^2}u\right)+c_2\frac{\partial w}{\partial r}+\frac{c_1}{2}\left(\frac{\partial}{\partial r}+\frac{1-\upsilon}{r}\right)\left(\frac{\partial w}{\partial r}\right)^2-c_3\ddot{u}=0, \tag{3.20a}$$

$$c_4\left(\frac{\partial^4 w}{\partial r^4}+\frac{2}{r}\frac{\partial^3 w}{\partial r^3}-\frac{1}{r^2}\frac{\partial^2 w}{\partial r^2}+\frac{1}{r^3}\frac{\partial w}{\partial r}\right)+c_2\left(\frac{\partial u}{\partial r}+\frac{u}{r}+\frac{2w}{R}\right)+\frac{c_2}{2}\left(\frac{\partial w}{\partial r}\right)^2$$

$$-c_1\left(\frac{\partial}{\partial r}+\frac{1}{r}\right)\left[\frac{\partial w}{\partial r}\left(\frac{\partial}{\partial r}+\frac{\upsilon}{r}\right)u+\frac{(1+\upsilon)}{R}\frac{\partial w}{\partial r}w+\frac{1}{2}\left(\frac{\partial w}{\partial r}\right)^3\right]+c_3\ddot{w}=0, \tag{3.20b}$$

where,

$$c_1=\frac{2\mathrm{E}h}{1-\upsilon^2}, \qquad c_2=\frac{2\mathrm{E}h(1+\upsilon)}{R(1-\upsilon^2)}, \qquad c_3=2\rho h, \qquad c_4=\frac{2\mathrm{E}h^3}{3(1-\upsilon^2)}. \tag{3.21}$$

# CHAPTER 4

# LINEAR AXISYMMETRIC VIBRATIONS OF HOMOGENEOUS AND SANDWICH SPHERICAL SHELLS

## 4.1 Shooting Method

In order to determine the natural frequencies and mode shapes of a homogeneous and sandwich spherical shell, it is assumed that each of the normal modes executes simple harmonic motion with an associated natural frequency $\omega$. The result is that the period and phase of the motion are the same for all points in the shell. Since the free vibrations take place at the natural frequencies of the system and in general, the motion will consist of several simultaneous oscillations at the various natural frequencies of the system.

However, under certain specified conditions, all the coordinates will undergo harmonic motion corresponding to the natural frequencies of the system. When such motion takes place in every part of the system, the motion is called the principal mode of vibration of the normal-mode vibration. Although normal-mode vibrations represent a very restricted type of motion, they are extremely important in that the more general types of motion can be represented by the superposition of normal-mode vibrations.

With these considerations in mind, the time dependence of the shell variables can be removed by assuming that their spatial and temporal variations are separable. Therefore, we will assume that the frequencies for the components are the same:

$$u(r,t) = u(r)e^{i\omega t}, \tag{4.1a}$$

$$\beta(r,t) = \beta(r)e^{i\omega t}, \tag{4.1b}$$

$$w(r,t) = w(r)e^{i\omega t}. \tag{4.1c}$$

Let us take the refined model given by Equations (2.28). If Equations (4.1) are substituted into (2.28), the modes of free vibration ($u$, $\beta$, $w$) must satisfy the system of differential equations:

$$C_1(\frac{d^2u}{dr^2}+\frac{1}{r}\frac{du}{dr}-\frac{1}{r^2}u)+C_2\frac{dw}{dr}+C_3\omega^2u=0, \tag{4.2a}$$

$$C_4(\frac{d^2\beta}{dr^2}+\frac{1}{r}\frac{d\beta}{dr}-\frac{1}{r^2}\beta)-C_5(\frac{dw}{dr}+\beta)+C_6\omega^2\beta=0, \tag{4.2b}$$

$$C_5(\frac{d^2w}{dr^2}+\frac{1}{r}\frac{dw}{dr}+\frac{d\beta}{dr}+\frac{\beta}{r})-C_2(\frac{du}{dr}+\frac{u}{r}+\frac{2w}{R})+C_3\omega^2w=0. \tag{4.2c}$$

Then the governing differential equations become the ordinary differential equations (4.2). We use the *Shooting Method* [13, 14, 15] to find the frequency, $\omega$ using the boundary conditions to be given later. Equations (4.2) can be written as a system of first order differential equations and then integrated numerically using Runge-Kutta algorithm.

In order to demonstrate the various effects of the many parameters included in the above frequency analysis and to permit a more convenient manner by which the natural frequencies can be calculated, it is advantageous to introduce the following dimensionless ratios:

$$r_\rho=\frac{\rho_2}{\rho_1}, \qquad r_h=\frac{2h_2}{h_1}, \qquad r_\mu=\frac{\mu_2}{\mu_1}=\frac{\frac{E_2}{2(1+\upsilon_2)}}{\frac{E_1}{2(1+\upsilon_1)}}=\frac{E_2(1+\upsilon_1)}{E_1(1+\upsilon_2)},$$

$$r_1=\frac{E_2(1-\upsilon_1^2)}{E_1(1-\upsilon_2^2)}, \qquad r_2=\frac{1+\upsilon_2}{1+\upsilon_1}. \tag{4.3}$$

In (4.3), the subscript 1 refers to the core and the subscript 2 refers to either face layer inasmuch as the sandwich construction implies face layers of the same thickness and material. Furthermore, the total thickness of the composite shell is given by

$$2h = 2h_1 + 4h_2. \tag{4.4}$$

For the purpose of the dimensionless frequency, the ratio $\frac{\omega}{\omega_o}$ will be employed [1],

where, $$\omega_o = \frac{1}{2h}\sqrt{\frac{\mu_1}{\rho_1}} = \frac{1}{2h}\sqrt{\frac{\mathrm{E}_1}{2\rho_1(1+\upsilon_1)}}, \tag{4.5a}$$

$\omega_o$ is equal to the first simple-thickness shear frequency of an infinite homogeneous plate divided by $\pi$. The rise $H$ is related to the radius $a$ of the edge and the mean radius $R$ of the sphere by $H = \frac{a^2}{2R}$. For the sandwich case, the $\omega_o$ is defined by

$$\omega_o = \mathrm{P}\sqrt{\frac{k_g k_s(1+3r_\rho r_h)}{12(1+r_h)^2}}, \tag{4.5b}$$

where P represents the lowest simple thickness-shear frequency. Reduction to the homogeneous case, by taking $k_s = \frac{12}{\pi^2}$, $k_g = 1$, and $r_h = 0$ yields,

$$\omega_o = \frac{\mathrm{P}}{\pi}. \tag{4.5c}$$

By taking (2.29) in terms of the dimensionless ratios in (4.3) yields,

$$C_1 = \frac{2\mathrm{E}_1 h_1}{1-\upsilon_1^2}[1+r_h r_1], \qquad C_2 = \frac{2\mathrm{E}_1 h_1(1+\upsilon_1)}{R(1-\upsilon_1^2)}[1+r_h r_1 r_2], \qquad C_3 = 2\rho_1 h_1[1+r_h r_\rho],$$

$$C_4 = \frac{2\mathrm{E}_1 h_1^3}{3(1-\upsilon_1^2)}[1+3r_h r_1], \qquad C_5 = \frac{\mathrm{E}_1 h_1}{k_s(1+\upsilon_1)}, \qquad C_6 = k_g\frac{2\rho_1 h_1^3}{3}[1+3r_h r_\rho]. \tag{4.6}$$

For the sandwich case $k_s = 1$, for the homogeneous case $k_s = \frac{12}{\pi^2}$ while $k_g = 1$, and $\frac{1}{R} = \frac{2H}{a^2}$.

The case now considered is an ordinary sandwich spherical shell with a cellular cellulose acetate core and aluminum face layers of equal thickness for which $r_\rho = 34.4$, $r_\mu = 1683$, $r_1 = 2177$, $r_2 = 1.189$, $\upsilon_1 = 0.09091$, $\upsilon_2 = 0.29709$, $E_1 = 5297$psi, $E_2 = 10.5 \times 10^6$ psi, $\rho_1 = 0.00031$ lb/in$^3$, and $\rho_2 = 0.010664$ lb/in$^3$. The geometrical ratios are chosen as $r_h = \frac{1}{10}$ and $\frac{2h}{a} = \frac{1}{20}$, which are typical values for thin sandwich spherical shells. The total shell thickness $2h$ is taken to be $\frac{3}{10}$ inch. Then $a$ is 6 inches, and $h_1 = \frac{3}{22}$ inch by (4.4) and $r_h = \frac{1}{10}$. Finally, for the refined model, we get $k_s = k_g = 1$. From [1], $\omega_o$ is equal to 9,350 cps because the lowest simple thickness-shear frequency of the associated infinite sandwich plate is 10,600 cps from (4.5b). Values for the rise start with $\frac{H}{2h} = 0$ for the circular plate and terminate with $\frac{H}{2h} = 6$, which is equivalent to a ratio of total thickness to middle surface radius, $\frac{2h}{a} = \frac{1}{20}$. However, Koplik [1] and most of the previous papers only considered the maximum rise equal to 5.

In order to investigate the homogeneous spherical shell, $r_h$ is set to be zero and the dimensionless ratios $r_\rho$, $r_1$ and $r_2$ are automatically eliminated from equations (4.6).

A steel shell is chosen with Poisson's ratio, $\upsilon_1$ taken as 0.3 and $\frac{2h}{a} = \frac{1}{20}$, where $h_1 = h$.

Then, $E_1 = 29 \times 10^6$ psi, $\rho_1 = 0.02696$ lb/in$^3$, and $h_1 = \frac{3}{20}$ by taking $a = 6$ inches. From [1], $\omega_o$ is equal to 67,800 cps because the lowest simple thickness-shear frequency is 213,000 cps from (4.5c).

The foregoing two Sections, (4.2) and (4.3) present the results of the refined model and classical model, respectively. Three boundary conditions will be applied to each model for both sandwich and homogeneous cases: (1) clamped on the outside and free on the inside, (2) simply supported on the outside and free on the outside, (3) free on the outside and free on the inside. The dimensionless radius, i.e. $\frac{r}{a}$ at the outer edge boundary is equal to 1, where $a(=6\,\text{inches})$ is the outer radius. Four different dimensionless sizes of holes, $\varepsilon = \frac{b}{a} = 0,\ 0.1,\ 0.2,\ 0.3$ are applied to the inner edge boundary, where b is the radius of the hole at the center. Using the shooting method, we obtain almost the same values of the natural frequency $\omega$ as found in [1]. The transverse deflection $w$ normalized to be the magnitude of 1 at the hole is plotted in figures later.

## 4.2 Refined Model

Three boundary cases of the refined model for both sandwich and homogeneous spherical shells are presented in this section. A free boundary condition is applied at the inner edge with three different boundaries at the outer edge: clamped edge, simply supported edge and free edge. It should be noted that displacement in the $u$ direction at free boundary

edge is set equal to zero. The free inner boundary becomes zero by plugging it with a rigid central ring.

The displacement boundary conditions are now obtained by substituting (2.15), (2.17) and (2.18) into (2.26):

For the clamped outer boundary, $r = 1$:

$$u(1)=0, \qquad \beta(1)=0, \qquad w(1)=0, \tag{4.7a}$$

For the simply supported outer boundary, $r = 1$:

$$u(1)=0, \qquad (1+3r_h r_1)\frac{d\beta(r)}{dr}\Big|_{r=1} + (\upsilon_1 + 3\upsilon_2 r_h r_1)\frac{\beta(r)}{r}\Big|_{r=1} = 0,$$

$$w(1)=0. \tag{4.7b}$$

For the free outer boundary, $r = 1$:

$$u(1)=0, \qquad (1+3r_h r_1)\frac{d\beta(r)}{dr}\Big|_{r=1} + (\upsilon_1 + 3\upsilon_2 r_h r_1)\frac{\beta(r)}{r}\Big|_{r=1} = 0,$$

$$\frac{dw(r)}{dr}\Big|_{r=1} + \beta(r)\Big|_{r=1} = 0. \tag{4.7c}$$

For the free inner boundary, $r = \frac{b}{a} = \varepsilon$:

$$u(\varepsilon)=0, \qquad (1+3r_h r_1)\frac{d\beta(r)}{dr}\Big|_{r=\varepsilon} + (\upsilon_1 + 3\upsilon_2 r_h r_1)\frac{\beta(r)}{r}\Big|_{r=\varepsilon} = 0,$$

$$\frac{dw(r)}{dr}\Big|_{r=\varepsilon} + \beta(r)\Big|_{r=\varepsilon} = 0. \tag{4.7d}$$

In the following three sub-sections, (4.2.1), (4.2.2) and (4.2.3) we will present the results for the clamped outer boundary, simply supported outer boundary and free outer boundary, respectively. Each sub-section consists of both sandwich and homogeneous cases. For each sandwich or homogeneous case we have four tables (a, b, c, d) and two

plots (Figures a and b). Table (a) shows the dimensionless frequency $\frac{\omega}{\omega_o}$ as a function of curvature or the rise $\frac{H}{2h}$ from 0 to 6 and the dimensionless size of the hole, $\varepsilon = \frac{b}{a}$ from 0 to 0.3, where $\omega_o = 9{,}350$ cps for the sandwich case and 67800 cps for the homogeneous case. Table (b) is Table (a) multiplied by $\omega_o$. Table (c) illustrates the dependence of $\frac{\omega}{\omega_o}$ with different sizes of holes for a shell having the maximum allowable rise, $\frac{H}{2h} = 6$, compared with those of a circular plate with zero rise, $\frac{H}{2h} = 0$. Table (d) shows how $\frac{\omega}{\omega_o}$ varies curvature for a shell with no center hole, i.e. $\varepsilon = 0$, compared with a shell with a hole, $\varepsilon = 0.3$.

Figure (a) and Figure (b) plot the mode shapes with the normalized transverse displacement $w$ as the ordinate and dimensionless radial coordinate $\frac{r}{a}$ as the abscissa.

### 4.2.1 Clamped and Free Case

In order to get the natural frequencies and the normal mode shapes of free vibration of refined model, Equations (4.2) are first written into a system by using the fourth-order Runge-Kutta algorithm. By the displacement boundary conditions found in (4.7a), the six shooting boundary values at the outer edge are set:

$u(1) = 0$, $u'(1) = \alpha$, $\beta(1) = 0$, $\beta'(1) = \gamma$, $w(1) = 0$ and $w'(1) = 0$,

and using an initial guess for $\omega$,

where the prime indicates differentiation with respect to $r$. Hence, $\alpha$, $\gamma$ & $\omega$ are the unknowns. The shooting method is used to find $\alpha$, $\gamma$ & $\omega$ so that the system (4.2) satisfies the boundary conditions.

The numerical results for the sandwich case (both tracers, $k_s$ and $k_g$ equal to unity) are given in Table 4.1.a and Table 4.1.b, showing that the frequency increases with increase of the rise $\frac{H}{2h}$ and the size of hole $\varepsilon$. Comparing our results for $\frac{b}{a}=0$ with that by Koplik [1] we find that Koplik gave $\frac{\omega}{\omega_o}$ from 0.05172 for zero rise to 0.26960 for a maximum rise equal to 5, which leads to less than 0.2 percent of error.

**Table 4.1.a** Refined Model of Dimensionless Frequencies of Clamped-Free Sandwich Case

$\omega/\omega_o$

| H/2h | b/a=0 | b/a=0.1 | b/a=0.2 | b/a=0.3 |
|---|---|---|---|---|
| 0 | 0.05182 | 0.05336 | 0.05741 | 0.06360 |
| 1 | 0.08910 | 0.09037 | 0.09354 | 0.09818 |
| 2 | 0.14177 | 0.14404 | 0.14927 | 0.15599 |
| 3 | 0.18414 | 0.18680 | 0.19332 | 0.20305 |
| 4 | 0.22611 | 0.22859 | 0.23466 | 0.24412 |
| 5 | 0.26926 | 0.27157 | 0.27709 | 0.28577 |
| 6 | 0.31300 | 0.31524 | 0.32042 | 0.32848 |

**Table 4.1.b** Refined Model of Fundamental Frequencies of Clamped-Free Sandwich Case

$\omega$

| H/2h | b/a=0 | b/a=0.1 | b/a=0.2 | b/a=0.3 |
|---|---|---|---|---|
| 0 | 484.5 | 498.9 | 534.8 | 594.7 |
| 1 | 833.1 | 845.0 | 874.6 | 918.0 |
| 2 | 1325.5 | 1346.8 | 1395.7 | 1458.5 |
| 3 | 1721.7 | 1746.6 | 1807.6 | 1898.5 |
| 4 | 2114.1 | 2137.4 | 2194.0 | 2282.6 |
| 5 | 2517.6 | 2539.2 | 2590.8 | 2671.9 |
| 6 | 2926.6 | 2947.5 | 2995.9 | 3071.4 |

**Table 4.1.c** Increase of Dimensionless Frequency with Rise According to the Refined Model of Clamped-Free Sandwich Case

| $b/a$ | $\omega/\omega_o$ for H/2h = 0 | $\omega/\omega_o$ for H/2h = 6 | $\Delta\omega/\omega_o$ | % Increase of $\omega/\omega_o$ |
|---|---|---|---|---|
| 0 | 0.05182 | 0.31300 | 0.26118 | 504 % |
| 0.1 | 0.05336 | 0.31524 | 0.26188 | 490 % |
| 0.2 | 0.05741 | 0.32042 | 0.26301 | 458 % |
| 0.3 | 0.06360 | 0.32848 | 0.26488 | 416 % |

**Table 4.1.d** Increase of Dimensionless Frequency with Size of Hole According to the Refined Model of Clamped-Free Sandwich Case

| H/2h | $\omega/\omega_0$ for b/a=0 | $\omega/\omega_0$ for b/a =0.3 | $\Delta\omega/\omega_0$ | % Increase of $\omega/\omega_0$ |
|---|---|---|---|---|
| 0 | 0.05182 | 0.06360 | 0.01178 | 22.7% |
| 1 | 0.08910 | 0.09818 | 0.00908 | 10.2% |
| 2 | 0.14177 | 0.15599 | 0.01422 | 10.0% |
| 3 | 0.18414 | 0.20305 | 0.01891 | 10.3% |
| 4 | 0.22611 | 0.24412 | 0.01801 | 8.0% |
| 5 | 0.26926 | 0.28577 | 0.01651 | 6.1% |
| 6 | 0.31300 | 0.32848 | 0.01548 | 4.9% |

We note that in Table 4.1.c, the frequencies $\frac{\omega}{\omega_o}$ increase between 416 percent and 504 percent from the zero rise to the maximum allowable rise in the four different sizes of holes. However, Table 4.1.d demonstrates that the frequencies increase between 4.9 percent and 22.7 percent from $\frac{b}{a} = 0$ to the maximum dimensionless hole, $\frac{b}{a} = 0.3$ in the seven different rises. The mode shapes are plotted in Figure 4.1.a and Figure 4.1.b. The former shows the graph with $\frac{b}{a} = 0$ with different rises while the latter is the case of the dimensionless hole, $\frac{b}{a} = 0.3$.

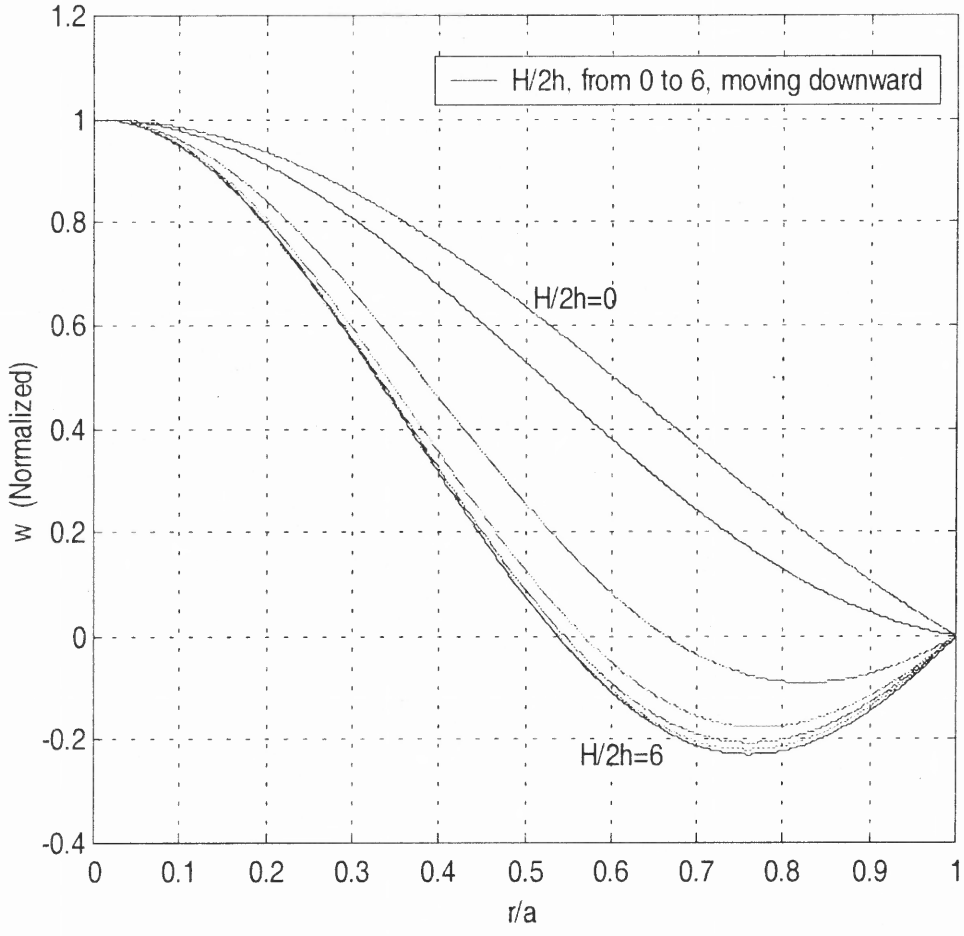


**Figure 4.1.a** Mode Shapes of Sandwich Refined Model with b/a=0 for Clamped Outside and Free Inside Case

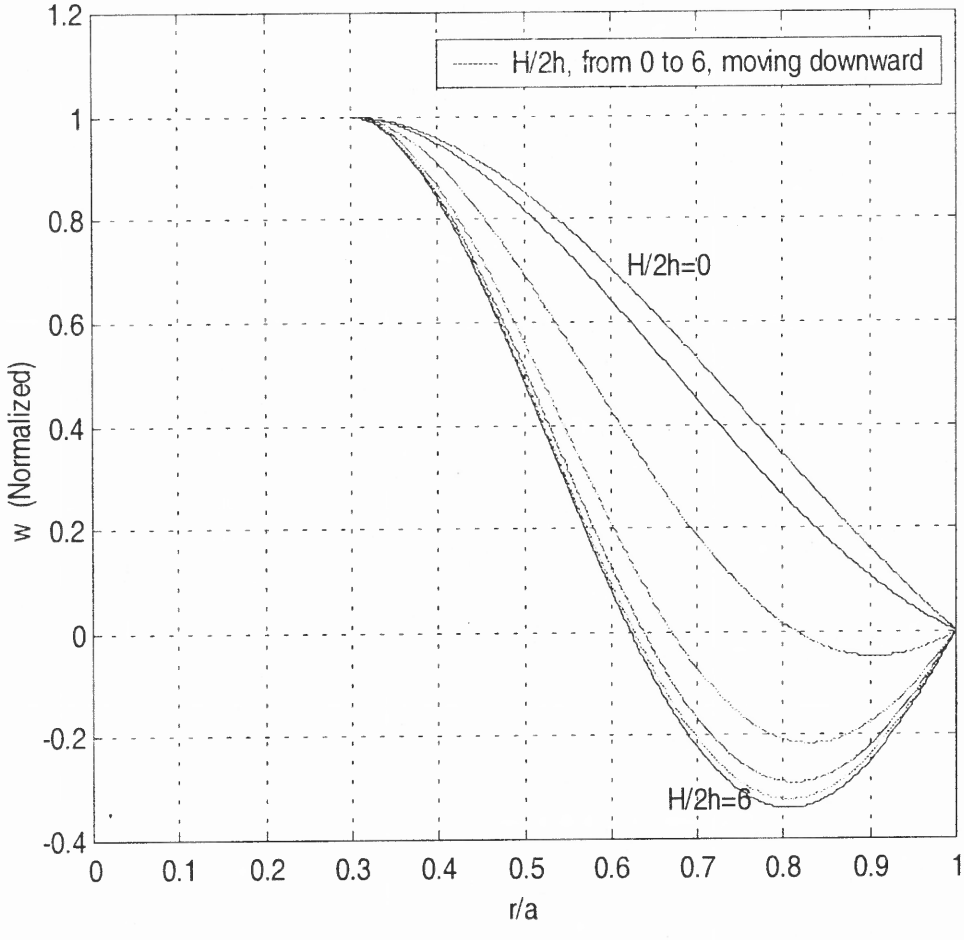


**Figure 4.1.b** Mode shapes of Sandwich Refined Model with b/a=0.3 for Clamped Outside and Free Inside Case

To calculate frequencies of a homogeneous shell based on the refined theory we further put $r_h = 0$, $k_s = \frac{12}{\pi^2}$ and $k_g = 1$ in Equation (4.6). Similar to the sandwich case, Table 4.2.a and Table 4.2.b show that the frequency of the homogeneous shell increases with the bigger hole and the curvature. Comparing the present results with the no hole case with the data by Koplik [1], it was found that $\frac{\omega}{\omega_o}$ is equal to 0.01237 for zero rise which yields a result 0.4 percent higher, while $\frac{\omega}{\omega_o}$ is equal to 0.05257 for rise of 5 which only leads to 0.04 percent of error.

**Table 4.2.a** Refined Model of Dimensionless Frequencies of Clamped-Free Homogeneous Case

$\omega / \omega_o$

| H/2h | b/a=0 | B/a=0.1 | b/a=0.2 | b/a=0.3 |
|---|---|---|---|---|
| 0 | 0.01242 | 0.01705 | 0.02109 | 0.02678 |
| 1 | 0.01681 | 0.02072 | 0.02426 | 0.02941 |
| 2 | 0.02564 | 0.02899 | 0.03188 | 0.03614 |
| 3 | 0.03526 | 0.03881 | 0.04147 | 0.04512 |
| 4 | 0.04441 | 0.04887 | 0.05175 | 0.05517 |
| 5 | 0.05259 | 0.05842 | 0.06206 | 0.06567 |
| 6 | 0.05988 | 0.06690 | 0.07190 | 0.07623 |

**Table 4.2.b** Refined Model of Fundamental Frequencies of Clamped-Free Homogeneous Case

$\omega$

| H/2h | b/a=0 | b/a=0.1 | b/a=0.2 | b/a=0.3 |
|---|---|---|---|---|
| 0 | 842.1 | 1156.0 | 1429.9 | 1815.7 |
| 1 | 1139.7 | 1404.8 | 1644.8 | 1994.0 |
| 2 | 1738.4 | 1965.5 | 2161.5 | 2450.3 |
| 3 | 2390.6 | 2631.3 | 2811.7 | 3059.1 |
| 4 | 3011.0 | 3313.4 | 3508.7 | 3740.5 |
| 5 | 3565.6 | 3960.9 | 4207.7 | 4452.4 |
| 6 | 4059.9 | 4535.8 | 4874.8 | 5168.4 |

**Table 4.2.c** Increase of Dimensionless Frequency with Rise According to the Refined Model of a Clamped-Free Homogeneous Case

| $b/a$ | $\omega/\omega_o$ for H/2h = 0 | $\omega/\omega_o$ for H/2h = 6 | $\Delta\omega/\omega_o$ | % Increase of $\omega/\omega_o$ |
|---|---|---|---|---|
| 0 | 0.01242 | 0.05988 | 0.04746 | 382% |
| 0.1 | 0.01705 | 0.06690 | 0.04985 | 292% |
| 0.2 | 0.02109 | 0.07190 | 0.05081 | 241% |
| 0.3 | 0.02678 | 0.07623 | 0.04945 | 185% |

**Table 4.2.d** Increase of Dimensionless Frequency with Size of Hole According to the Refined Model of a Clamped-Free Homogeneous Case

| H/2h | $\omega/\omega_0$ for b/a=0 | $\omega/\omega_0$ for b/a =0.3 | $\Delta\omega/\omega_0$ | % Increase of $\omega/\omega_0$ |
|---|---|---|---|---|
| 0 | 0.01242 | 0.02678 | 0.01436 | 115.6% |
| 1 | 0.01681 | 0.02941 | 0.01260 | 75.0% |
| 2 | 0.02564 | 0.03614 | 0.01050 | 41.0% |
| 3 | 0.03526 | 0.04512 | 0.00986 | 28.0% |
| 4 | 0.04441 | 0.05517 | 0.01076 | 24.2% |
| 5 | 0.05259 | 0.06567 | 0.01308 | 24.9% |
| 6 | 0.05988 | 0.07623 | 0.01635 | 27.3% |

Table 4.2.c illustrates that the frequencies increase between 185 percent to 382 percent from zero rise to the maximum allowable rise in the four different size of hole cases. Table 4.2.d shows that the frequencies increase between 24.2 percent to 115.6 percent from $\frac{b}{a} = 0$ to the maximum dimensionless hole, $\frac{b}{a} = 0.3$ in the seven different rise cases. Figure 4.2.a and Figure 4.2.b plot the mode shapes for zero rise and a rise of six with different sizes of holes, respectively.

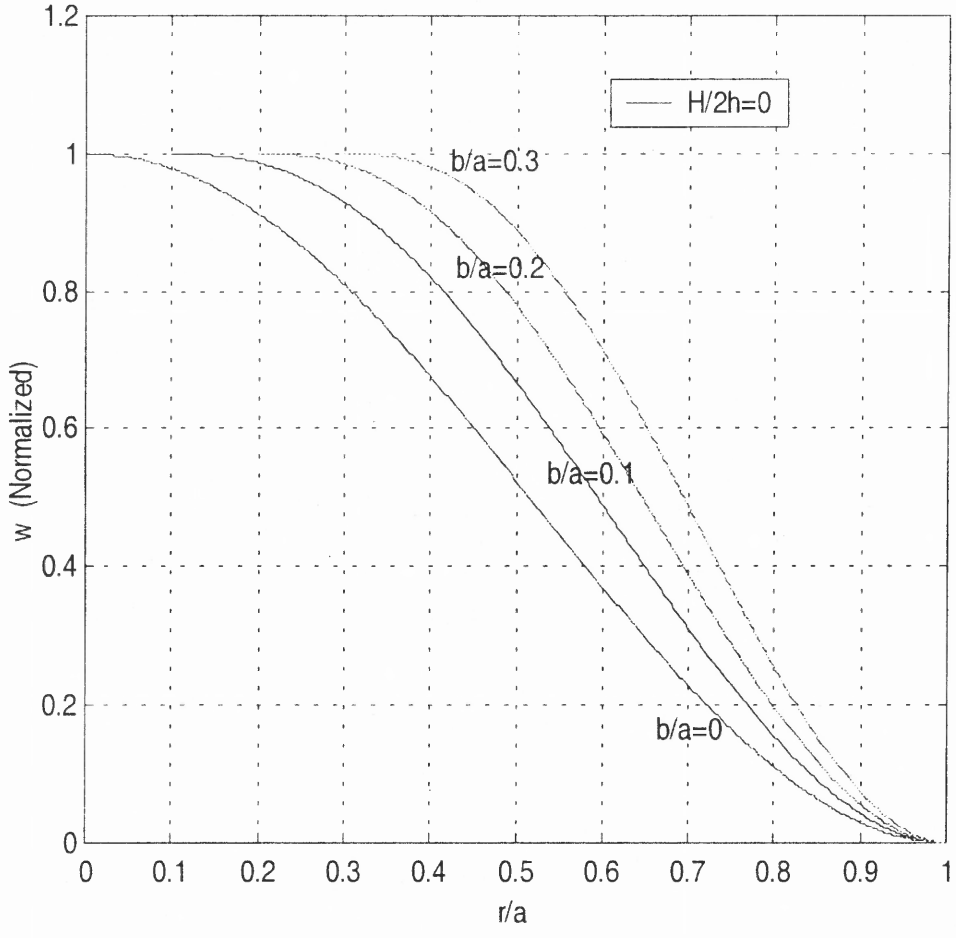


**Figure 4.2.a** Mode Shapes of Homogeneous Refined Model for H/2h=0 with Different Sizes of Holes for Clamped Outside and Free Inside Case

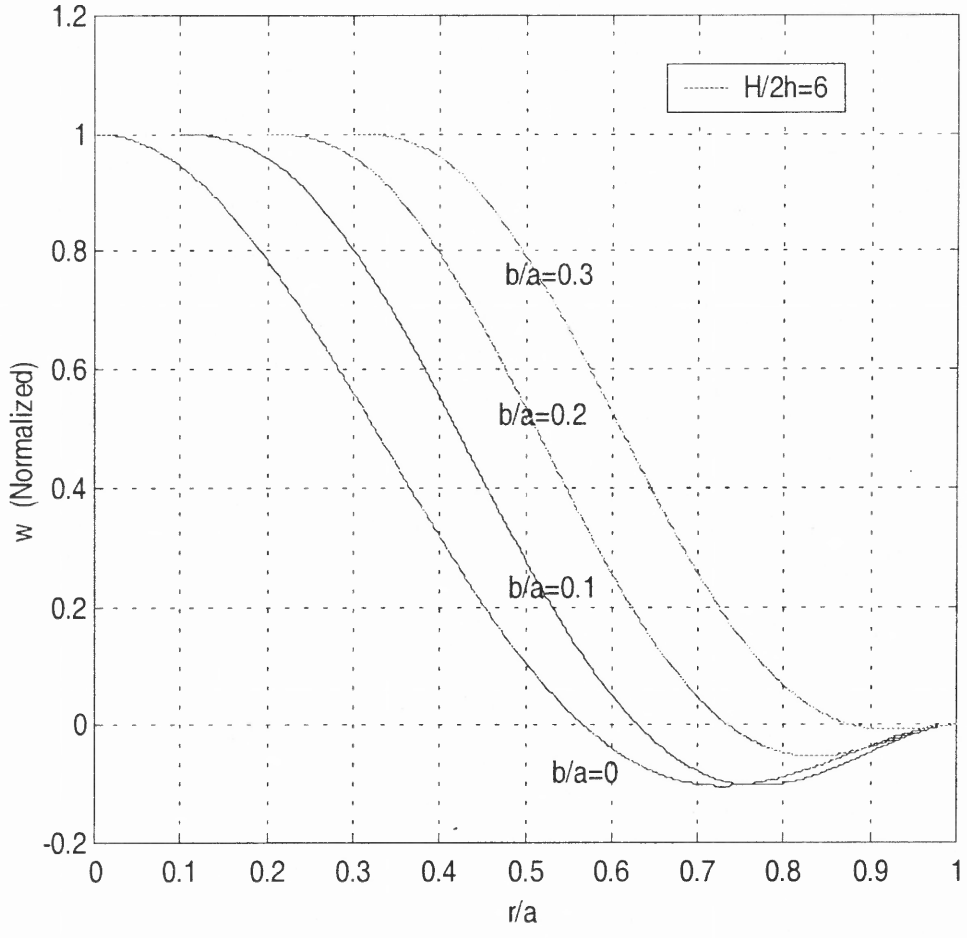


**Figure 4.2.b** Mode Shapes of Homogeneous Refined Model for H/2h=6 with Different Sizes of Holes for Clamped Outside and Free Inside Case

### 4.2.2 Simply Supported and Free Case

Similar to the clamped on outside and free on inside case, Equations (4.2) are first written into a system by using the fourth-order Runge-Kutta algorithm. From the displacement boundary conditions found in (4.7b), the six shooting boundary values, $u(1)$, $u'(1)$, $\beta(1)$, $\beta'(1)$, $w(1)$ and $w'(1)$ at the outer edge are set:

$$u(1)=0,\ u'(1)=\alpha,\ \beta(1)=\gamma,\ \beta'(1)=\frac{-(\upsilon_1+3\upsilon_2 r_h r_1)}{(1+3r_h r_1)}\gamma,\ w(1)=0 \text{ and } w'(1)=\lambda,$$

where $\alpha$, $\gamma$ & $\omega$ are the unknowns, and $\lambda$ is found to be independent of $\omega$ and is set equal to one in the analysis. Then the three unknowns, $\alpha$, $\gamma$ & $\omega$ are determined by employing the *Shooting Method* stated in the previous section.

Table 4.3.a and Table 4.3.b present the frequency of the sandwich case in which the frequency increases with increase in rise and the size of hole.

**Table 4.3.a** Refined Model of Dimensionless Frequencies of Simply Supported-Free Sandwich Case

$\omega / \omega_o$

| H/2h | b/a=0 | b/a=0.1 | b/a=0.2 | b/a=0.3 |
|---|---|---|---|---|
| 0 | 0.04083 | 0.04221 | 0.04591 | 0.05166 |
| 1 | 0.08443 | 0.08537 | 0.08777 | 0.09144 |
| 2 | 0.14123 | 0.14328 | 0.14784 | 0.15342 |
| 3 | 0.18413 | 0.18679 | 0.19322 | 0.20261 |
| 4 | 0.22609 | 0.22859 | 0.23467 | 0.24408 |
| 5 | 0.26923 | 0.27156 | 0.27711 | 0.28579 |
| 6 | 0.31297 | 0.31522 | 0.32043 | 0.32852 |

**Table 4.3.b** Refined Model of Fundamental Frequencies of Simply Supported-Free Sandwich Case

$\omega$

| H/2h | b/a=0 | b/a=0.1 | b/a=0.2 | b/a=0.3 |
|---|---|---|---|---|
| 0 | 381.7 | 394.7 | 429.3 | 483.0 |
| 1 | 789.4 | 798.2 | 820.7 | 854.9 |
| 2 | 1320.5 | 1339.7 | 1382.3 | 1434.5 |
| 3 | 1721.7 | 1746.5 | 1806.6 | 1894.4 |
| 4 | 2114.0 | 2137.3 | 2194.2 | 2282.1 |
| 5 | 2517.3 | 2539.1 | 2591.0 | 2672.2 |
| 6 | 2926.2 | 2947.3 | 2996.1 | 3071.6 |

As shown in Table 4.3.c, there is a noticeable increase of the frequency from 536 percent to 667 percent from zero rise to the maximum allowable rise in the four different size of hole cases. Table 4.3.d demonstrates that the frequencies increase from 5.0 percent to 26.5 percent from $\frac{b}{a} = 0$ to the maximum dimensionless hole, $\frac{b}{a} = 0.3$ in the seven different rise cases. The mode shapes are plotted in Figure 4.3.a and Figure 4.3.b. The former plots the case of $\frac{H}{2h} = 0$ with different hole sizes, while the latter shows the rise of six.

**Table 4.3.c** Increase of Dimensionless Frequency with Rise According to the Refined Model of a Simply Supported-Free Sandwich Case

| $b/a$ | $\omega/\omega_o$ for H/2h = 0 | $\omega/\omega_o$ for H/2h = 6 | $\Delta\omega/\omega_o$ | % Increase of $\omega/\omega_o$ |
|---|---|---|---|---|
| 0 | 0.04083 | 0.31297 | 0.27214 | 667 % |
| 0.1 | 0.04221 | 0.31522 | 0.27301 | 647 % |
| 0.2 | 0.04591 | 0.32043 | 0.27452 | 598 % |
| 0.3 | 0.05166 | 0.32852 | 0.27686 | 536 % |

**Table 4.3.d** Increase of Dimensionless Frequency with Size of Hole According to the Refined Model of a Simply Supported-Free Sandwich Case

| H/2h | $\omega/\omega_0$ for b/a=0 | $\omega/\omega_0$ for b/a =0.3 | $\Delta\omega/\omega_0$ | % Increase of $\omega/\omega_0$ |
|---|---|---|---|---|
| 0 | 0.04083 | 0.05166 | 0.01083 | 26.5% |
| 1 | 0.08443 | 0.09144 | 0.00701 | 8.3% |
| 2 | 0.14123 | 0.15342 | 0.01219 | 8.6% |
| 3 | 0.18413 | 0.20261 | 0.01848 | 10.0% |
| 4 | 0.22609 | 0.24408 | 0.01799 | 8.0% |
| 5 | 0.26923 | 0.28579 | 0.01656 | 6.2% |
| 6 | 0.31297 | 0.32852 | 0.01555 | 5.0% |

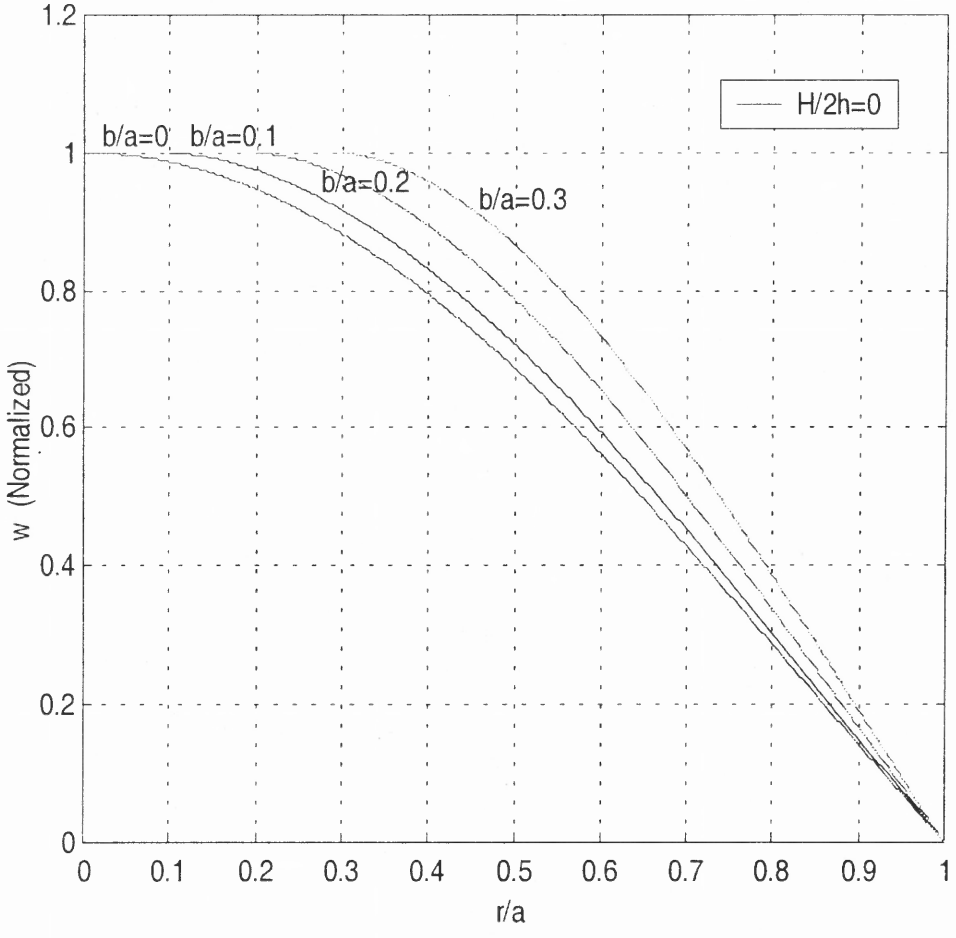


**Figure 4.3.a** Mode Shapes of Sandwich Refined Model for H/2h=0 with Different Sizes of Holes for Simply Supported Outside and Free Inside Case

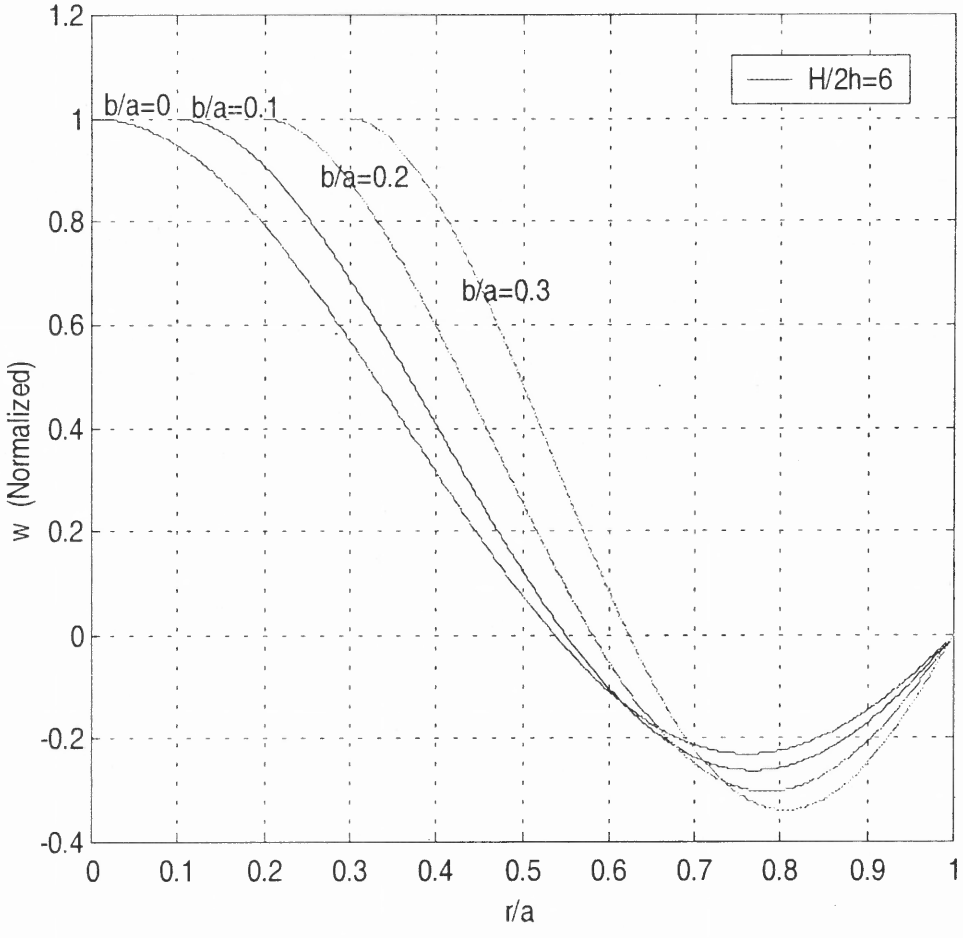


**Figure 4.3.b** Mode Shapes of Sandwich Refined Model for H/2h=6 with Different Sizes of Holes for Simply Supported Outside and Free Inside Case

Table 4.4.a and Table 4.4.b show that the frequency of the homogeneous shell increases with the size of hole and the curvature.

**Table 4.4.a** Refined Model of Dimensionless Frequencies of Simply Supported-Free Homogeneous Case

$\omega / \omega_o$

| H/2h | b/a=0 | b/a=0.1 | b/a=0.2 | b/a=0.3 |
|---|---|---|---|---|
| 0 | 0.00603 | 0.00908 | 0.01145 | 0.01473 |
| 1 | 0.01362 | 0.01551 | 0.01712 | 0.01953 |
| 2 | 0.02481 | 0.02662 | 0.02786 | 0.02957 |
| 3 | 0.03526 | 0.03822 | 0.03962 | 0.04113 |
| 4 | 0.04357 | 0.04898 | 0.05144 | 0.05315 |
| 5 | 0.05042 | 0.05732 | 0.06241 | 0.06522 |
| 6 | 0.05692 | 0.06378 | 0.07088 | 0.07689 |

**Table 4.4.b** Refined Model of Fundamental Frequencies of Simply Supported-Free Homogeneous Case

$\omega$

| H/2h | b/a=0 | b/a=0.1 | b/a=0.2 | b/a=0.3 |
|---|---|---|---|---|
| 0 | 408.8 | 615.6 | 776.3 | 998.7 |
| 1 | 923.4 | 1051.6 | 1160.7 | 1324.1 |
| 2 | 1682.1 | 1804.8 | 1888.9 | 2004.8 |
| 3 | 2390.6 | 2591.3 | 2686.2 | 2788.6 |
| 4 | 2954.0 | 3320.8 | 3487.6 | 3603.6 |
| 5 | 3418.5 | 3886.3 | 4231.4 | 4421.9 |
| 6 | 3859.2 | 4324.3 | 4805.7 | 5213.1 |

The frequencies shown in Table 4.4.c increase between 422 percent and 844 percent from the zero rise to the maximum allowable rise in the four different size of hole cases. Table 4.4.d shows that the frequencies increase between 16.6 percent to 144.3 percent from $\frac{b}{a} = 0$ to the maximum dimensionless hole, $\frac{b}{a} = 0.3$ in the seven different rise cases. Figure 4.4.a and Figure 4.4.b plot the mode shapes for no hole case and the dimensionless hole size of 0.2 with different rises, respectively.

**Table 4.4.c** Increase of Dimensionless Frequency with Rise According to the Refined Model of a Simply Supported-Free Homogeneous Case

| $b/a$ | $\omega/\omega_o$ for H/2h = 0 | $\omega/\omega_o$ for H/2h = 6 | $\Delta\omega/\omega_o$ | % Increase of $\omega/\omega_o$ |
|---|---|---|---|---|
| 0 | 0.00603 | 0.05692 | 0.05089 | 844 % |
| 0.1 | 0.00908 | 0.06378 | 0.05470 | 602 % |
| 0.2 | 0.01145 | 0.07088 | 0.05943 | 519 % |
| 0.3 | 0.01473 | 0.07689 | 0.06216 | 422 % |

**Table 4.4.d** Increase of Dimensionless Frequency with Size of Hole According to the Refined Model of a Simply Supported-Free Homogeneous Case

| H/2h | $\omega/\omega_0$ for b/a=0 | $\omega/\omega_0$ for b/a =0.3 | $\Delta\omega/\omega_0$ | % Increase of $\omega/\omega_0$ |
|---|---|---|---|---|
| 0 | 0.00603 | 0.01473 | 0.00870 | 144.3% |
| 1 | 0.01362 | 0.01953 | 0.00591 | 43.4% |
| 2 | 0.02481 | 0.02957 | 0.00476 | 19.2% |
| 3 | 0.03526 | 0.04113 | 0.00587 | 16.6% |
| 4 | 0.04357 | 0.05315 | 0.00958 | 22.0% |
| 5 | 0.05042 | 0.06522 | 0.01480 | 29.4% |
| 6 | 0.05692 | 0.07689 | 0.01997 | 35.1% |

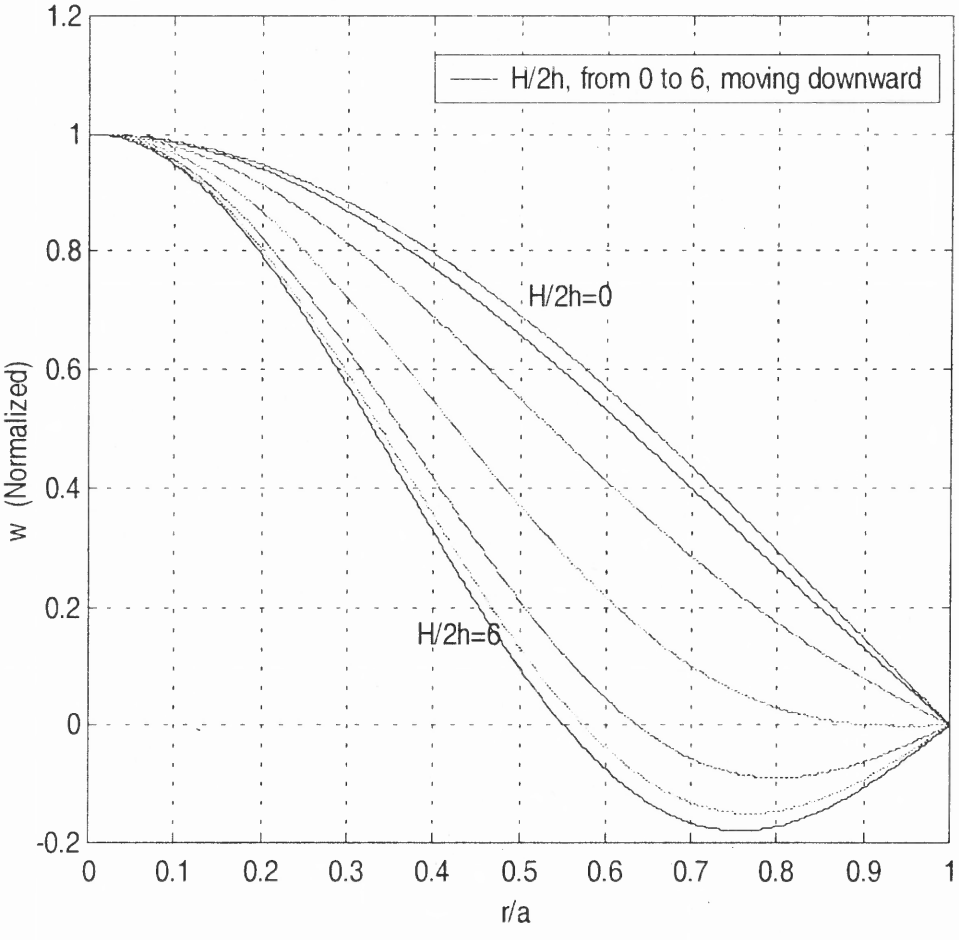


**Figure 4.4.a** Mode Shapes of Homogeneous Refined Model with b/a=0 for Simply Supported Outside and Free Inside Case

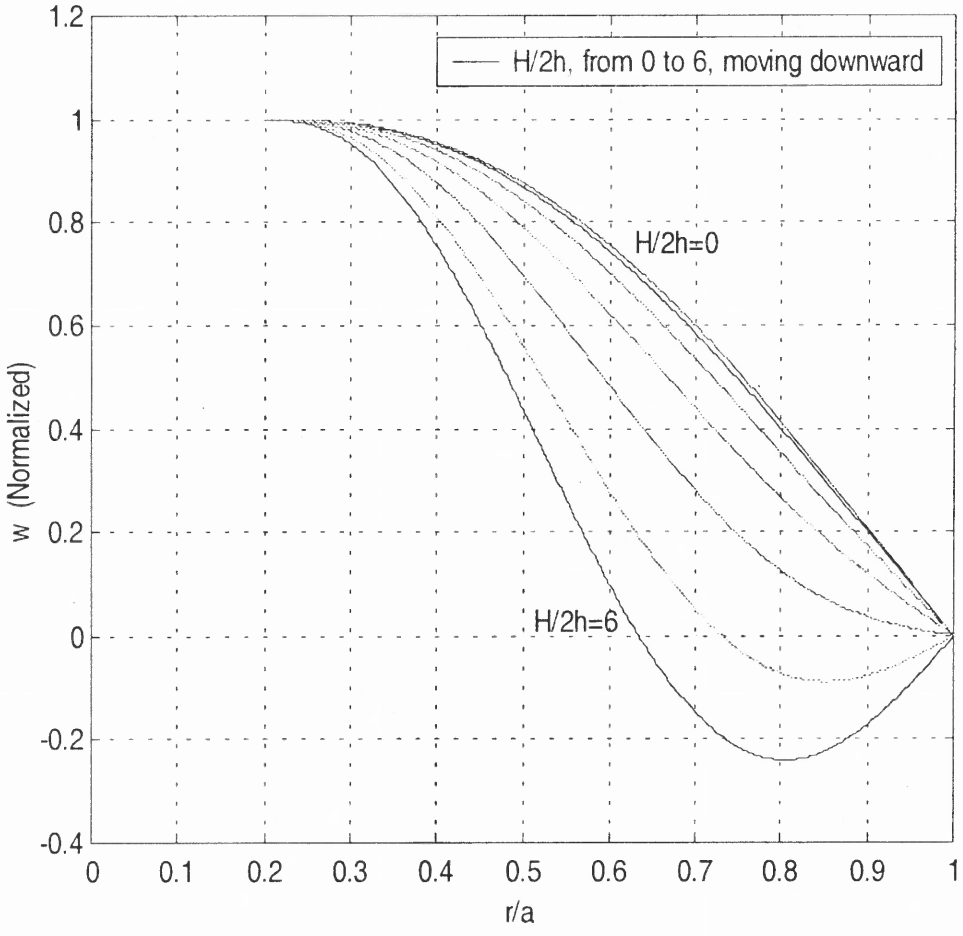


**Figure 4.4.b** Mode Shapes of Homogeneous Refined Model with b/a=0.2 for Simply Supported Outside and Free Inside Case

### 4.2.3 Free and Free Case

To employ the fourth-order Runge-Kutta algorithm for Equations (4.2) written into a system, the six shooting boundary values, $u(1)$, $u'(1)$, $\beta(1)$, $\beta'(1)$, $w(1)$ and $w'(1)$ at the outer edge from (4.7c) are:

$$u(1)=0,\quad u'(1)=\lambda,\quad \beta(1)=\gamma,\quad \beta'(1)=\frac{-(\upsilon_1+3\upsilon_2 r_h r_1)}{(1+3r_h r_1)}\gamma,\quad w(1)=\alpha \quad \text{and} \quad w'(1)=-\gamma,$$

where $\alpha$, $\gamma$ & $\omega$ are the unknowns, and $\lambda$ is found to be independent of $\omega$ in the analysis and taken as one in value.

By using the procedures of the Shooting *Method*, the numerical results for the sandwich case are obtained in Table 4.5.a and Table 4.5.b. Similar to the previous two boundary cases, the frequency increases with the size of hole and the rise.

**Table 4.5.a** Refined Model of Dimensionless Frequencies of Free-Free Sandwich Case $\omega/\omega_o$

| H/2h | b/a=0 | b/a=0.1 | b/a=0.2 | b/a=0.3 |
|---|---|---|---|---|
| 0 | 0.08126 | 0.08400 | 0.09124 | 0.12460 |
| 1 | 0.09512 | 0.09751 | 0.10384 | 0.11382 |
| 2 | 0.12797 | 0.12979 | 0.13465 | 0.14251 |
| 3 | 0.16875 | 0.17021 | 0.17402 | 0.18026 |
| 4 | 0.21257 | 0.21384 | 0.21705 | 0.22225 |
| 5 | 0.25744 | 0.25865 | 0.26157 | 0.26620 |
| 6 | 0.30242 | 0.30366 | 0.30654 | 0.31096 |

**Table 4.5.b** Refined Model of Fundamental Frequencies of Free-Free Sandwich Case

$\omega$

| H/2h | b/a=0 | b/a=0.1 | b/a=0.2 | b/a=0.3 |
|---|---|---|---|---|
| 0 | 759.8 | 785.4 | 853.1 | 958.0 |
| 1 | 889.4 | 911.7 | 970.9 | 1064.3 |
| 2 | 1196.5 | 1213.6 | 1258.9 | 1332.5 |
| 3 | 1577.9 | 1591.5 | 1627.1 | 1685.4 |
| 4 | 1987.6 | 1999.4 | 2029.4 | 2078.0 |
| 5 | 2407.1 | 2418.4 | 2445.6 | 2488.9 |
| 6 | 2827.6 | 2839.3 | 2866.1 | 2907.5 |

It can be seen from Table 4.5.c, that the frequencies increase between 150 percent to 272 percent from the zero rise to the maximum allowable rise in the four different size of hole cases. Table 4.5.d shows that the frequencies increase between 2.8 percent to 53.3 percent from $\frac{b}{a}=0$ to $\frac{b}{a}=0.3$ in the seven different rise cases. The mode shapes are plotted in Figure 4.5.a and Figure 4.5.b for the case with $\frac{b}{a}=0$ and the case with $\frac{b}{a}=0.3$, with different rises respectively. It should be noted that since both boundaries are set to be free, the normalized transverse deflection, $w$ at the outer edge boundary is not zero while the $w$-displacement at the inner boundary is normalized to be one.

**Table 4.5.c** Increase of Dimensionless Frequency with Rise According to the Refined Model of a Free-Free Sandwich Case

| $b/a$ | $\omega/\omega_o$ for H/2h = 0 | $\omega/\omega_o$ for H/2h = 6 | $\Delta\omega/\omega_o$ | % Increase of $\omega/\omega_o$ |
|---|---|---|---|---|
| 0 | 0.08126 | 0.30242 | 0.22116 | 272 % |
| 0.1 | 0.08400 | 0.30366 | 0.21966 | 262 % |
| 0.2 | 0.09124 | 0.30654 | 0.21530 | 236 % |
| 0.3 | 0.12460 | 0.31096 | 0.18636 | 150 % |

**Table 4.5.d** Increase of Dimensionless Frequency with Size of Hole According to the Refined Model of a Free-Free Sandwich Case

| H/2h | $\omega / \omega_0$ for b/a=0 | $\omega / \omega_0$ for b/a =0.3 | $\Delta\omega / \omega_0$ | % Increase of $\omega / \omega_0$ |
|---|---|---|---|---|
| 0 | 0.08126 | 0.12460 | 0.04334 | 53.3% |
| 1 | 0.09512 | 0.11382 | 0.01870 | 19.7% |
| 2 | 0.12797 | 0.14251 | 0.01454 | 11.4% |
| 3 | 0.16875 | 0.18026 | 0.01151 | 6.8% |
| 4 | 0.21257 | 0.22225 | 0.00968 | 4.6% |
| 5 | 0.25744 | 0.26620 | 0.00876 | 3.4% |
| 6 | 0.30242 | 0.31096 | 0.00854 | 2.8% |

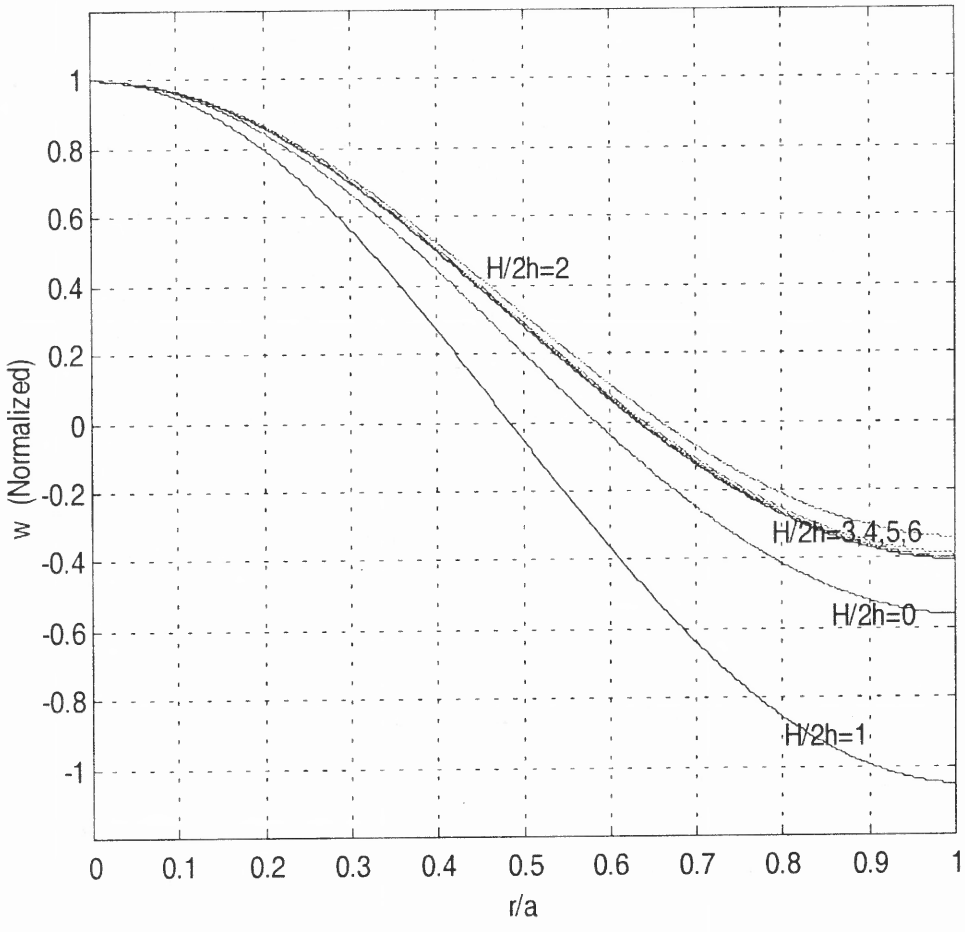


**Figure 4.5.a** Mode Shapes of Sandwich Refined Model with b/a=0 for Free Outside and Free Inside Case

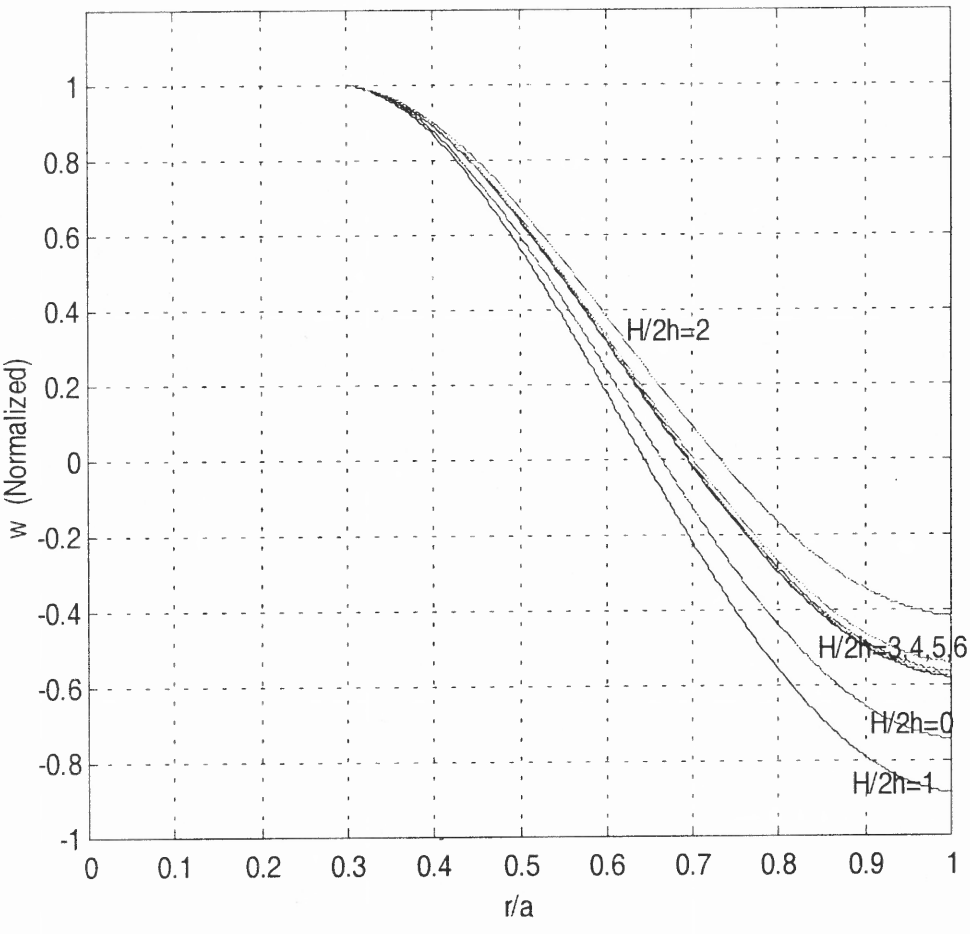


**Figure 4.5.b** Mode Shapes of Sandwich Refined Model with b/a=0.3 for Free Outside and Free Inside Case

Similar to the sandwich case, Table 4.6.a and Table 4.6.b show that the frequency of the homogeneous shell increases with the size of hole and the curvature.

**Table 4.6.a** Refined Model of Dimensionless Frequencies of Free-Free Homogeneous Case

$\omega / \omega_o$

| H/2h | b/a=0 | b/a=0.1 | b/a=0.2 | b/a=0.3 |
|---|---|---|---|---|
| 0 | 0.02566 | 0.03419 | 0.04256 | 0.05450 |
| 1 | 0.02687 | 0.03510 | 0.04329 | 0.05507 |
| 2 | 0.03021 | 0.03770 | 0.04541 | 0.05674 |
| 3 | 0.03503 | 0.04164 | 0.04872 | 0.05940 |
| 4 | 0.04077 | 0.04654 | 0.05295 | 0.06290 |
| 5 | 0.04702 | 0.05208 | 0.05788 | 0.06709 |
| 6 | 0.05354 | 0.05801 | 0.06327 | 0.07180 |

**Table 4.6.b** Refined Model of Fundamental Frequencies of Free-Free Homogeneous Case

$\omega$

| H/2h | b/a=0 | b/a=0.1 | b/a=0.2 | b/a=0.3 |
|---|---|---|---|---|
| 0 | 1739.7 | 2318.1 | 2885.6 | 3695.1 |
| 1 | 1821.8 | 2379.8 | 2935.1 | 3733.7 |
| 2 | 2048.2 | 2556.1 | 3078.8 | 3847.0 |
| 3 | 2375.0 | 2823.2 | 3303.2 | 4027.3 |
| 4 | 2764.2 | 3155.4 | 3590.0 | 4264.6 |
| 5 | 3188.0 | 3531.0 | 3924.3 | 4548.7 |
| 6 | 3630.0 | 3933.1 | 4289.7 | 4868.0 |

**Table 4.6.c** Increase of Dimensionless Frequency with Rise According to the Refined Model of a Free-Free Homogeneous Case

| $b/a$ | $\omega / \omega_o$ for H/2h = 0 | $\omega / \omega_o$ for H/2h = 6 | $\Delta\omega / \omega_o$ | % Increase of $\omega / \omega_o$ |
|---|---|---|---|---|
| 0 | 0.02566 | 0.05354 | 0.02788 | 109 % |
| 0.1 | 0.03419 | 0.05801 | 0.02382 | 70.0 % |
| 0.2 | 0.04256 | 0.06327 | 0.02071 | 49.0 % |
| 0.3 | 0.05450 | 0.07180 | 0.01730 | 32.0 % |

**Table 4.6.d** Increase of Dimensionless Frequency with Size of Hole According to the Refined Model of a Free-Free Homogeneous Case

| H/2h | $\omega/\omega_0$ for b/a=0 | $\omega/\omega_0$ for b/a =0.3 | $\Delta\omega/\omega_0$ | % Increase of $\omega/\omega_0$ |
|---|---|---|---|---|
| 0 | 0.02566 | 0.05450 | 0.02884 | 112.4% |
| 1 | 0.02687 | 0.05507 | 0.02820 | 104.9% |
| 2 | 0.03021 | 0.05674 | 0.02653 | 87.8% |
| 3 | 0.03503 | 0.05940 | 0.02437 | 69.6% |
| 4 | 0.04077 | 0.06290 | 0.02213 | 54.3% |
| 5 | 0.04702 | 0.06709 | 0.02007 | 42.7% |
| 6 | 0.05354 | 0.07180 | 0.01826 | 34.1% |

Table 4.6.c demonstrates that the frequencies increase between 32 percent and 109 percent from zero rise to the maximum allowable rise in the four different size of hole cases. Table 4.6.d shows that the frequencies increase between 34.1 percent to 112.4 percent from $\frac{b}{a}=0$ to $\frac{b}{a}=0.3$ in the seven different rise cases. Figure 4.6.a and Figure 4.6.b plot the mode shapes for zero rise and rise of six with different sizes of holes, respectively.

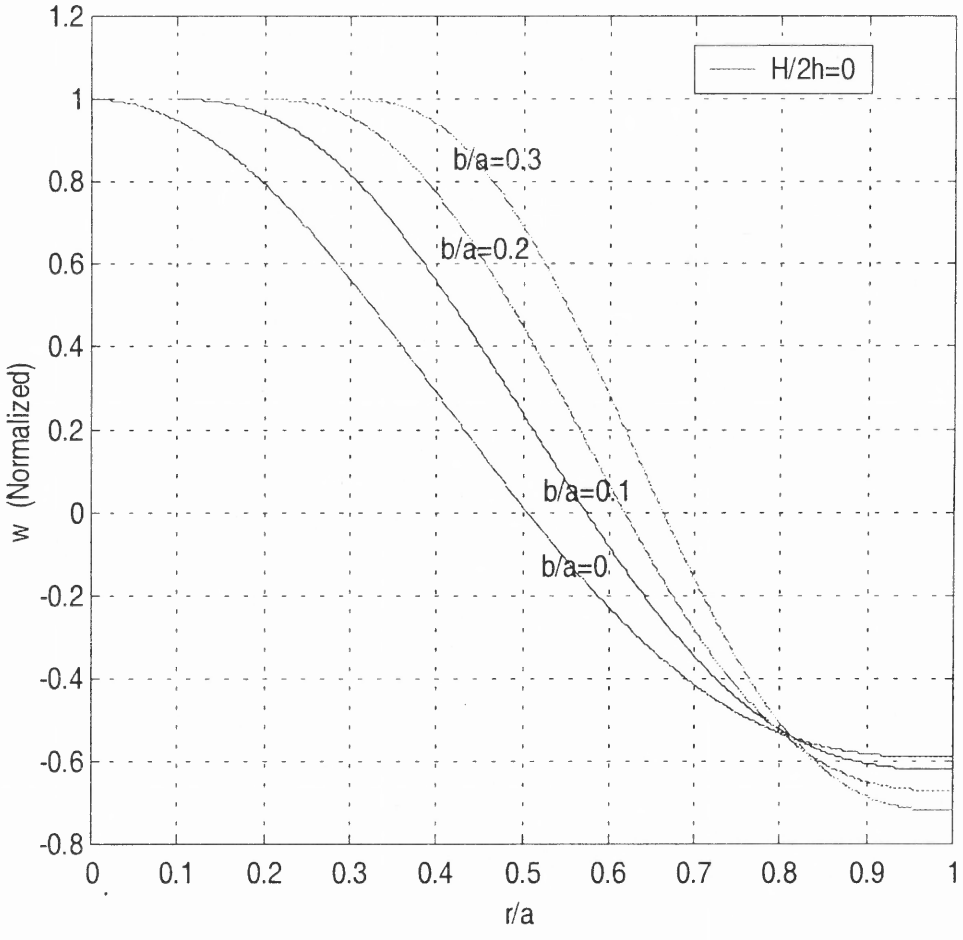


**Figure 4.6.a** Mode Shapes of Homogeneous Refined Model for H/2h=0 with Different Sizes of Holes for Free Outside and Free Inside Case

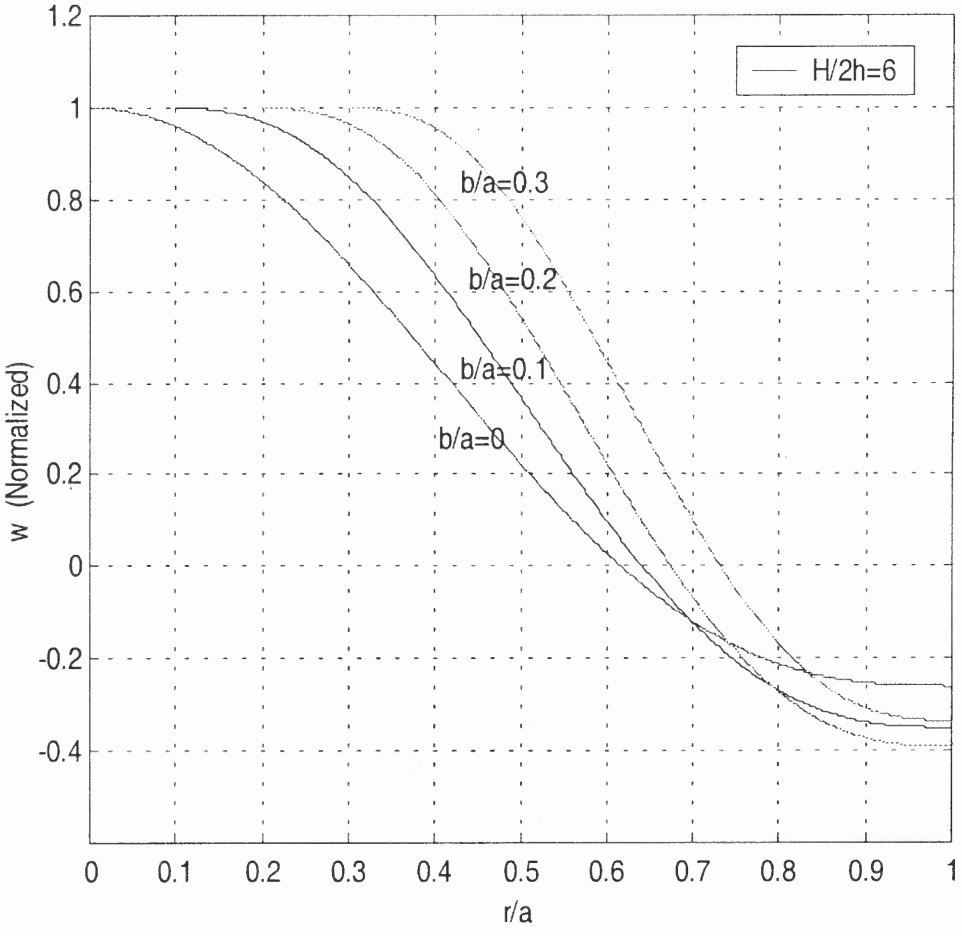


**Figure 4.6.b** Mode Shapes of Homogeneous Refined Model for H/2h=6 with Different Sizes of Holes for Free Outside and Free Inside Case

## 4.3 Classical Model

Similar to the refined model presented in Section (4.2), three boundary cases of the classical model for both sandwich and homogeneous shells are shown in this section. A free boundary is applied at the inner edge with three different boundaries at the outer edge: clamped edge, simply supported edge and free edge, respectively.

Substituting the solution forms from (4.1a) and (4.1b) into (2.30) we have,

$$C_1\left(\frac{d^2u}{dr^2}+\frac{1}{r}\frac{du}{dr}-\frac{1}{r^2}u\right)+C_2\frac{dw}{dr}+C_3\omega^2 u=0, \tag{4.8a}$$

$$C_4\left(\frac{d^4w}{dr^4}+\frac{2}{r}\frac{d^3w}{dr^3}-\frac{1}{r^2}\frac{d^2w}{dr^2}+\frac{1}{r^3}\frac{dw}{dr}\right)+C_2\left(\frac{du}{dr}+\frac{u}{r}+\frac{2w}{R}\right)-C_3\omega^2 w=0, \tag{4.8b}$$

where $C_1$ to $C_4$ are found in (4.6).

To obtain results for the classical model, the tracers $k_s$ and $k_g$ are set equal to zero by neglecting the effects of transverse shear deformation and rotatory inertia, respectively. Such assumptions lead to the displacement boundary conditions described in (2.26b) and (2.26c) in terms of $w$-displacement only. Hence, now taking $k_s = 0$ in Equation (2.18), yields $\beta = -\frac{dw}{dr}$ which is (2.25e). In order to get the outer displacement boundary condition in (2.26b), we first substitute (2.25e) into the (2.15b), (2.15c) and (2.17a) and then (2.26b) at $r = 1$ becomes,

$$(1+3r_h r_1)\frac{d^2w(r)}{dr^2}\Big|_{r=1}+(\upsilon_1+3\upsilon_2 r_h r_1)\frac{1}{r}\frac{dw(r)}{dr}\Big|_{r=1}=0.$$

To evaluate the displacement boundary condition in (2.26c) in terms of the $w$-displacement, set $k_g = 0$ in (2.25b) which give:

$$Q_{rz}^{(1)} = (\frac{dM_{rr}^{(1)}}{dr} - h_1 \frac{dN_{rr}^{(2)}}{dr} + h_1 \frac{dN_{rr}^{(3)}}{dr}) + (\frac{M_{rr}^{(1)}}{r} - h_1 \frac{N_{rr}^{(2)}}{r} + h_1 \frac{N_{rr}^{(3)}}{r})$$

$$- (\frac{M_{\theta\theta}^{(1)}}{r} - h_1 \frac{N_{\theta\theta}^{(2)}}{r} + h_1 \frac{N_{\theta\theta}^{(3)}}{r})$$

Substituting (2.15) and (2.17) together with (2.25e), (2.26c) at $r = 1$ yields,

$$\frac{d^3w(r)}{dr^3} + \frac{1}{r}\frac{d^2w(r)}{dr^2} - \frac{1}{r^2}\frac{dw(r)}{dr}\Big|_{r=1} = 0.$$

The clamped outer displacement boundaries at $r = 1$ are,

$$u(1) = 0, \qquad w(1) = 0, \qquad \frac{dw(r)}{dr}|_{r=1} = 0. \tag{4.9a}$$

The simply supported outer displacement boundaries at $r = 1$ are,

$$u(1) = 0, \qquad w(1) = 0,$$

$$(1 + 3r_h r_1)\frac{d^2w(r)}{dr^2}|_{r=1} + (\upsilon_1 + 3\upsilon_2 r_h r_1)\frac{1}{r}\frac{dw(r)}{dr}|_{r=1} = 0. \tag{4.9b}$$

The free outer displacement boundaries at $r = 1$ are,

$$u(1) = 0,$$

$$(1 + 3r_h r_1)\frac{d^2w(r)}{dr^2}|_{r=1} + (\upsilon_1 + 3\upsilon_2 r_h r_1)\frac{1}{r}\frac{dw(r)}{dr}|_{r=1} = 0, \tag{4.9c}$$

$$\frac{d^3w(r)}{dr^3} + \frac{1}{r}\frac{d^2w(r)}{dr^2} - \frac{1}{r^2}\frac{dw(r)}{dr}\Big|_{r=1} = 0.$$

The free inner displacement boundaries at $r = \frac{b}{a} = \varepsilon$ are

$$u(\varepsilon) = 0,$$

$$(1 + 3r_h r_1)\frac{d^2w(r)}{dr^2}|_{r=\varepsilon} + (\upsilon_1 + 3\upsilon_2 r_h r_1)\frac{1}{r}\frac{dw(r)}{dr}|_{r=\varepsilon} = 0, \tag{4.9d}$$

$$\frac{d^3w(r)}{dr^3}+\frac{1}{r}\frac{d^2w(r)}{dr^2}-\frac{1}{r^2}\frac{dw(r)}{dr}\Bigg|_{r=\varepsilon}=0.$$

The following three sub-sections, (4.3.1), (4.3.2) and (4.3.3) will present the results of clamped outer boundary, simply supported outer boundary and free outer boundary, respectively. Each sub-section consists of both the sandwich and homogeneous cases. Each sandwich or homogeneous case will demonstrate four tables (a, b, c, d, e) and two plots (Figures a and b). Table (a) shows the dimensionless frequency, $\frac{\omega}{\omega_o}$ by varying the curvature or the rise $\frac{H}{2h}$ from 0 to 6 and the dimensionless size of the hole, $\varepsilon=\frac{b}{a}$ from 0 to 0.3, where $\omega_o=9{,}350$ cps for the sandwich case and 67,800 cps for the homogeneous case. Table (b) gives the fundamental natural frequency, $\omega$, which is Table (a) multiplied by $\omega_o$. Table (c) illustrates the results of $\frac{\omega}{\omega_o}$ with different sizes of holes for the shell having the maximum allowable rise, $\frac{H}{2h}=6$, compared with those for a circular plate with zero rise, $\frac{H}{2h}=0$. Table (d) shows the results of $\frac{\omega}{\omega_o}$ with varied curvature for the shell with no center hole, $\varepsilon=0$, compared with those for the shell with hole, $\varepsilon=0.3$. Table (e) illustrates the comparison results for the plate case, i.e. $\frac{H}{2h}=0$ with the analytical solutions by Leissa [10].

Figure (a) and Figure (b) plot the mode shapes with the normalized transverse displacement $w$ as the ordinate and the dimensionless radial coordinate $\frac{r}{a}$ as the abscissa.

### 4.3.1 Clamped and Free Case

In order to obtain the natural frequencies and the normal mode shapes of free vibration for the refined model, Equations (4.8) are first written into a system by using the fourth-order Runge-Kutta algorithm. From the displacement boundary conditions found in (4.9a), the six shooting boundary values, $u(1)$, $u'(1)$, $w(1)$, $w'(1)$, $w''(1)$ and $w'''(1)$ at the outer edge are set: $u(1) = 0$, $u'(1) = \alpha$, $w(1) = 0$, $w'(1) = 0$, $w''(1) = \lambda$, $w'''(1) = \gamma$.

$\alpha$, $\gamma$ & $\omega$ are the unknowns, and $\lambda$ is set equal to one as in the previous cases.

The three unknowns, $\alpha$, $\gamma$ & $\omega$ are determined by employing the *Shooting Method*. The numerical results for the sandwich case are presented in Table 4.7.a and Table 4.7.b, in which the frequency increases as the rise and the size of hole become bigger, except the case between the hole size of 0 and 0.2.

Comparing the present results for $\frac{H}{2h} = 0$ with the analytical solution in Table 4.7.e, we observe that the values of the frequencies are quite close to each other, except in the case of $\frac{b}{a} = 0$.

**Table 4.7.a** Classical Model of Dimensionless Frequencies of Clamped-Free Sandwich Case

$\omega / \omega_o$

| H/2h | b/a=0 | b/a=0.1 | b/a=0.2 | b/a=0.3 |
|---|---|---|---|---|
| 0 | 0.12593 | 0.12094 | 0.12336 | 0.13526 |
| 1 | 0.14413 | 0.13951 | 0.14151 | 0.15206 |
| 2 | 0.18807 | 0.18388 | 0.18521 | 0.19366 |
| 3 | 0.24325 | 0.23910 | 0.24003 | 0.24723 |
| 4 | 0.30212 | 0.29764 | 0.29860 | 0.30566 |
| 5 | 0.36087 | 0.35578 | 0.35737 | 0.36547 |
| 6 | 0.41707 | 0.41125 | 0.41424 | 0.42469 |

**Table 4.7.b** Classical Model of Fundamental Frequencies of Clamped-Free Sandwich Case

$\omega$

| H/2h | b/a=0 | b/a=0.1 | b/a=0.2 | b/a=0.3 |
|---|---|---|---|---|
| 0 | 1177.4 | 1130.8 | 1153.5 | 1264.6 |
| 1 | 1347.6 | 1304.4 | 1323.1 | 1421.7 |
| 2 | 1758.5 | 1719.3 | 1731.7 | 1810.7 |
| 3 | 2274.4 | 2235.6 | 2244.2 | 2311.6 |
| 4 | 2824.8 | 2782.9 | 2791.9 | 2857.9 |
| 5 | 3374.1 | 3326.6 | 3341.1 | 3417.1 |
| 6 | 3899.6 | 3845.2 | 3873.1 | 3970.9 |

We notice that in Table 4.7.c, the frequencies increase over two hundred percent from the zero rise to the maximum allowable rise in the four different size of hole cases. However, Table 4.7.d illustrates that the frequencies increase between 1.2 percent and 7.4 percent from $\frac{b}{a}=0$ to $\frac{b}{a}=0.3$ in the seven different rise cases. Figure 4.7.a plots the mode shapes of the case with $\frac{b}{a}=0$ with different rises, while Figure 4.7.b plots the case of the dimensionless hole, $\frac{b}{a}=0.3$.

**Table 4.7.c** Increase of Dimensionless Frequency with Rise According to the Classical Model of a Clamped-Free Sandwich Case

| $b/a$ | $\omega/\omega_o$ for H/2h = 0 | $\omega/\omega_o$ for H/2h = 6 | $\Delta\omega/\omega_o$ | % Increase of $\omega/\omega_o$ |
|---|---|---|---|---|
| 0 | 0.12593 | 0.41707 | 0.29114 | 231% |
| 0.1 | 0.12094 | 0.41125 | 0.29031 | 240% |
| 0.2 | 0.12336 | 0.41424 | 0.29088 | 236% |
| 0.3 | 0.13526 | 0.42469 | 0.28943 | 214% |

**Table 4.7.d** Increase of Dimensionless Frequency with Size of Hole According to the Classical Model of a Clamped-Free Sandwich Case

| H/2h | $\omega/\omega_0$ for b/a=0 | $\omega/\omega_0$ for b/a =0.3 | $\Delta\omega/\omega_0$ | % Increase of $\omega/\omega_0$ |
|---|---|---|---|---|
| 0 | 0.12593 | 0.13526 | 0.00933 | 7.4% |
| 1 | 0.14413 | 0.15206 | 0.00793 | 5.5% |
| 2 | 0.18807 | 0.19366 | 0.00559 | 3.0% |
| 3 | 0.24325 | 0.24723 | 0.00398 | 1.6% |
| 4 | 0.30212 | 0.30566 | 0.00354 | 1.2% |
| 5 | 0.36087 | 0.36547 | 0.00460 | 1.3% |
| 6 | 0.41707 | 0.42469 | 0.00762 | 1.8% |

**Table 4.7.e** Comparison of Classical Model of Dimensionless Frequency of Circular Plate for Clamped-Free Sandwich Case ($\frac{H}{2h}=0$)

$\omega/\omega_0$

| | b/a=0 | b/a=0.1 | b/a=0.2 | b/a=0.3 |
|---|---|---|---|---|
| Present Study | 0.12593 | 0.12094 | 0.12336 | 0.13526 |
| Leissa [10] | 0.12066 | 0.12002 | 0.12300 | 0.13503 |
| % error | 4.4% | 0.8% | 0.3% | 0.2% |

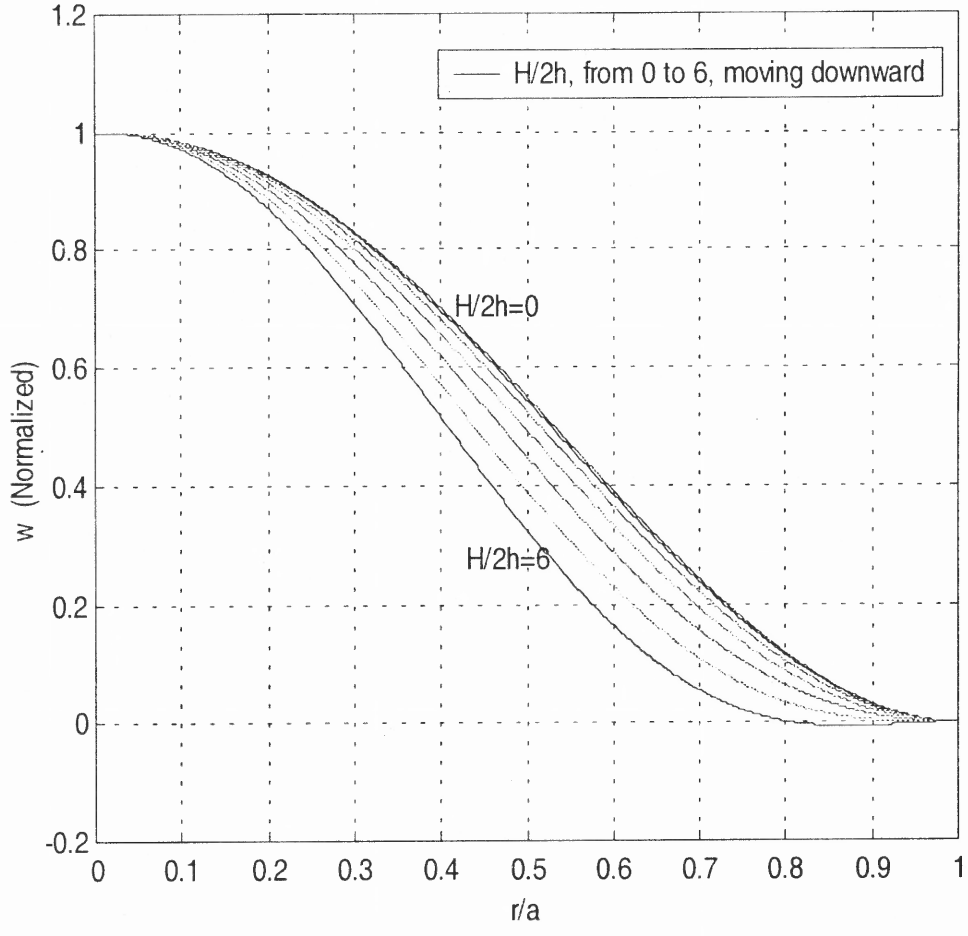


**Figure 4.7.a** Mode Shapes of Sandwich Classical Model with b/a=0 for Clamped Outside and Free Inside Case

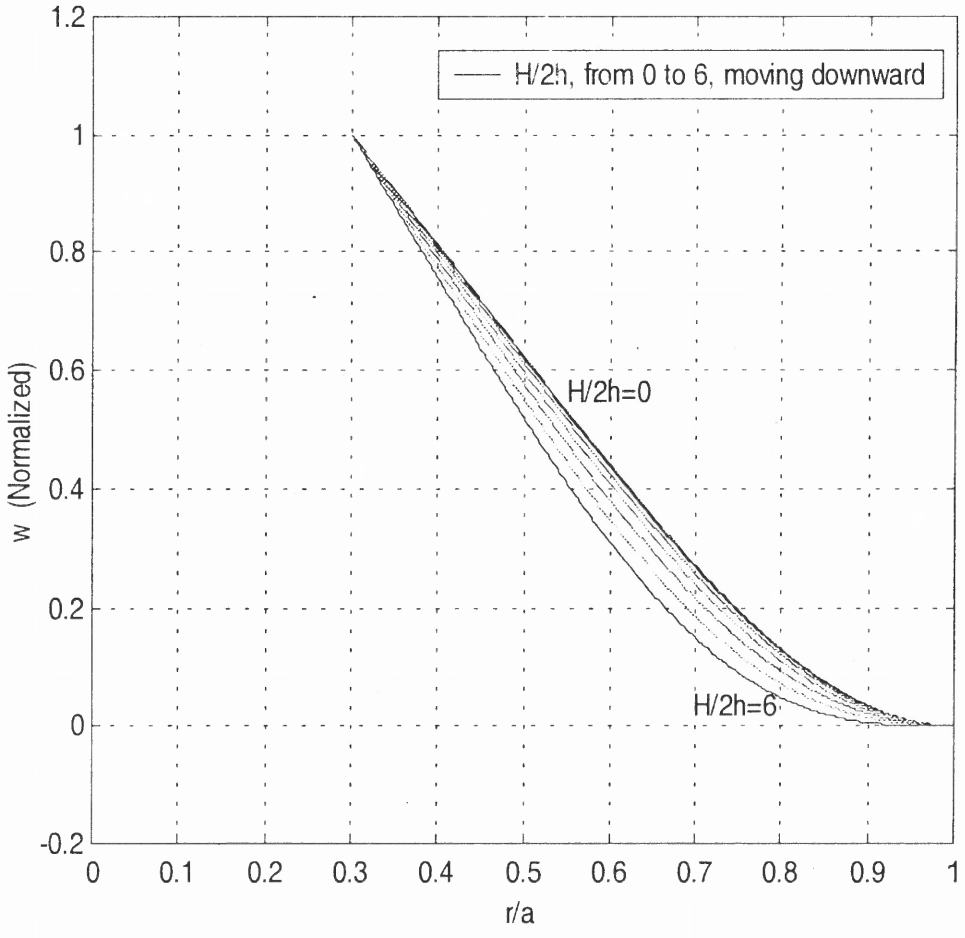


**Figure 4.7.b** Mode Shapes of Sandwich Classical Model with b/a=0.3 for Clamped Outside and Free Inside Case

To calculate the frequencies of a homogeneous shell based on the classical theory we further put $r_h = 0$, $k_s = 0$ and $k_g = 0$ in Equation (4.6). Similar to the sandwich case, Table 4.8.a and Table 4.8.b show that the frequency of the homogeneous shell increases with the bigger hole and the curvature, except for the case where the hole size $\frac{b}{a} = 0.1$.

Comparing the present results for $\frac{H}{2h} = 0$ with the analytical solution in Table 4.8.e, the values of the frequencies are quite close to each other, except in the case of $\frac{b}{a} = 0$.

**Table 4.8.a** Classical Model of Dimensionless Frequencies of Clamped-Free Homogeneous Case

$\omega / \omega_o$

| H/2h | b/a=0 | b/a=0.1 | b/a=0.2 | b/a=0.3 |
|---|---|---|---|---|
| 0 | 0.01301 | 0.01249 | 0.01273 | 0.01396 |
| 1 | 0.01729 | 0.01683 | 0.01699 | 0.01795 |
| 2 | 0.02605 | 0.02561 | 0.02570 | 0.02642 |
| 3 | 0.03575 | 0.03523 | 0.03534 | 0.03610 |
| 4 | 0.04510 | 0.04445 | 0.04474 | 0.04585 |
| 5 | 0.05353 | 0.05275 | 0.05339 | 0.05515 |
| 6 | 0.06101 | 0.06019 | 0.06119 | 0.06373 |

**Table 4.8.b** Classical Model of Fundamental Frequencies of Clamped-Free Homogeneous Case

$\omega$

| H/2h | b/a=0 | b/a=0.1 | b/a=0.2 | b/a=0.3 |
|---|---|---|---|---|
| 0 | 882.1 | 846.8 | 863.1 | 946.5 |
| 1 | 1172.3 | 1141.1 | 1151.9 | 1217.0 |
| 2 | 1766.2 | 1736.4 | 1742.5 | 1791.3 |
| 3 | 2423.9 | 2388.6 | 2396.1 | 2447.6 |
| 4 | 3057.8 | 3013.7 | 3033.4 | 3108.6 |
| 5 | 3629.3 | 3576.5 | 3619.8 | 3739.2 |
| 6 | 4136.5 | 4080.9 | 4148.7 | 4320.9 |

Table 4.8.c demonstrates that the frequency increases over three hundred percent from zero rise to the maximum allowable rise in the four different size of hole cases. Table 4.8.d illustrates that the frequency increase between 1.0 percent and 7.3 percent from $\frac{b}{a} = 0$ to the maximum dimensionless hole, $\frac{b}{a} = 0.3$ in the seven different rise cases. Figure 4.8.a and Figure 4.8.b plot the mode shapes for zero rise and rise of six with different sizes of holes, respectively.

**Table 4.8.c** Increase of Dimensionless Frequency with Rise According to the Classical Model of a Clamped-Free Homogeneous Case

| $b/a$ | $\omega/\omega_o$ for H/2h = 0 | $\omega/\omega_o$ for H/2h = 6 | $\Delta\omega/\omega_o$ | % Increase of $\omega/\omega_o$ |
|---|---|---|---|---|
| 0 | 0.01301 | 0.06101 | 0.04800 | 369 % |
| 0.1 | 0.01249 | 0.06019 | 0.04770 | 382 % |
| 0.2 | 0.01273 | 0.06119 | 0.04846 | 381 % |
| 0.3 | 0.01396 | 0.06373 | 0.04977 | 357 % |

**Table 4.8.d** Increase of Dimensionless Frequency with Size of Hole According to the Classical Model of a Clamped-Free Homogeneous Case

| H/2h | $\omega/\omega_0$ for b/a=0 | $\omega/\omega_0$ for b/a =0.3 | $\Delta\omega/\omega_0$ | % Increase of $\omega/\omega_0$ |
|---|---|---|---|---|
| 0 | 0.01301 | 0.01396 | 0.00095 | 7.3% |
| 1 | 0.01729 | 0.01795 | 0.00066 | 3.8% |
| 2 | 0.02605 | 0.02642 | 0.00037 | 1.4% |
| 3 | 0.03575 | 0.03610 | 0.00035 | 1.0% |
| 4 | 0.04510 | 0.04585 | 0.00075 | 1.7% |
| 5 | 0.05353 | 0.05515 | 0.00162 | 3.0% |
| 6 | 0.06101 | 0.06373 | 0.00272 | 4.5% |

**Table 4.8.e** Comparison of Classical Model of Dimensionless Frequency of Circular Plate for Clamped-Free Homogeneous Case ($\frac{H}{2h}=0$)

$\omega/\omega_0$

| | b/a=0 | b/a=0.1 | b/a=0.2 | b/a=0.3 |
|---|---|---|---|---|
| Present Study | 0.01301 | 0.01249 | 0.01273 | 0.01396 |
| Leissa [10] | 0.01246 | 0.01239 | 0.01270 | 0.01394 |
| % error | 4.4% | 0.8% | 0.2% | 0.1% |

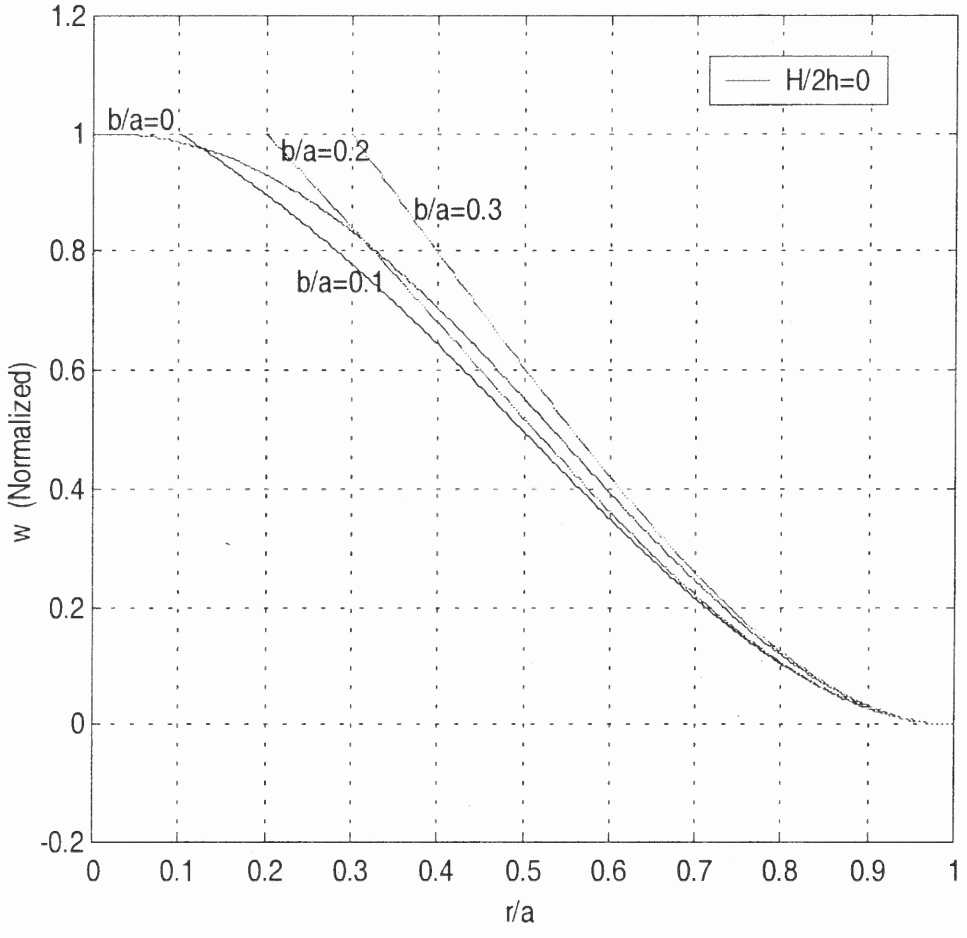


**Figure 4.8.a** Mode Shapes of Homogeneous Classical Model for H/2h=0 with Different Sizes of Holes for Clamped Outside and Free Inside Case

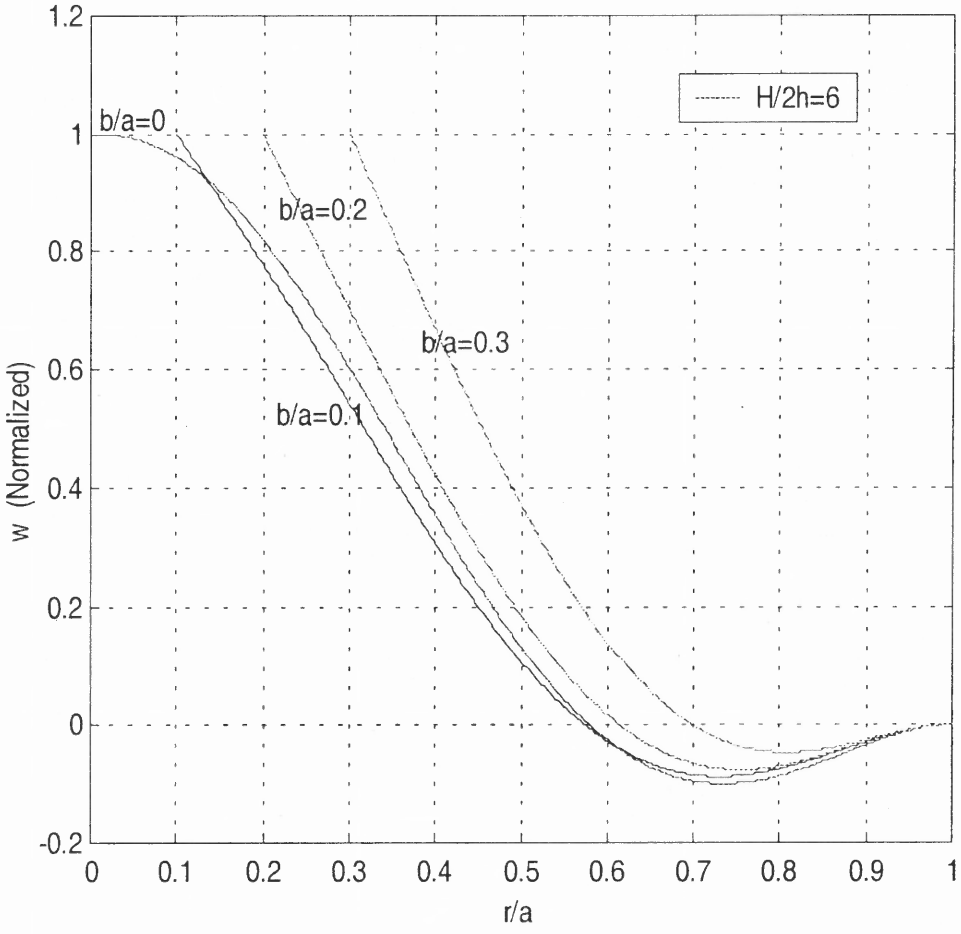


**Figure 4.8.b** Mode Shapes of Homogeneous Classical Model for H/2h=6 with Different Sizes of Holes for Clamped Outside and Free Inside Case

### 4.3.2 Simply Supported and Free Case

Similar to the clamped on outside and free on inside case, Equations (4.8) are first written into a system by using the fourth-order Runge-Kutta algorithm. From the displacement boundary conditions found in (4.9b), the six shooting boundary values, $u(1)$, $u'(1)$, $w(1)$, $w'(1)$, $w''(1)$ and $w'''(1)$ at the outer edge are set as follows:

$u(1)=0$, $u'(1)=\alpha$, $w(1)=0$, $w'(1)=\lambda$, $w''(1)=\dfrac{-(\upsilon_1+3\upsilon_2 r_h r_1)}{(1+3r_h r_1)}\lambda$, $w'''(1)=\gamma$, where $\alpha$, $\gamma$ & $\omega$ are the unknowns, and $\lambda$ is found to be independent of $\omega$ and taken equal to one in the analysis. Then the three unknowns, $\alpha$, $\gamma$ & $\omega$ are solved by employing the process from the *Shooting Method* stated in the previous section.

Table 4.9.a and Table 4.9.b present the frequency of the sandwich case in which the frequency increases with the increase of the rise, except for the case where the hole size $\dfrac{b}{a}=0.1$. However, the frequency fluctuates as the size of hole varies.

Comparing the present results for $\dfrac{H}{2h}=0$ with the analytical solution in Table 4.9.e, we observe that the values of the frequencies are quite close to each other, except for the case of $\dfrac{b}{a}=0$.

**Table 4.9.a** Classical Model of Dimensionless Frequencies of Simply Supported-Free Sandwich Case

$\omega / \omega_o$

| H/2h | b/a=0 | b/a=0.1 | b/a=0.2 | b/a=0.3 |
|---|---|---|---|---|
| 0 | 0.06218 | 0.05795 | 0.05594 | 0.05519 |
| 1 | 0.09792 | 0.09495 | 0.09354 | 0.09307 |
| 2 | 0.16292 | 0.16046 | 0.15934 | 0.15921 |
| 3 | 0.23223 | 0.22946 | 0.22858 | 0.22922 |
| 4 | 0.29970 | 0.29594 | 0.29582 | 0.29842 |
| 5 | 0.36074 | 0.35540 | 0.35540 | 0.36429 |
| 6 | 0.41190 | 0.40527 | 0.41041 | 0.42434 |

**Table 4.9.b** Classical Model of Dimensionless Frequencies of Simply Supported-Free Sandwich Case

$\omega$

| H/2h | b/a=0 | b/a=0.1 | b/a=0.2 | b/a=0.3 |
|---|---|---|---|---|
| 0 | 581.3 | 541.8 | 523.0 | 516.0 |
| 1 | 979.2 | 887.8 | 874.6 | 870.2 |
| 2 | 1523.3 | 1500.2 | 1489.9 | 1488.6 |
| 3 | 2171.4 | 2145.5 | 2137.3 | 2143.9 |
| 4 | 2802.2 | 2767.0 | 2766.0 | 2790.3 |
| 5 | 3373.0 | 3323.0 | 3323.0 | 3406.1 |
| 6 | 3851.3 | 3789.3 | 3837.3 | 3967.6 |

As shown in Table 4.9.c, there is a noticeable increase of the frequency from 562 percent to 669 percent from the zero rise to the maximum allowable rise in the four different size of hole cases. Table 4.9.d shows that the frequencies fluctuate between 0.4 percent to 11.2 percent from $\frac{b}{a} = 0$ to the maximum dimensionless hole, $\frac{b}{a} = 0.3$ in the seven different rise cases. The mode shapes are plotted in Figure 4.9.a and Figure 4.9.b. The former shows the case of $\frac{H}{2h} = 0$ with different hole sizes, while the latter plots the rise of six.

**Table 4.9.c** Increase of Dimensionless Frequency with Rise According to the Classical Model of a Simply Supported-Free Sandwich Case

| $b/a$ | $\omega/\omega_o$ for H/2h = 0 | $\omega/\omega_o$ for H/2h = 6 | $\Delta\omega/\omega_o$ | % Increase of $\omega/\omega_o$ |
|---|---|---|---|---|
| 0 | 0.06218 | 0.41190 | 0.34972 | 562 % |
| 0.1 | 0.05795 | 0.40527 | 0.34732 | 599 % |
| 0.2 | 0.05594 | 0.41041 | 0.35447 | 634 % |
| 0.3 | 0.05519 | 0.42434 | 0.36915 | 669 % |

**Table 4.9.d** Increase of Dimensionless Frequency with Size of Hole According to the Classical Model of a Simply Supported-Free Sandwich Case

| H/2h | $\omega/\omega_0$ for b/a=0 | $\omega/\omega_0$ for b/a =0.3 | $\Delta\omega/\omega_0$ | % Increase (+) or Decrease (-) of $\omega/\omega_0$ |
|---|---|---|---|---|
| 0 | 0.06218 | 0.05519 | -0.00699 | -11.2% |
| 1 | 0.09792 | 0.09307 | -0.00485 | -5.0% |
| 2 | 0.16292 | 0.15921 | -0.00371 | -2.3% |
| 3 | 0.23223 | 0.22922 | -0.00301 | -1.3% |
| 4 | 0.29970 | 0.29842 | -0.00128 | -0.4% |
| 5 | 0.36074 | 0.36429 | 0.00355 | 1.0% |
| 6 | 0.41190 | 0.42434 | 0.01244 | 3.0% |

**Table 4.9.e** Comparison of Classical Model of Dimensionless Frequency of Circular Plate for Simply Supported-Free Sandwich Case ($\frac{H}{2h} = 0$)

$\omega/\omega_0$

| | b/a=0 | b/a=0.1 | b/a=0.2 | b/a=0.3 |
|---|---|---|---|---|
| Present Study | 0.06218 | 0.05795 | 0.05594 | 0.05519 |
| Leissa [10] | 0.05823 | 0.05728 | 0.05570 | 0.05509 |
| % error | 6.8% | 1.2% | 0.4% | 0.2% |

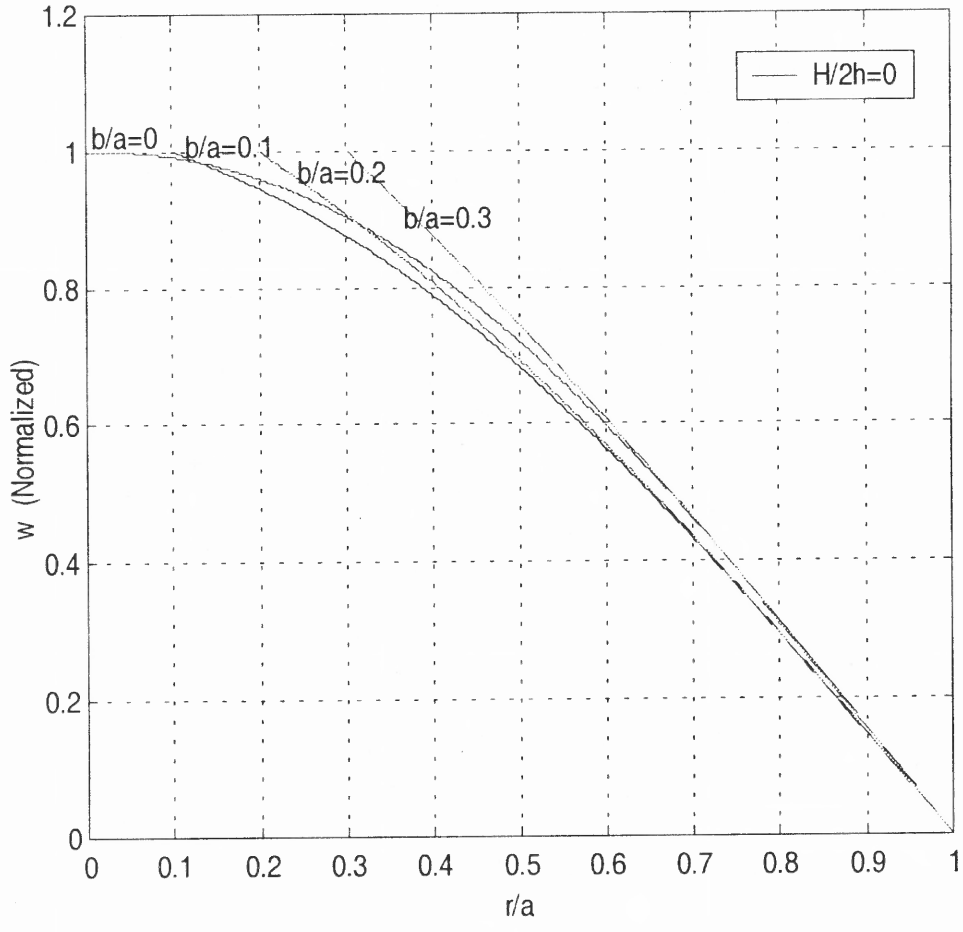


**Figure 4.9.a** Mode Shapes of Sandwich Classical Model for H/2h=0 with Different Sizes of Holes for Simply Supported Outside and Free Inside Case

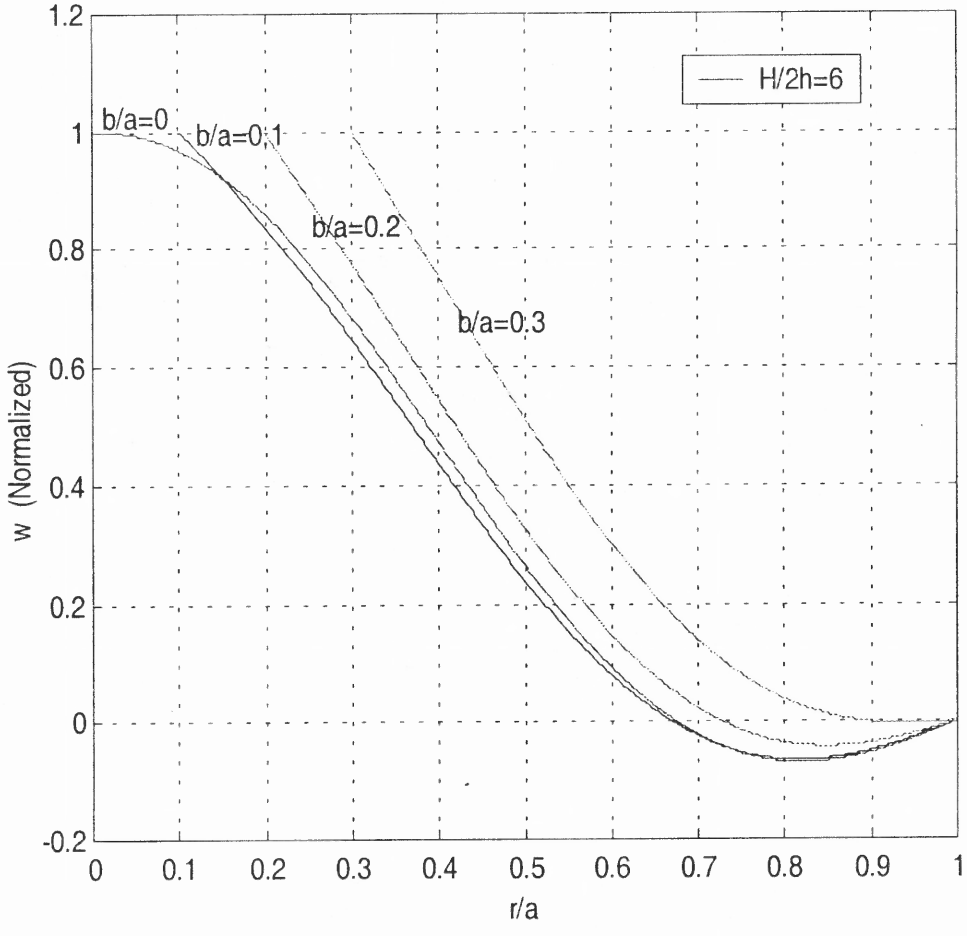


**Figure 4.9.b** Mode Shapes of Sandwich Classical Model for H/2h=6 with Different Sizes of Holes for Simply Supported Outside and Free Inside Case

Table 4.10.a and Table 4.10.b show that the changes of frequency of the homogeneous shell are similar to those of the sandwich case discussed above.

**Table 4.10.a** Classical Model of Dimensionless Frequencies of Simply Supported-Free Homogeneous Case

$\omega / \omega_o$

| H/2h | b/a=0 | b/a=0.1 | b/a=0.2 | b/a=0.3 |
|---|---|---|---|---|
| 0 | 0.00643 | 0.00599 | 0.00578 | 0.00570 |
| 1 | 0.01386 | 0.01359 | 0.01346 | 0.01343 |
| 2 | 0.02507 | 0.02477 | 0.02468 | 0.02476 |
| 3 | 0.03574 | 0.03523 | 0.03532 | 0.03585 |
| 4 | 0.04436 | 0.04361 | 0.04416 | 0.04574 |
| 5 | 0.05132 | 0.05055 | 0.05140 | 0.05394 |
| 6 | 0.05782 | 0.05713 | 0.05811 | 0.06104 |

**Table 4.10.b** Classical Model of Fundamental Frequencies of Simply Supported-Free Homogeneous Case

$\omega$

| H/2h | b/a=0 | b/a=0.1 | b/a=0.2 | b/a=0.3 |
|---|---|---|---|---|
| 0 | 436.0 | 406.1 | 391.9 | 386.5 |
| 1 | 939.7 | 921.4 | 912.6 | 910.6 |
| 2 | 1699.7 | 1679.4 | 1673.3 | 1678.7 |
| 3 | 2423.2 | 2388.6 | 2394.7 | 2430.6 |
| 4 | 3007.6 | 2956.8 | 2994.0 | 3101.2 |
| 5 | 3479.5 | 3427.3 | 3484.9 | 3657.1 |
| 6 | 3920.2 | 3873.4 | 3939.9 | 4138.5 |

The frequencies shown in Table 4.10.c increase between 799 percent and 971 percent from the zero rise to the maximum allowable rise in the four different size of hole cases. Table 4.10.d demonstrates that the frequency fluctuates between 0.3 percent and 11.4 percent from $\frac{b}{a} = 0$ to $\frac{b}{a} = 0.3$ in the seven different rise cases.

Figure 4.10.a and Figure 4.10.b show the mode shapes for the zero hole case and the dimensionless hole size of 0.2 with different rises, respectively.

**Table 4.10.c** Increase of Dimensionless Frequency with Rise According to the Classical Model of a Simply Supported-Free Homogeneous Case

| $b/a$ | $\omega/\omega_o$ for H/2h = 0 | $\omega/\omega_o$ for H/2h = 6 | $\Delta\omega/\omega_o$ | % Increase of $\omega/\omega_o$ |
|---|---|---|---|---|
| 0 | 0.00643 | 0.05782 | 0.05139 | 799 % |
| 0.1 | 0.00599 | 0.05713 | 0.05114 | 854 % |
| 0.2 | 0.00578 | 0.05811 | 0.05233 | 905 % |
| 0.3 | 0.0057 | 0.06104 | 0.05534 | 971 % |

**Table 4.10.d** Increase of Dimensionless Frequency with Size of Hole According to the Classical Model of a Simply Supported-Free Homogeneous Case

| H/2h | $\omega/\omega_0$ for b/a=0 | $\omega/\omega_0$ for b/a =0.3 | $\Delta\omega/\omega_0$ | % Increase (+) or Decrease (-) of $\omega/\omega_0$ |
|---|---|---|---|---|
| 0 | 0.00643 | 0.00570 | -0.00073 | -11.4% |
| 1 | 0.01386 | 0.01343 | -0.00043 | -3.1% |
| 2 | 0.02507 | 0.02476 | -0.00031 | -1.2% |
| 3 | 0.03574 | 0.03585 | 0.00011 | 0.3% |
| 4 | 0.04436 | 0.04574 | 0.00138 | 3.1% |
| 5 | 0.05132 | 0.05394 | 0.00262 | 5.1% |
| 6 | 0.05782 | 0.06104 | 0.00322 | 5.6% |

**Table 4.10.e** Comparison of Classical Model of Dimensionless Frequency of Circular Plate for Simply Supported-Free Homogeneous Case ($\frac{H}{2h} = 0$)

$\omega/\omega_0$

| | b/a=0 | b/a=0.1 | b/a=0.2 | b/a=0.3 |
|---|---|---|---|---|
| Present Study | 0.00643 | 0.00599 | 0.00578 | 0.00570 |
| Leissa [10] | 0.00602 | 0.00592 | 0.00575 | 0.00569 |
| % error | 6.8% | 1.2% | 0.5% | 0.2% |

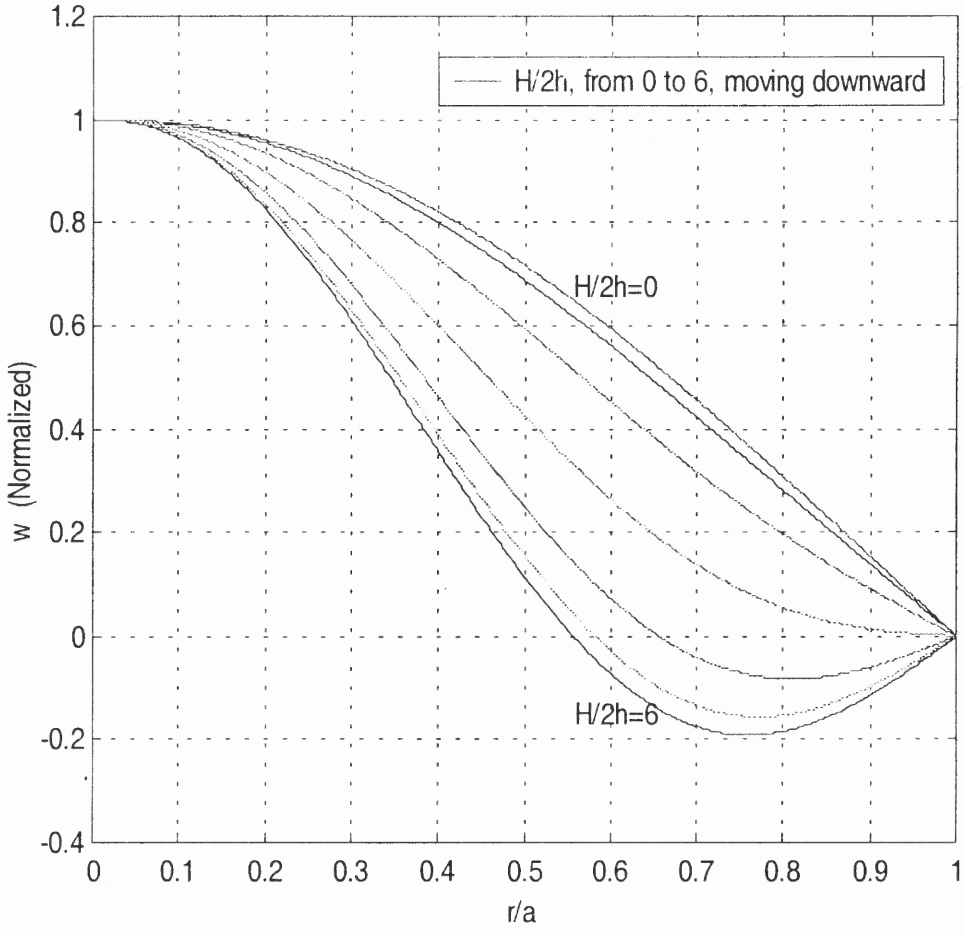


**Figure 4.10.a** Mode Shapes of Homogeneous Classical Model with b/a=0 for Simply Supported Outside and Free Inside Case

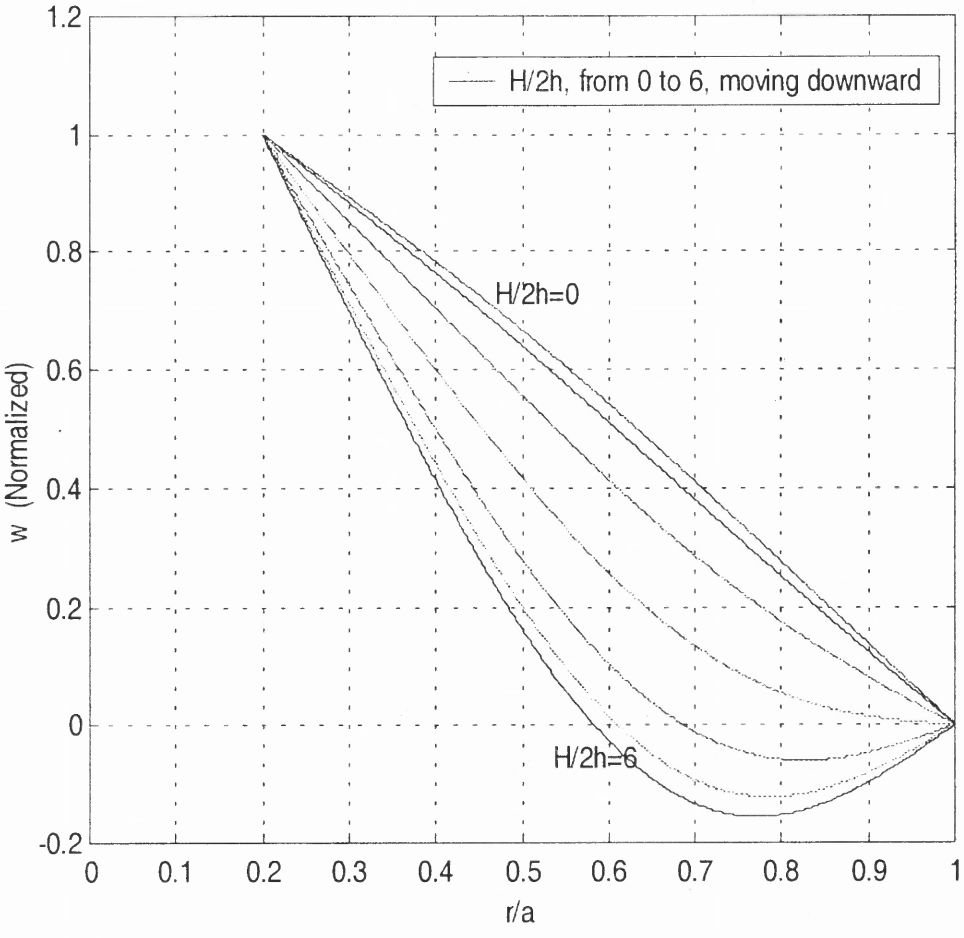


**Figure 4.10.b** Mode Shapes of Homogeneous Classical Model with b/a=0.2 for Simply Supported Outside and Free Inside Case

### 4.3.3 Free and Free Case

To apply the fourth-order Runge-Kutta algorithm for Equations (4.8) written into a system, the six shooting boundary values, $u(1)$, $u'(1)$, $w(1)$, $w'(1)$, $w''(1)$ and $w'''(1)$ at the outer edge are set as follows:

$$u(1)=0, \qquad u'(1)=\alpha, \qquad w(1)=\gamma, \qquad w'(1)=\lambda, \qquad w''(1)=\frac{-(\upsilon_1+3\upsilon_2 r_h r_1)}{(1+3r_h r_1)}\lambda,$$

$$w'''(1)=\frac{(\upsilon_1+3\upsilon_2 r_h r_1)}{(1+3r_h r_1)}\lambda+\lambda,$$

where $\alpha$, $\gamma$ & $\omega$ are the unknowns, and $\lambda$ is independent of $\omega$ in the analysis and taken as one in value.

Using the procedures of the *Shooting Method*, we obtain the numerical results for the sandwich case in Table 4.11.a and Table 4.11.b. The frequency decreases with the larger hole and increases with the curvature. Comparing the present results for $\frac{H}{2h}=0$ with the analytical solution in Table 4.11.e, we observe that the values of the frequencies are quite close to each other, except in the case of $\frac{b}{a}=0$.

**Table 4.11.a** Classical Model of Dimensionless Frequencies of Free-Free Sandwich Case $\omega/\omega_o$

| H/2h | b/a=0 | B/a=0.1 | b/a=0.2 | b/a=0.3 |
|---|---|---|---|---|
| 0 | 0.11138 | 0.10439 | 0.09996 | 0.09876 |
| 1 | 0.12191 | 0.12326 | 0.11555 | 0.11158 |
| 2 | 0.14897 | 0.14383 | 0.14071 | 0.13993 |
| 3 | 0.18521 | 0.18112 | 0.17877 | 0.17826 |
| 4 | 0.22591 | 0.22619 | 0.22089 | 0.22069 |
| 5 | 0.26864 | 0.26596 | 0.26479 | 0.26496 |
| 6 | 0.31213 | 0.30995 | 0.30935 | 0.30997 |

**Table 4.11.b** Classical Model of Fundamental Frequencies of Free-Free Sandwich Case $\omega$

| H/2h | b/a=0 | b/a=0.1 | b/a=0.2 | b/a=0.3 |
|---|---|---|---|---|
| 0 | 1041.4 | 976.0 | 934.6 | 923.5 |
| 1 | 1139.8 | 1152.4 | 1080.4 | 1043.3 |
| 2 | 1392.9 | 1344.8 | 1315.7 | 1308.3 |
| 3 | 1731.8 | 1693.5 | 1671.5 | 1666.8 |
| 4 | 2112.3 | 2081.5 | 2065.3 | 2063.4 |
| 5 | 2511.8 | 2486.7 | 2475.8 | 2477.3 |
| 6 | 2918.4 | 2898.0 | 2892.4 | 2898.3 |

As shown in Table 4.11.c, the frequencies increase between 180 percent and 214 percent from the zero rise to the maximum allowable rise in the four different size of hole cases. However, Table 4.11.d illustrates that the frequencies decrease between 0.7 percent and 11.3 percent from $\frac{b}{a}=0$ to $\frac{b}{a}=0.3$ in the seven different rise cases. Figure 4.11.a plots the mode shapes of the case with $\frac{b}{a}=0$ with different rises. Figure 4.11.b plots the case of the dimensionless hole, $\frac{b}{a}=0.3$, in which they have the same mode shapes. Similar to the refined model shown in Section (4.2.3), the $w$ deflection is normalized to be unity at the inner boundary.

**Table 4.11.c** Increase of Dimensionless Frequency with Rise According to the Classical Model of a Free-Free Sandwich Case

| $b/a$ | $\omega/\omega_o$ for H/2h = 0 | $\omega/\omega_o$ for H/2h = 6 | $\Delta\omega/\omega_o$ | % Increase of $\omega/\omega_o$ |
|---|---|---|---|---|
| 0 | 0.11138 | 0.31213 | 0.20075 | 180 % |
| 0.1 | 0.10439 | 0.30995 | 0.20556 | 197 % |
| 0.2 | 0.09996 | 0.30935 | 0.20939 | 209 % |
| 0.3 | 0.09876 | 0.30997 | 0.21121 | 214 % |

**Table 4.11.d** Increase of Dimensionless Frequency with Size of Hole According to the Classical Model of a Free-Free Sandwich Case

| H/2h | $\omega/\omega_0$ for b/a=0 | $\omega/\omega_0$ for b/a =0.3 | $\Delta\omega/\omega_0$ | % Increase (+) or Decrease (-) of $\omega/\omega_0$ |
|---|---|---|---|---|
| 0 | 0.11138 | 0.09876 | -0.01262 | -11.3% |
| 1 | 0.12191 | 0.11158 | -0.01033 | -8.5% |
| 2 | 0.14897 | 0.13993 | -0.00904 | -6.1% |
| 3 | 0.18521 | 0.17826 | -0.00695 | -3.8% |
| 4 | 0.22591 | 0.22069 | -0.00522 | -2.3% |
| 5 | 0.26864 | 0.26496 | -0.00368 | -1.4% |
| 6 | 0.31213 | 0.30997 | -0.00216 | -0.7% |

**Table 4.11.e** Comparison of Classical Model of Dimensionless Frequency of Circular Plate for Free-Free Sandwich Case $(\frac{H}{2h} = 0)$

$\omega/\omega_0$

| | b/a=0 | b/a=0.1 | b/a=0.2 | b/a=0.3 |
|---|---|---|---|---|
| Present Study | 0.11138 | 0.10439 | 0.09996 | 0.09876 |
| Leissa [10] | 0.10625 | 0.10358 | 0.09974 | 0.09870 |
| % error | 3.5% | 0.5% | 0.2% | 0.1% |

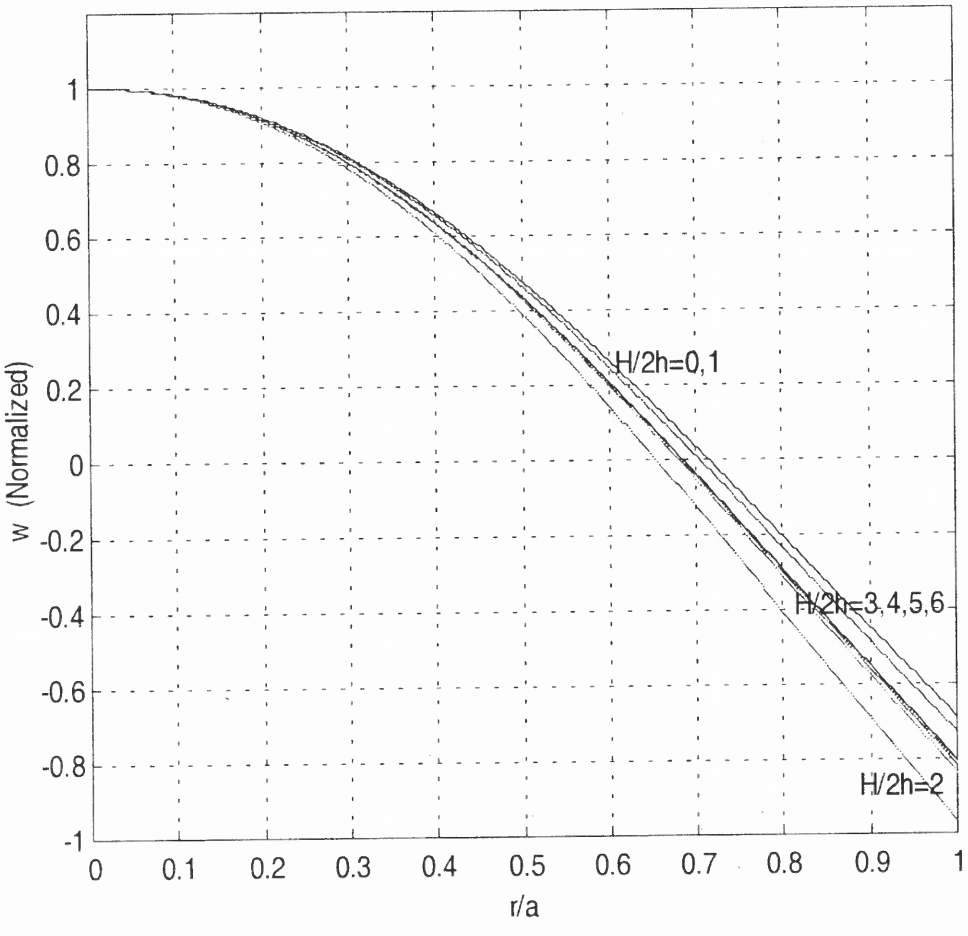


**Figure 4.11.a** Mode Shapes of Sandwich Classical Model with b/a=0 for Free Outside and Free Inside Case

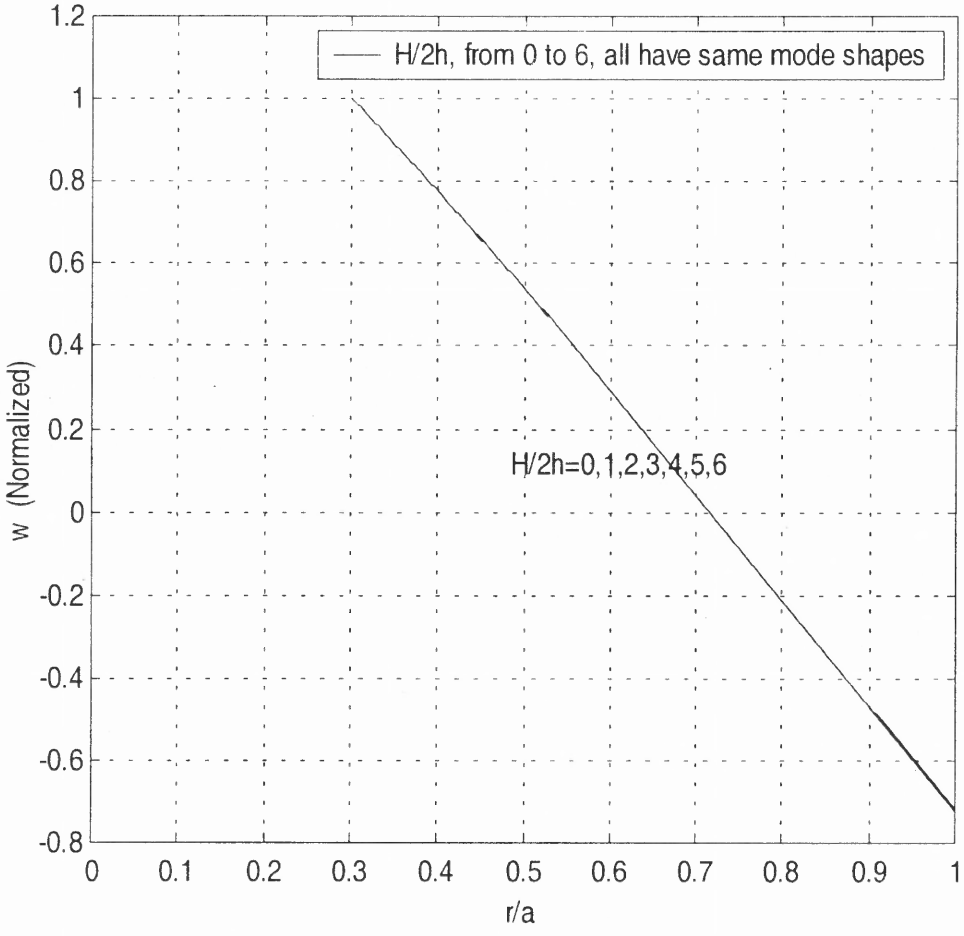


**Figure 4.11.b** Mode Shapes of Sandwich Classical Model with b/a=0.3 for Free Outside and Free Inside Case

Similar to the sandwich case, Table 4.12.a and Table 4.12.b show that the frequency of the homogeneous shell increases with the curvature but decrease with the bigger hole. Similarly, Table 4.12.e shows that the values of the frequencies are close to that of the analytical solution.

**Table 4.12.a** Classical Model of Dimensionless Frequencies of Free-Free Homogeneous Case

$\omega / \omega_o$

| H/2h | b/a=0 | b/a=0.1 | b/a=0.2 | b/a=0.3 |
|---|---|---|---|---|
| 0 | 0.01152 | 0.01079 | 0.01032 | 0.01020 |
| 1 | 0.01405 | 0.01346 | 0.01309 | 0.01299 |
| 2 | 0.01977 | 0.01935 | 0.01911 | 0.01905 |
| 3 | 0.02665 | 0.02635 | 0.02618 | 0.02616 |
| 4 | 0.03394 | 0.03370 | 0.03360 | 0.03362 |
| 5 | 0.04134 | 0.04116 | 0.04112 | 0.04119 |
| 6 | 0.04874 | 0.04860 | 0.04863 | 0.04877 |

**Table 4.12.b** Classical Model of Fundamental Frequencies of Free-Free Homogeneous Case

$\omega$

| H/2h | b/a=0 | b/a=0.1 | b/a=0.2 | b/a=0.3 |
|---|---|---|---|---|
| 0 | 781.1 | 731.6 | 699.7 | 691.6 |
| 1 | 952.6 | 912.6 | 887.5 | 880.7 |
| 2 | 1340.4 | 1311.9 | 1295.7 | 1291.6 |
| 3 | 1806.9 | 1786.5 | 1775.0 | 1773.6 |
| 4 | 2301.1 | 2284.9 | 2278.1 | 2279.4 |
| 5 | 2802.9 | 2790.6 | 2787.9 | 2792.7 |
| 6 | 3304.6 | 3295.1 | 3297.1 | 3306.6 |

The frequencies presented in Table 4.12.c increase over 300 percent from the zero rise to the maximum rise in the four different size of hole cases. Table 4.12.d illustrates that the frequencies decrease between 0.1 percent and 11.5 percent from $\frac{b}{a}=0$ to $\frac{b}{a}=0.3$ in the seven different rise cases.

Figure 4.12.a and Figure 4.12.b plot the mode shapes for zero rise and rise of six with different sizes of holes, respectively.

**Table 4.12.c** Increase of Dimensionless Frequency with Rise According to the Classical Model of a Simply Free-Free Homogeneous Case

| $b/a$ | $\omega/\omega_o$ for H/2h = 0 | $\omega/\omega_o$ for H/2h = 6 | $\Delta\omega/\omega_o$ | % Increase of $\omega/\omega_o$ |
|---|---|---|---|---|
| 0 | 0.01152 | 0.04874 | 0.03722 | 323 % |
| 0.1 | 0.01079 | 0.04860 | 0.03781 | 350 % |
| 0.2 | 0.01032 | 0.04863 | 0.03831 | 371% |
| 0.3 | 0.01020 | 0.04877 | 0.03857 | 378 % |

**Table 4.12.d** Increase of Dimensionless Frequency with Size of Hole According to the Classical Model of a Free-Free Sandwich Case

| H/2h | $\omega/\omega_0$ for b/a=0 | $\omega/\omega_0$ for b/a =0.3 | $\Delta\omega/\omega_0$ | % Increase (+) or Decrease (-) of $\omega/\omega_0$ |
|---|---|---|---|---|
| 0 | 0.01152 | 0.01020 | -0.00132 | -11.5% |
| 1 | 0.01405 | 0.01299 | -0.00106 | -7.5% |
| 2 | 0.01977 | 0.01905 | -0.00072 | -3.6% |
| 3 | 0.02665 | 0.02616 | -0.00049 | -1.8% |
| 4 | 0.03394 | 0.03362 | -0.00032 | -0.9% |
| 5 | 0.04134 | 0.04119 | -0.00015 | -0.4% |
| 6 | 0.04874 | 0.04877 | 0.00003 | 0.1% |

**Table 4.12.e** Comparison of Classical Model of Dimensionless Frequency of Circular Plate for Free-Free Homogeneous Case ($\frac{H}{2h} = 0$)

$\omega / \omega_0$

| | b/a=0 | b/a=0.1 | b/a=0.2 | b/a=0.3 |
|---|---|---|---|---|
| Present Study | 0.01152 | 0.01079 | 0.01032 | 0.01020 |
| Leissa [10] | 0.01098 | 0.01070 | 0.01030 | 0.01019 |
| % error | 4.9% | 0.8% | 0.2% | 0.1% |

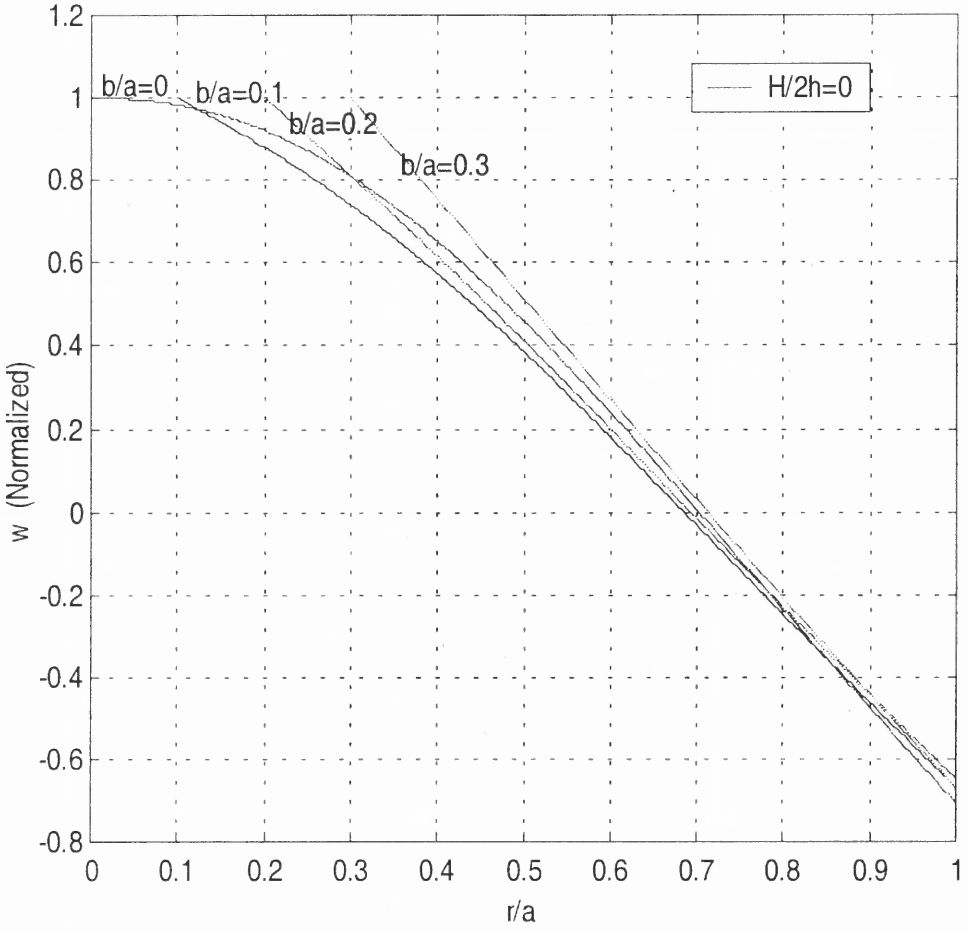


**Figure 4.12.a** Mode Shapes of Homogeneous Classical Model for H/2h=0 with Different Sizes of Holes for Free Outside and Free Inside Case

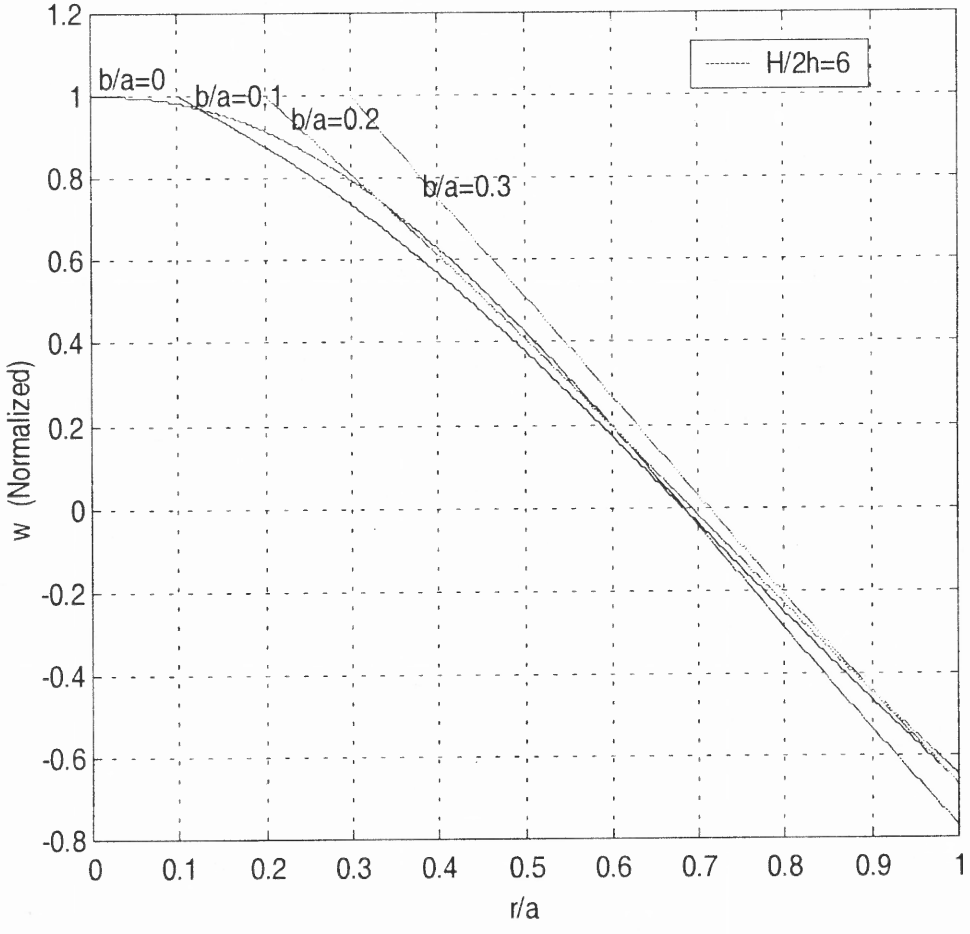


**Figure 4.12.b** Mode Shapes of Homogeneous Classical Model for H/2h=6 with Different Sizes of Holes for Free Outside and Free Inside Case

## 4.4 Comparison of Results for Two Models

The fundamental frequency changes with the rise for the three boundary cases with $\frac{b}{a} = 0.3$ are plotted in Figure 4.13. The solid lines represent the sandwich case while the cross lines represent the homogeneous case, where the notation c-f is the clamped on outside and free on inside, ss-f is the simply supported on outside and free on inside, and f-f is free on inside and free on inside. It can be seen that there are big differences in frequency between the three boundary conditions in the homogeneous case, especially when the rise is small.

The following six figures show the comparison results for the two models with the three boundary cases. In each boundary case, two figures will be presented, in which figure (a) plots the sandwich case and figure (b) plots the homogeneous case. The solid line represents the classical model and the cross line represents the refined model.

As shown Figure 4.14.b of the clamped on outside and free on inside boundary case, the error is insignificantly small between the models when $\frac{b}{a} = 0$ so that the use of the classical theory in calculating the fundamental frequencies is fully justified. This contrasts with the case of the sandwich shell shown in Figure 4.14.a for which results of the classical model deviated from those of the refined model. The same conclusion can be applied in the simply supported on outside and free on inside boundary case as shown in the comparison of Figure 4.15.a and Figure 4.15.b. However, there is no such phenomenon in the free on outside and free on inside boundary case as shown in the comparison of Figure 4.16.a and Figure 4.16.b.

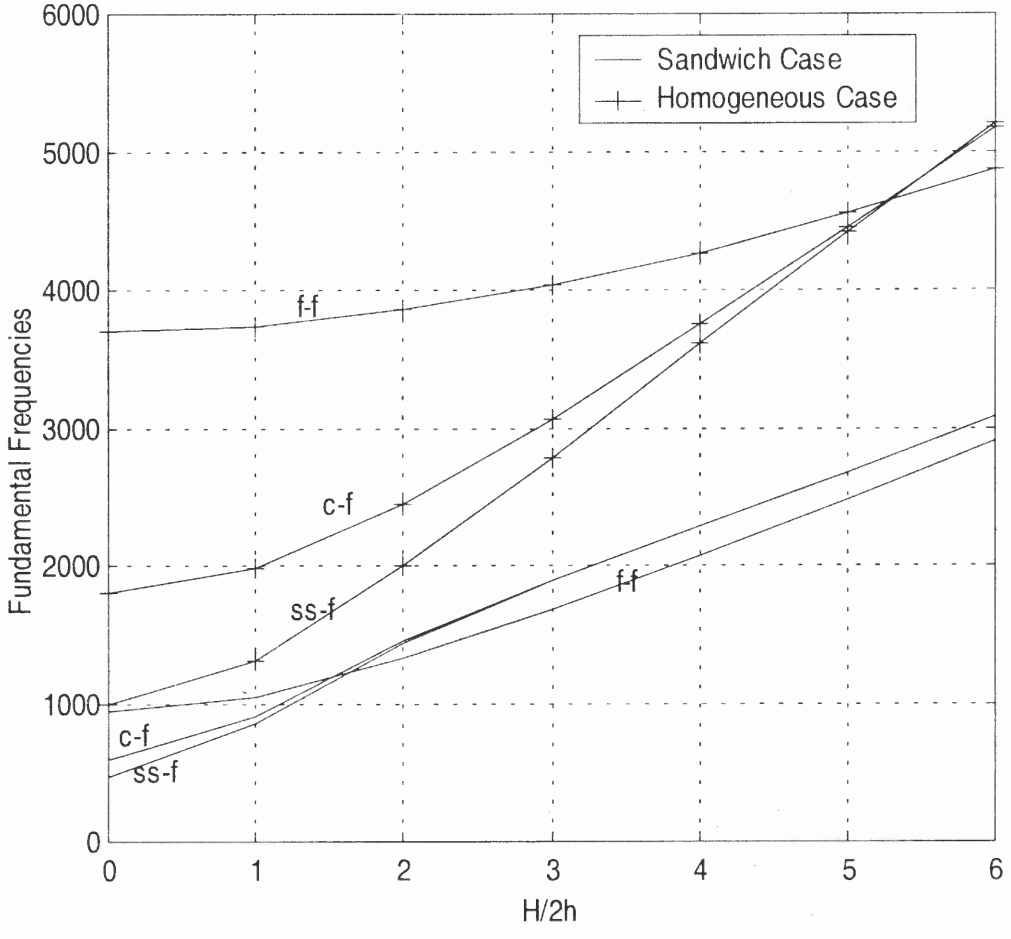


**Figure 4.13** Axisymmetric Vibrations of Refined Model with b/a=0.3 for Clamped, Simply Supported and Free Spherical Shells

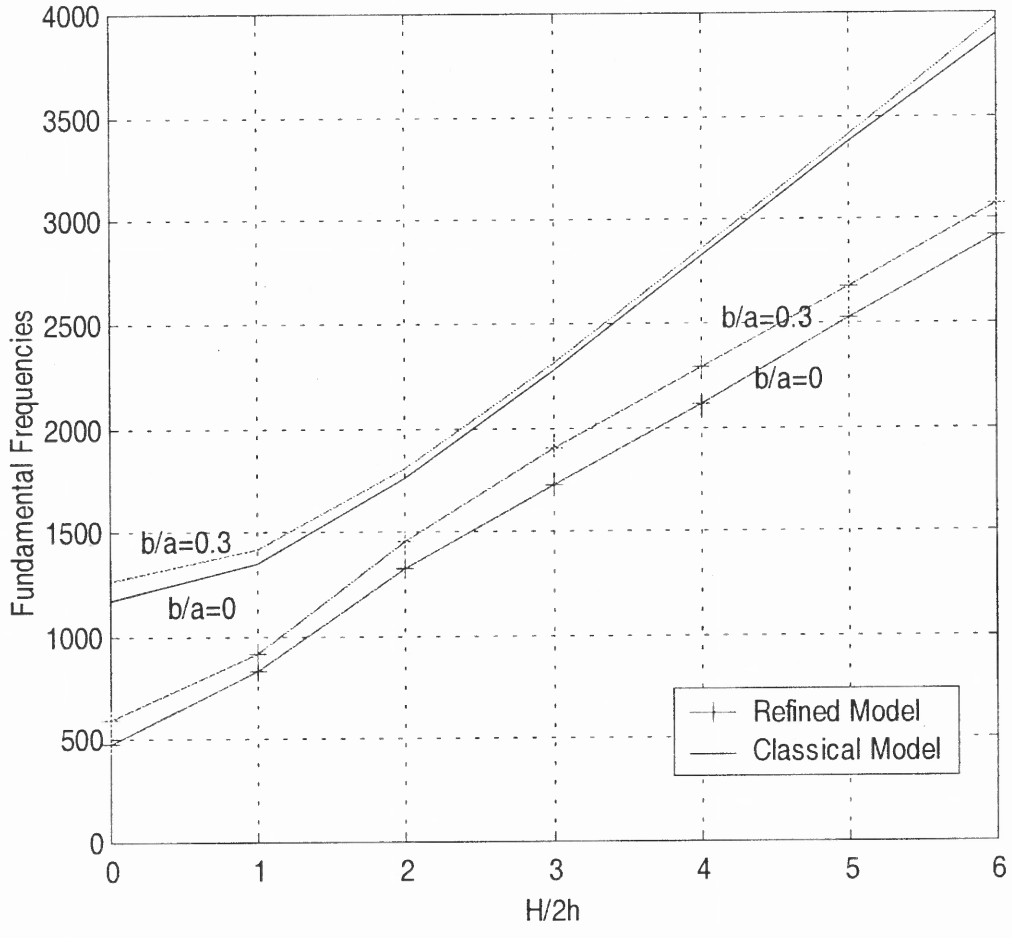


**Figure 4.14.a** Axisymmetric Vibrations of Sandwich Spherical Shells for Clamped Outside and Free Inside Case

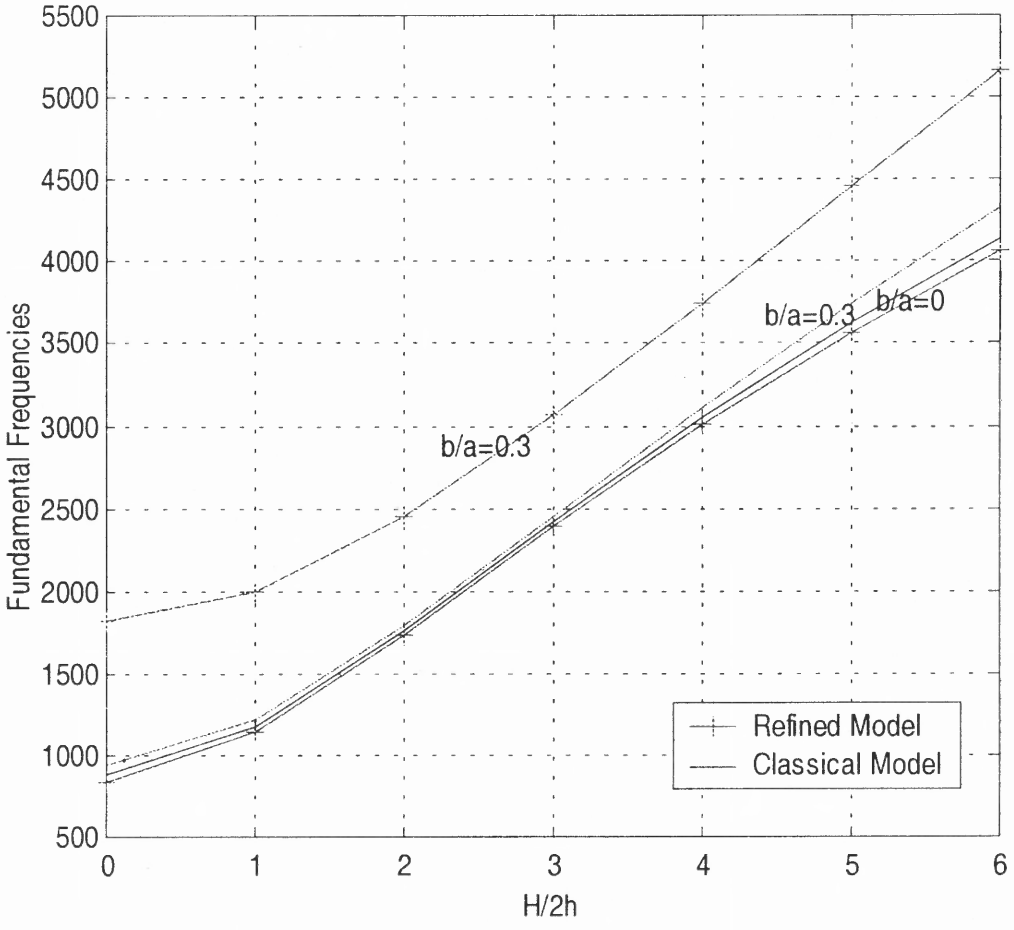


**Figure 4.14.b** Axisymmetric Vibrations of Homogeneous Spherical Shells for Clamped Outside and Free Inside Case

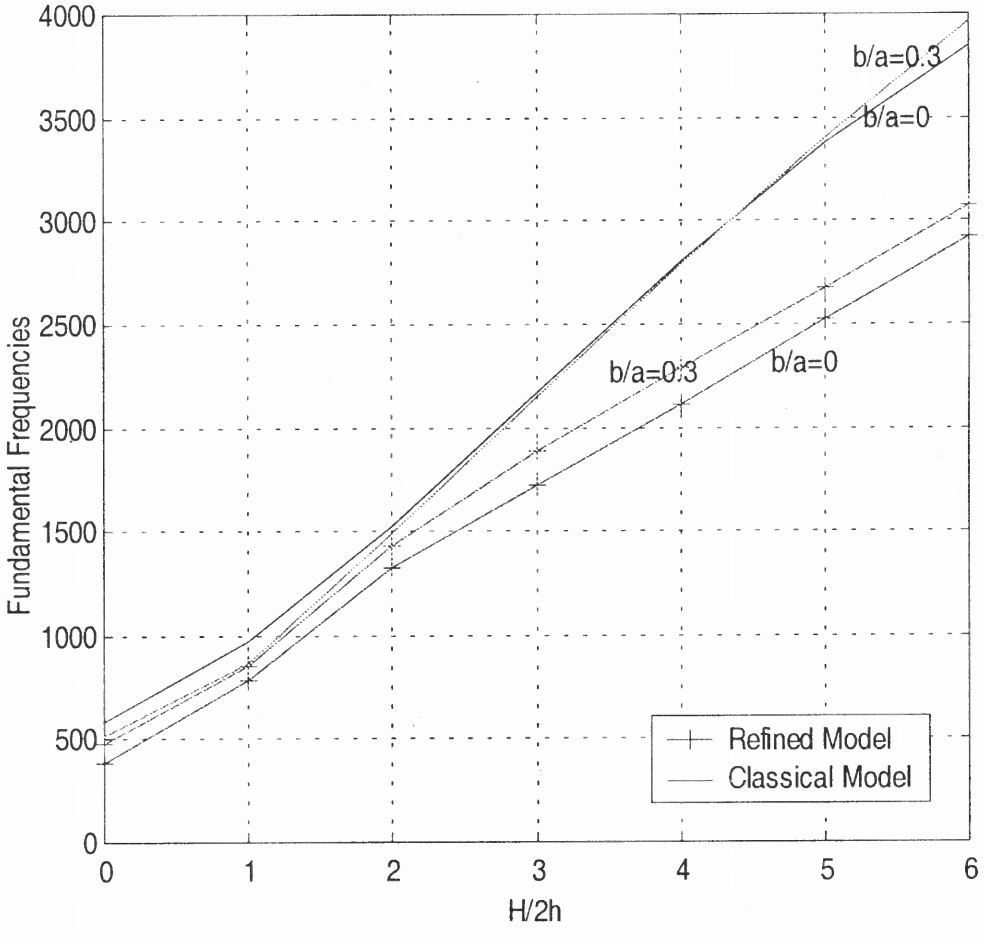


**Figure 4.15.a** Axisymmetric Vibrations of Sandwich Spherical Shells for Simply Supported Outside and Free Inside Case

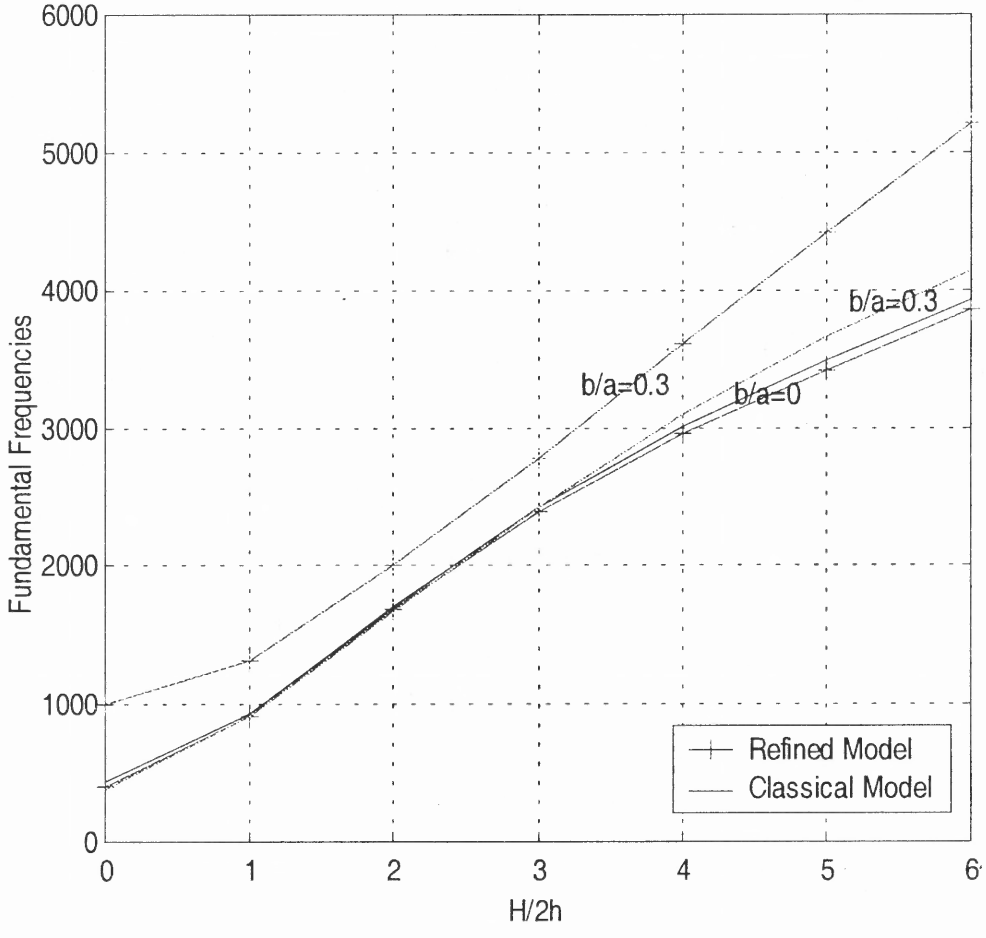


**Figure 4.15.b** Axisymmetric Vibrations of Homogeneous Spherical Shells for Simply Supported Outside and Free Inside Case

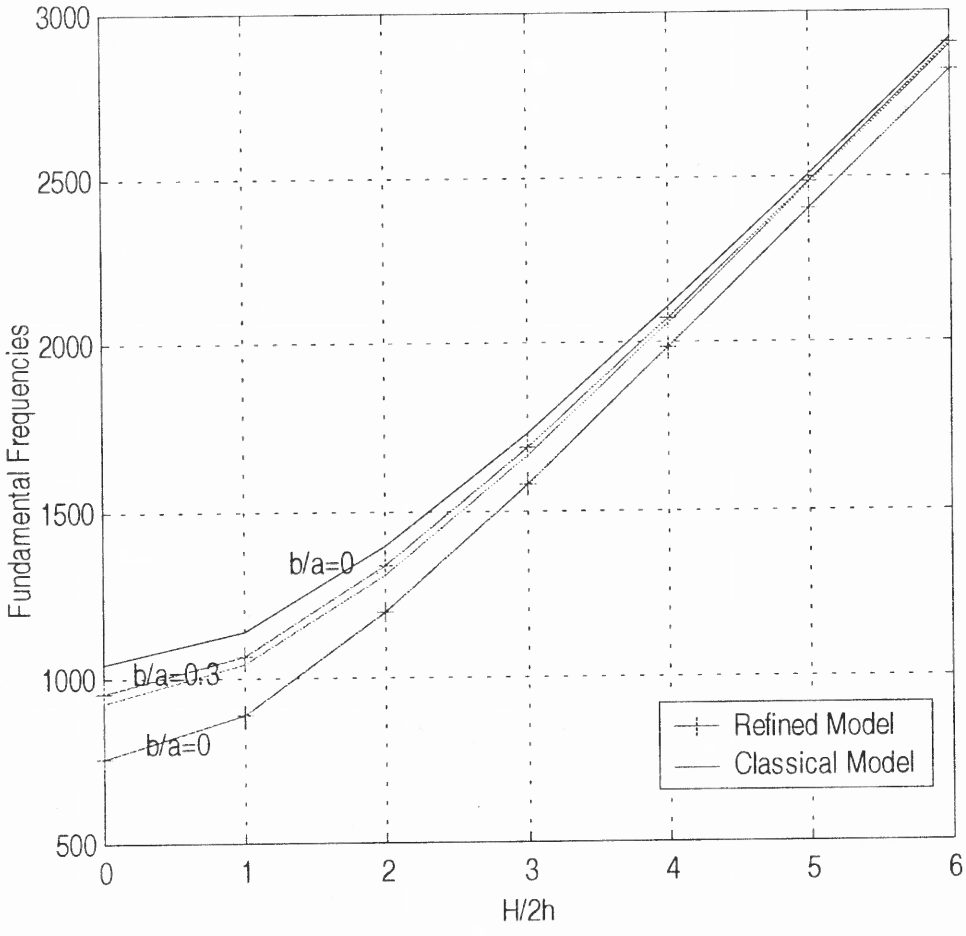


**Figure 4.16.a** Axisymmetric Vibrations of Sandwich Spherical Shells for Free Outside and Free Inside Case

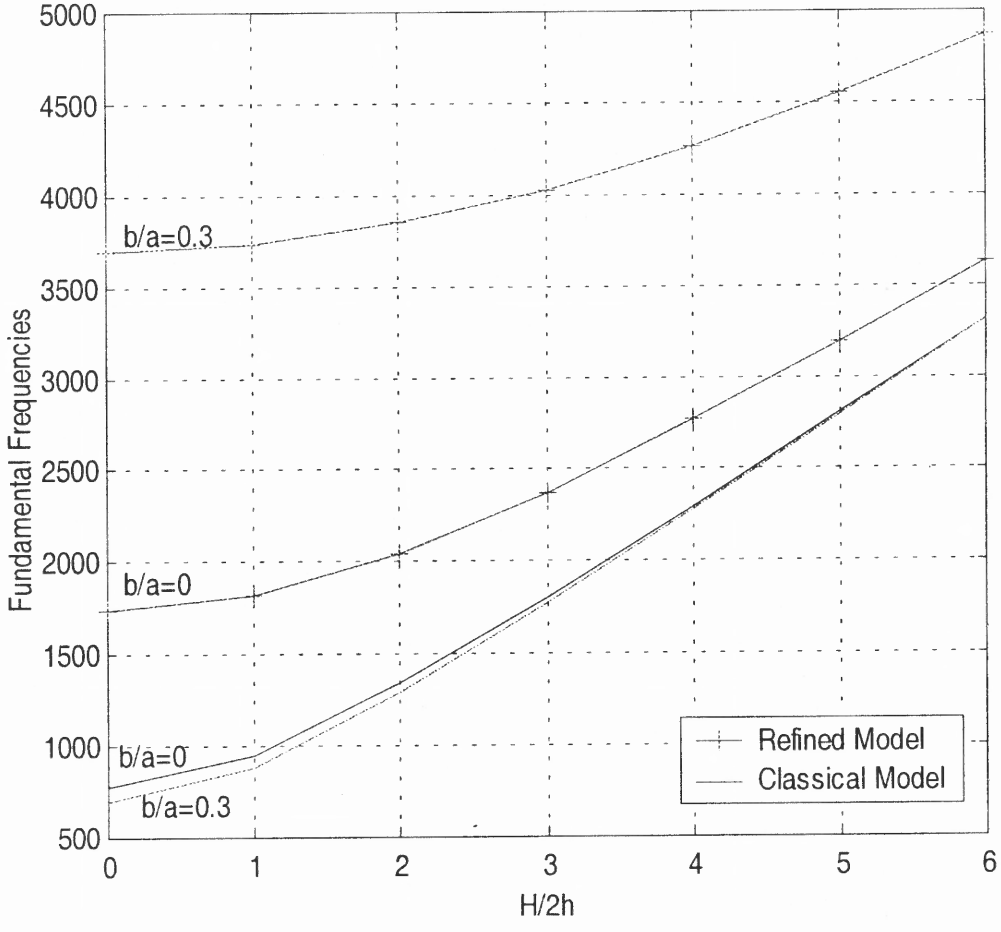


**Figure 4.16.b** Axisymmetric Vibrations of Homogeneous Spherical Shells for Free Outside and Free Inside Case

# CHAPTER 5

# NONLINEAR AXISYMMETRIC VIBRATIONS OF HOMOGENEOUS SPHERICAL SHELLS

## 5.1 Finite Difference Method

In our previous work on linear vibrations of spherical shells, we were able to obtain the numerical solution by means of the shooting method. However, the assumption of the displacement forms $u(r,t) = u(r)e^{i\omega t}$, $\beta(r,t) = \beta(r)e^{i\omega t}$, and $w(r,t) = w(r)e^{i\omega t}$ in (4.1) is no longer valid in the nonlinear case. For example, the classical model for the nonlinear axisymmetric displacement equations of a homogeneous spherical shell were given previously (3.20) as follows:

$$c_1\left(\frac{\partial^2 u}{\partial r^2}+\frac{1}{r}\frac{\partial u}{\partial r}-\frac{1}{r^2}u\right)+c_2\frac{\partial w}{\partial r}+\frac{c_1}{2}\left(\frac{\partial}{\partial r}+\frac{1-\upsilon}{r}\right)\left(\frac{\partial w}{\partial r}\right)^2-c_3\ddot{u}=0, \tag{5.1a}$$

$$c_4\left(\frac{\partial^4 w}{\partial r^4}+\frac{2}{r}\frac{\partial^3 w}{\partial r^3}-\frac{1}{r^2}\frac{\partial^2 w}{\partial r^2}+\frac{1}{r^3}\frac{\partial w}{\partial r}\right)+c_2\left(\frac{\partial u}{\partial r}+\frac{u}{r}+\frac{2w}{R}\right)+\frac{c_2}{2}\left(\frac{\partial w}{\partial r}\right)^2$$

$$-c_1\left(\frac{\partial}{\partial r}+\frac{1}{r}\right)\left[\frac{\partial w}{\partial r}\left(\frac{\partial}{\partial r}+\frac{\upsilon}{r}\right)u+\frac{(1+\upsilon)}{R}\frac{\partial w}{\partial r}w+\frac{1}{2}\left(\frac{\partial w}{\partial r}\right)^3\right]+c_3\ddot{w}=0, \tag{5.1b}$$

where,

$$c_1=\frac{2Eh}{1-\upsilon^2},\qquad c_2=\frac{2Eh(1+\upsilon)}{R(1-\upsilon^2)},\qquad c_3=2\rho h,\qquad c_4=\frac{2Eh^3}{3(1-\upsilon^2)}. \tag{5.1c}$$

Substituting $u(r,t) = u(r)e^{i\omega t}$ and $w(r,t) = w(r)e^{i\omega t}$ into (5.1a) and (5.1b) yields,

$$c_1\left(\frac{d^2 u}{dr^2}+\frac{1}{r}\frac{du}{dr}-\frac{1}{r^2}u\right)e^{i\omega t}+c_2\frac{dw}{dr}e^{i\omega t}+\frac{c_1}{2}\left(\frac{d}{dr}+\frac{1-\upsilon}{r}\right)\left(\frac{dw}{dr}\right)^2(e^{i\omega t})^2+c_3\omega^2 u e^{i\omega t}=0,$$

$$c_4\left(\frac{d^4 w}{dr^4}+\frac{2}{r}\frac{d^3 w}{dr^3}-\frac{1}{r^2}\frac{d^2 w}{dr^2}+\frac{1}{r^3}\frac{dw}{dr}\right)e^{i\omega t}+c_2\left(\frac{du}{dr}+\frac{u}{r}+\frac{2w}{R}\right)e^{i\omega t}+\frac{c_2}{2}\left(\frac{dw}{dr}\right)^2(e^{i\omega t})^2$$

$$-c_1(\frac{d}{dr}+\frac{1}{r})[\frac{dw}{dr}(\frac{d}{dr}+\frac{\upsilon}{r})u(e^{i\omega t})^2+\frac{(1+\upsilon)}{R}\frac{dw}{dr}w(e^{i\omega t})^2+\frac{1}{2}(\frac{dw}{dr})^3(e^{i\omega t})^3]$$

$$-c_3\omega^2 we^{i\omega t}=0.$$

Due to the nonlinear nature of Equations (5.1), the time dependence through $e^{i\omega t}$ cannot be eliminated.

In order to determine the solution of (5.1), a finite difference method is employed. Length and time are divided into a grid and we let,

$$u(\varepsilon+i\Delta r, j\Delta t)=u_i^j, \tag{5.2a}$$

$$w(\varepsilon+i\Delta r, j\Delta t)=w_i^j. \tag{5.2b}$$

$\varepsilon$ is the size of the hole, $i=0,1,.....,N$, and $j=0,1,.....,M$, $\Delta r=\frac{1-\varepsilon}{N}$, $N$ is the number of divisions, and $\Delta t=\frac{1}{M}$ is the time increment.

The governing differential equations (5.1) are approximated by using of the following formulas [16, 17, 18]:

$$\frac{\partial u(r,t)}{\partial r}=\frac{u_{i+1}^j-u_{i-1}^j}{2\Delta r}, \qquad \frac{\partial^2 u(r,t)}{\partial r^2}=\frac{u_{i+1}^j-2u_i^j+u_{i-1}^j}{\Delta r^2},$$

$$\frac{\partial^2 u(r,t)}{\partial t^2}=\frac{u_i^{j+1}-2u_i^j+u_i^{j-1}}{\Delta t^2}, \qquad \frac{\partial w(r,t)}{\partial r}=\frac{w_{i+1}^j-w_{i-1}^j}{2\Delta r},$$

$$\frac{\partial^2 w(r,t)}{\partial r^2}=\frac{w_{i+1}^j-2w_i^j+w_{i-1}^j}{\Delta r^2}, \qquad \frac{\partial^3 w(r,t)}{\partial r^3}=\frac{w_{i+2}^j-2w_{i+1}^j+2w_{i-1}^j-w_{i-2}^j}{2\Delta r^3},$$

$$\frac{\partial^4 w(r,t)}{\partial r^4}=\frac{w_{i+2}^j-4w_{i+1}^j+6w_i^j-4w_{i-1}^j+w_{i-2}^j}{\Delta r^4}, \qquad \frac{\partial^2 w(r,t)}{\partial t^2}=\frac{w_i^{j+1}-2w_i^j+w_i^{j-1}}{\Delta t^2}, \tag{5.2c}$$

where the subscript $i$ represents the radial position while the superscript $j$ represents the time position. Replacing (5.1) with the above approximation (5.2) and solving for the highest time increment, $u_i^{j+1}$, $w_i^{j+1}$ in terms of the lower time increment, we have the equations:

$$u_i^{j+1} = f_1(u_s^j, u_s^{j-1}, w_s^j), \tag{5.3a}$$

$$w_i^{j+1} = f_2(u_s^j, w_s^{j-1}, w_s^j), \tag{5.3b}$$

where $u_s = u_{i+1}, u_i, u_{i-1}$, and $w_s = w_{i+2}, w_{i+1}, w_i, \ldots$.etc., $f_1$ and $f_2$ contain all terms at time step $j$ and $j-1$.

Here we have a two time step method. We need the values of the variables at time $j-1$, and $j$ to find the values at time $j+1$ in (5.3). Similarly, the boundary conditions are also approximated by using (5.2c) since they involve derivatives. Let the initial condition for the rise, $\frac{H}{2h} = 0$, be the analytical solutions [10],

$$u(r,0) = A_1 J_1(\omega r) + A_2 Y_1(\omega r), \tag{5.4a}$$

$$w(r,0) = A_0 J_0(kr) + B_0 Y_0(kr) + C_0 I_0(kr) + D_0 K_0(kr), \tag{5.4b}$$

where $k^4 = \frac{c_3}{c_4}\omega^2$, $J_0, J_1, Y_0, Y_1, I_0$, and $K_0$ are Bessel functions.

We take this initial condition to be the same as that chosen by [10] for the uncoupled version of (5.1).

To start the process, we assign the initial condition (5.4) to both $j = 0$ and $j = 1$ time steps in order to obtain the numerical solution at time step $j = 2$. Then continue the process to obtain solutions at any time step $j$. The constants $A_1, A_2, A_0, B_0, C_0$, and $D_0$ in (5.4) are calculated so that they satisfy the boundary conditions. We note that the

constants are going to be functions of the natural frequency $\omega$. In order to find the period $T$, we iterate in time and find how long it will take for the solution to come back to the initial curve. That is when $(\underline{u}^{j+N\Delta t}, \underline{w}^{j+N\Delta t})$ is almost the same as $(\underline{u}^{j}, \underline{w}^{j})$. Since $\Delta t$ is taken to be small, we will have $\left\|(\underline{u}^{j+N\Delta t}, \underline{w}^{j+N\Delta t}) - (\underline{u}^{j}, \underline{w}^{j})\right\|$ is small. Then the period $T$ is approximately equal to $N\Delta t$. From Figure 5.1.a, once the periodicity occurs, i.e. the period $T = \frac{2\pi}{\omega}$, the natural frequency $\omega$ is found.

## 5.2 Comparison with Results from Shooting Method

Before analyzing the nonlinear vibrations, we first use the finite difference method to solve for the linear vibrations and compare the results with those obtained by the shooting method presented in Chapter 4. We consider the clamped outer boundary and free inner boundary of homogeneous case of the classical model with the dimensionless hole size $\varepsilon = 0.2$ in Section (4.3.1). We then compare the linear version in Equations (5.1) by using the finite difference method.

Table 5.1 shows the results from the two methods. Figure 5.1.a through Figure 5.1.d represent the plots from the finite difference method (F.D.M.). The magnitude of the deflections is normalized to be one, as in the shooting method.

**Table 5.1** Comparison of Results for Linear Vibration

| H/2h with $\varepsilon = 0.2$ | $\omega = 2\pi / T$ Shooting Method | $\omega_w = 2\pi / T$ F.D.M. | % error |
|---|---|---|---|
| 0 | 863.1 | 842.3 | 2.4 % |
| 1 | 1151.9 | 1104.3 | 4.1 % |
| 2 | 1742.9 | 1712.0 | 1.8 % |
| 3 | 2396.1 | 2362.1 | 1.4 % |

It should be noted that by using the finite difference method, the natural frequencies of the $u$ and $w$ directions are found to be different. In Table 5.1, $\omega_w$ is the natural frequency in the $w$ direction, which is almost the same as the natural frequency $\omega$ found by the shooting method. But the natural frequency $\omega_u$ in the $u$ direction found by the finite difference method is equal to 24,272 cps with the rise $\frac{H}{2h} = 0 \text{ to } 3$, plotted in Figure 5.1.a. From the numerical results, we can stipulate that the value of $w(r, t)$ did not effect $u(r, t)$ in Equation (5.1a). Therefore Equation (5.1a) can be solved for $u(r, t)$. It is inserted in Equation (5.1b) as a known forcing term. Then Equation (5.1b) is solved as a nonhomogeneous equation. The solution for $w(r, t)$ would then be a linear combination of the homogeneous solution and the particular solution. However, we did not follow this path, instead we solve the simultaneous equation using a finite difference scheme. From Figures 5.1.b through 5.1.d, we observe that the periodicity reduces the accuracy when the rise $\frac{H}{2h}$ is increased. From [1], Koplik concluded that the $\omega_u$ is the higher predominantly extensional mode in both the uncoupled and coupled vibrations.

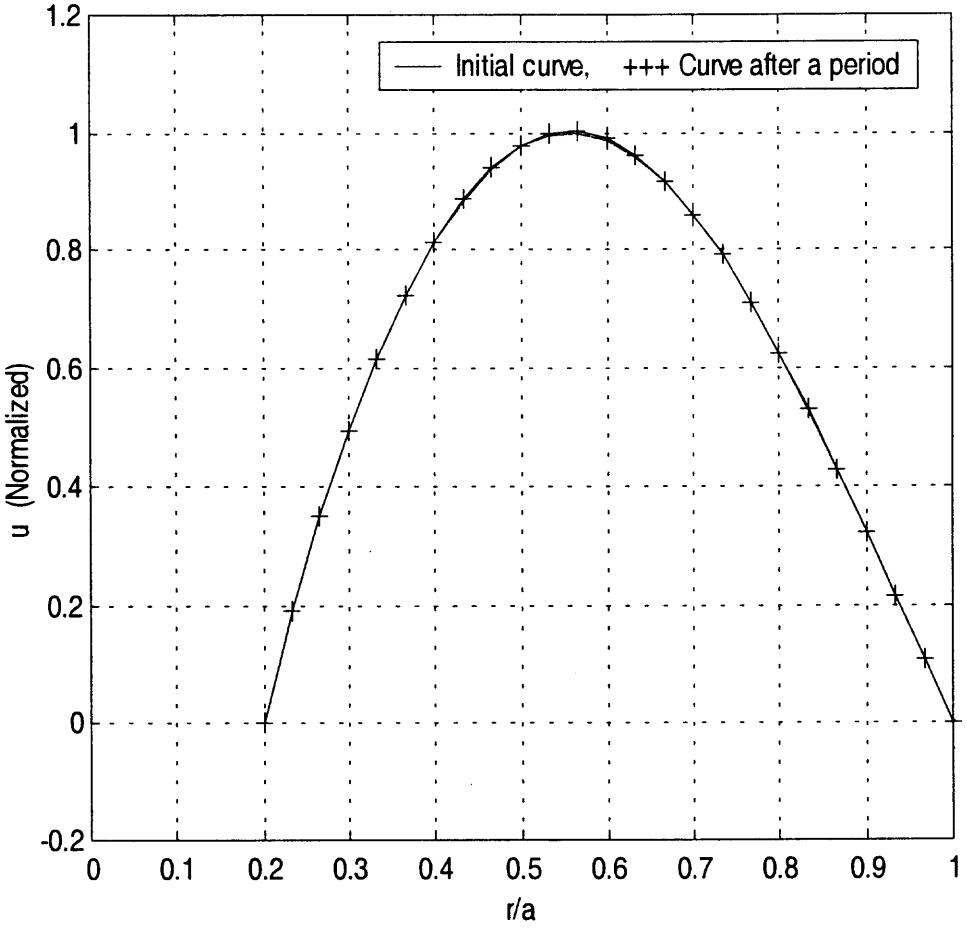


**Figure 5.1.a** Linear Vibrations in the *u* Direction with H/2h = 0 to 3

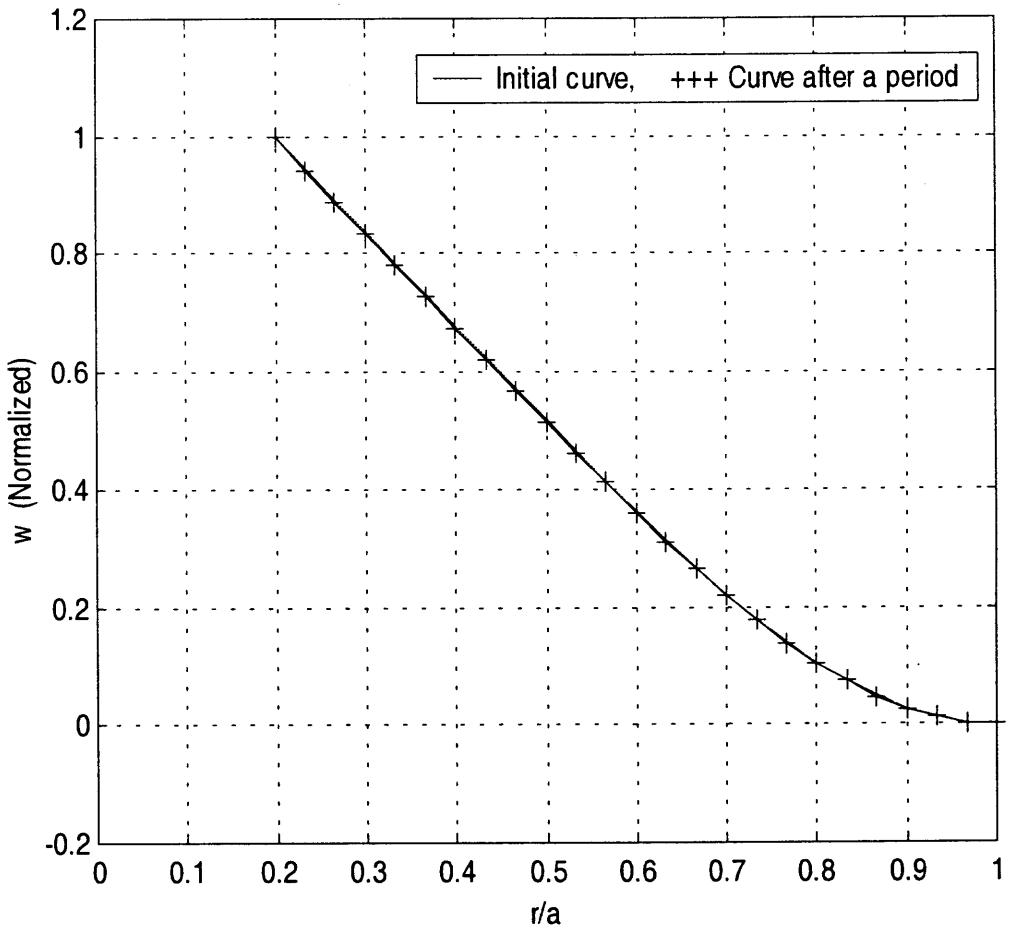


**Figure 5.1.b** Linear Vibrations in the *w* Direction with H/2h = 0

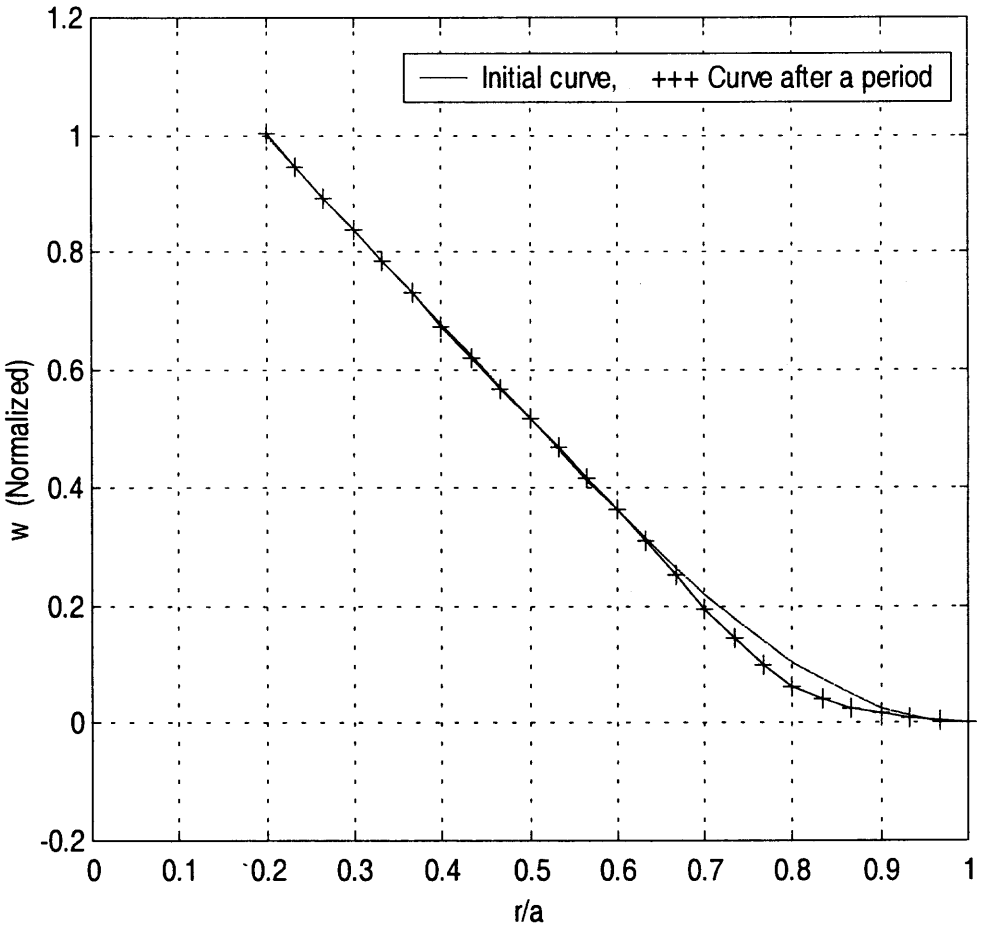


**Figure 5.1.c** Linear Vibrations in the *w* Direction with H/2h = 1

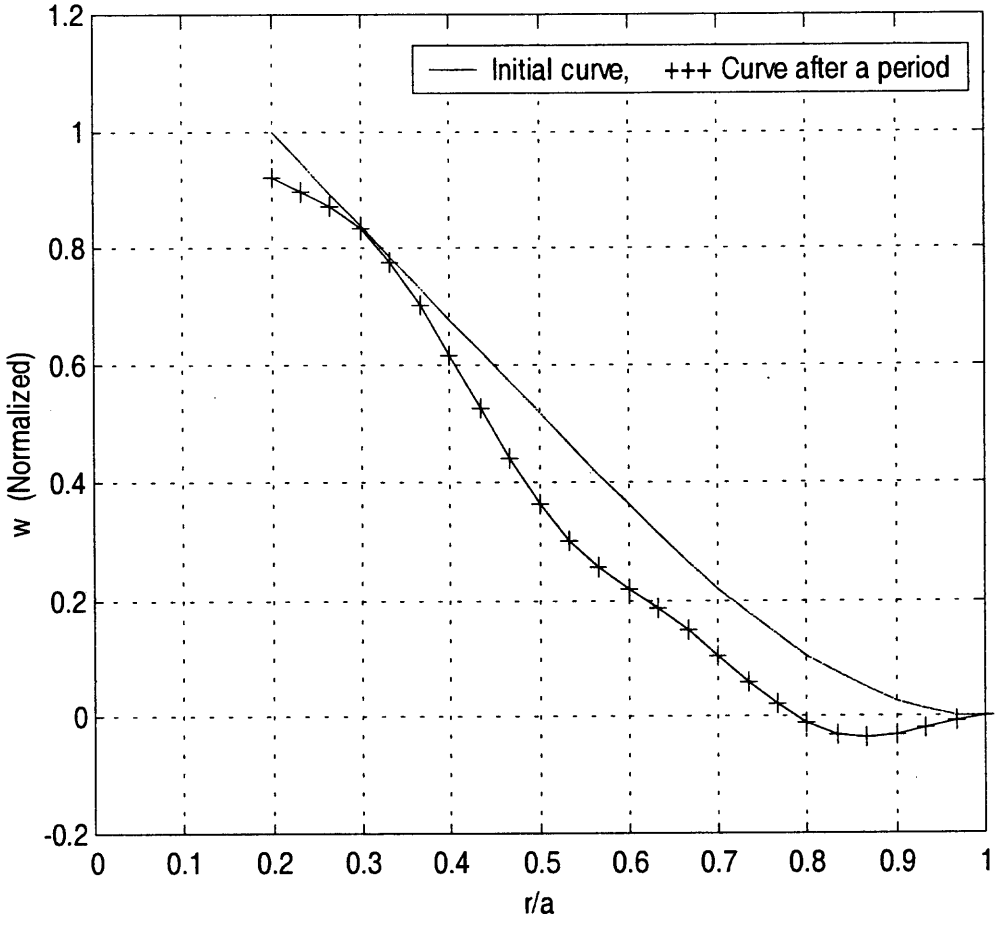


**Figure 5.1.d** Linear Vibrations in the *w* Direction with H/2h = 3

## 5.3 Comparison with Results of Linear Vibrations

This section presents the results of nonlinear vibrations of Equations (5.1) with the same boundary conditions used as in Section (5.2). Table 5.2 and Figure 5.2.a through Figure 5.2.d show the results for the nonlinear vibrations. We found that the nonlinear problem only behaves well when the magnitude of the deflection is small, say in the order of 0.01, as shown in the following four figures. Also, from Table 5.2 and Figure 5.2.b through Figure 5.2.d, we have periodicity when the magnitude of the deflections is small as is expected. Hence, we only expect periodicity when the variables in the nonlinear problem are small. We also observe that the natural frequency $\omega_u$ in the $u$ direction is equal to 23,489 cps with the rise $\frac{H}{2h} = 0 \text{ to } 3$, plotted in Figure 5.2.a. As the magnitude of the deflection increases, we loose periodicity. In other words, the magnitude does not return to the original position.

**Table 5.2** Comparison of Results for Nonlinear Vibration

| H/2h with $\dot{\varepsilon} = 0.2$ | $\omega_w = 2\pi / T$ Linear Case | $\omega_w = 2\pi / T$ Nonlinear Case |
|---|---|---|
| 0 | 842.3 | 1005.3 |
| 1 | 1104.3 | 1132.1 |
| 2 | 1712.0 | *Lack of Periodicity |
| 3 | 2362.1 | *Lack of Periodicity |

* Lack of Periodicity means the curve did not o back to the initial curve, see Figure 5.2.d.

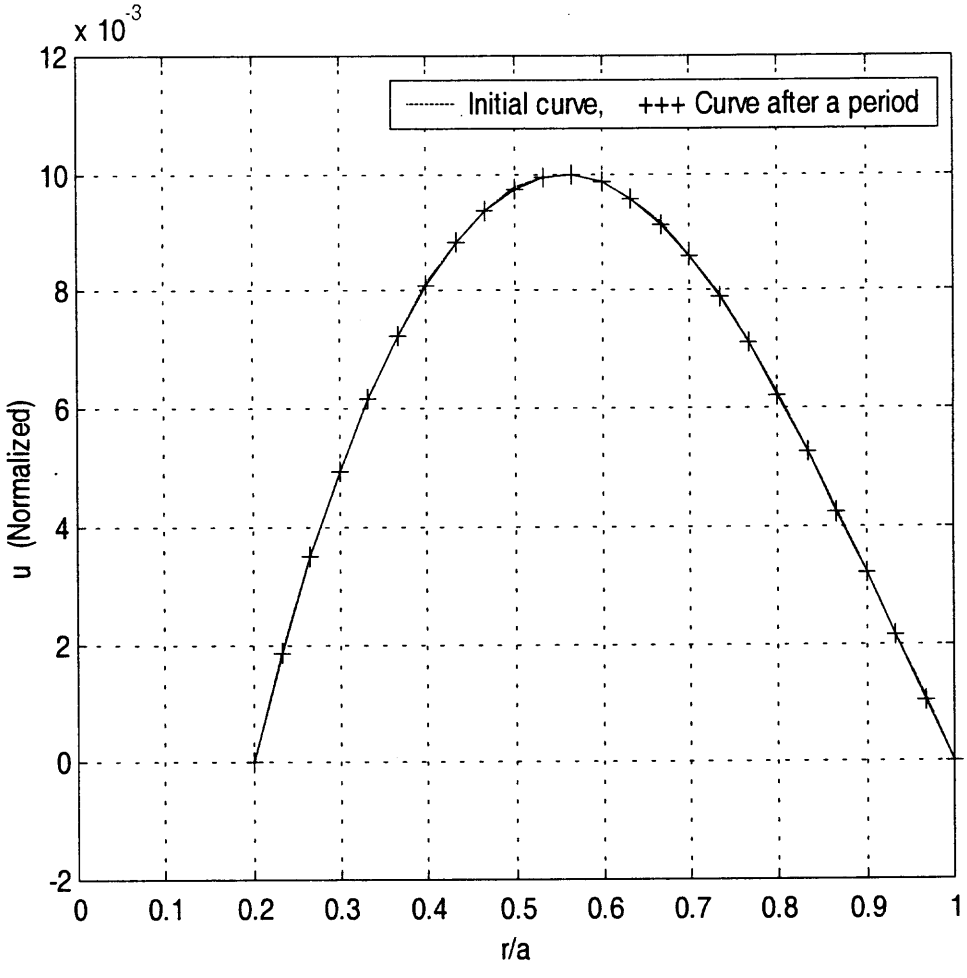


**Figure 5.2.a** Nonlinear Vibrations in the *u* Direction with H/2h = 0 to 3

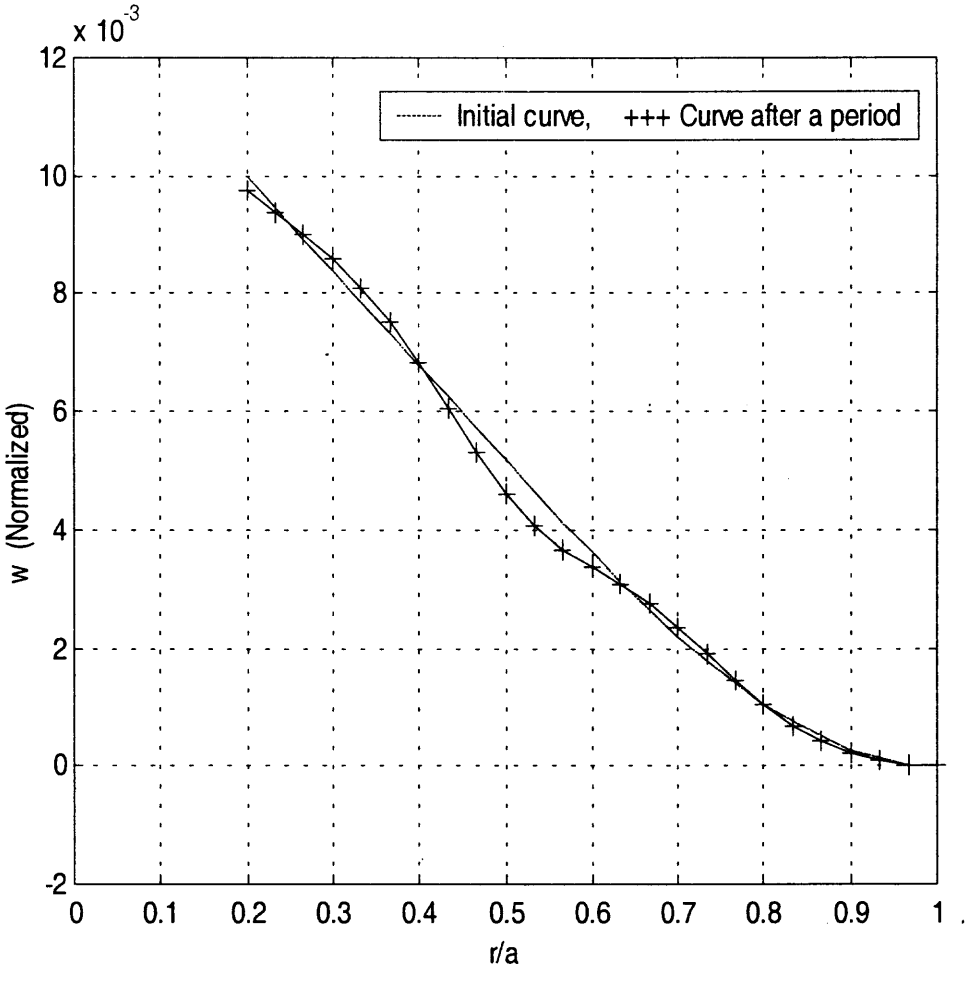


**Figure 5.2.b** Nonlinear Vibrations in the *w* Direction with H/2h = 0

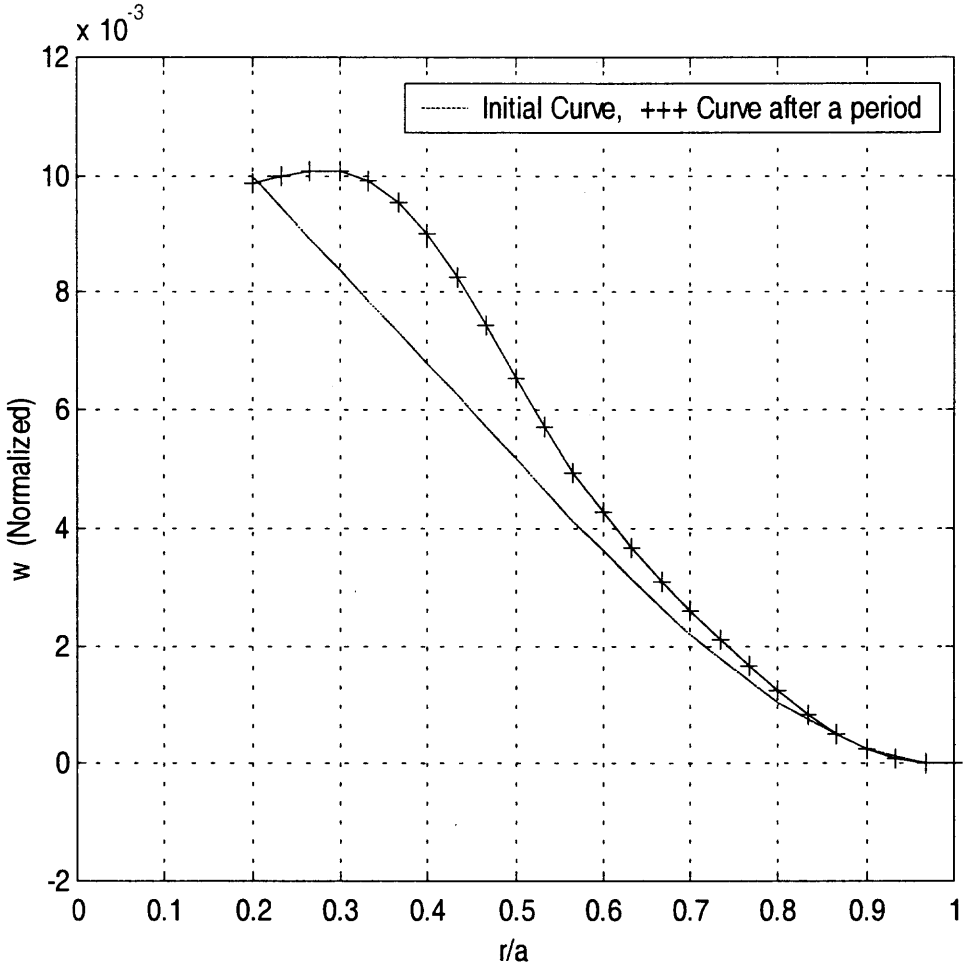


**Figure 5.2.c** Nonlinear Vibrations in the *w* Direction with H/2h = 1

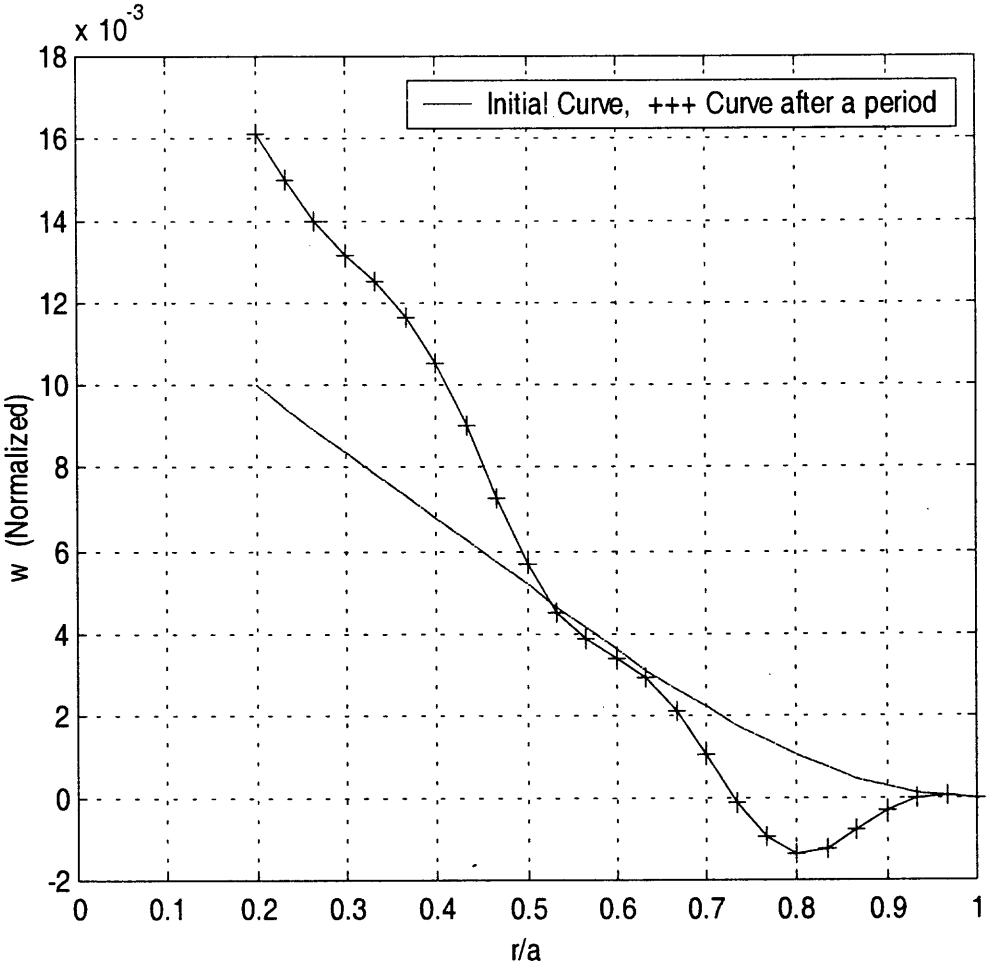


**Figure 5.2.d** Nonlinear Vibrations in the *w* Direction with H/2h = 3

# CHAPTER 6

# CONCLUSIONS

By starting with Hamilton's principle as well as the derivation based on [1, 2], we have succeeded in finding the equations for the solution for the natural frequencies of linear and nonlinear shallow spherical shells. The linear vibration case involves the analysis of both the sandwich and homogeneous spherical shells while the nonlinear equation case deals with the vibration of the homogeneous shells.

In the linear case, by using the Shooting Method, we assume the natural frequency is the same in all the displacement directions, $\beta$, $u$, or $w$. The analysis is applied for shells with varied curvature and size of central hole for three sets of outer boundary conditions, namely, clamped, simply supported and free. In all cases the inside edge condition remains free.

It is observed that the fundamental frequencies are extremely sensitive to curvature demonstrating increases in the frequencies of over 100% when comparing zero rise to the maximum rise, for all the boundary cases of both models. We have demonstrated that the fundamental frequencies increase with the bigger holes in the clamped boundary cases of both models, but only in simply supported, and free outer boundary cases of the refined model. It is noted that when the central hole is equal to zero, the classical model can be employed giving the same results as the refined model for the homogeneous case with clamped and simply supported outer boundary conditions. However, we see that the fundamental frequencies of the sandwich case in the classical model are far higher than those in the refined model. It is also observed that with the central hole of dimensionless radius, $\frac{b}{a} = 0.3$, the refined model for both sandwich and

homogeneous cases should be applied to find the frequency, except for the sandwich case of the free outer boundary condition, since the frequency calculated by the classical model gives results which deviate significantly from those of the refined model.

In the nonlinear case, the finite difference method is employed to analyze the natural frequency using the classical model for the homogeneous case with a clamped outer boundary condition and a dimensionless hole size of $\varepsilon = 0.2$. The period, $T$ is determined numerically, where the frequency $\omega$ is equal $\frac{2\pi}{T}$. The numerical results show that the fundamental frequencies are different in the $u$ and $w$ directions in either the uncoupled or coupled case. This leads to the conclusion that the assumption of the same natural frequency in each displacement direction is a very specific condition, consistent with the assumption of most of the previous researchers. As pointed out further, analytic work is needed to substantiate that the frequencies of the extension and transverse directions are not the same.

It is found that the nonlinear vibration of the spherical shell has a natural frequency, only in the case that the magnitude of the deflection is small, in the order of 0.01. We observed that the periodicity in the $w$ direction is significantly reduced in accuracy when the rise is equal to 3. However, the periodicity in the $u$ direction is much more stable. The natural frequency $\omega_u$ is over 20,000 cps, while the natural frequency in the $w$ direction, $\omega_w$ is around 1,000 cps.

In conclusion, it is noted that the shooting method is a powerful tool in determining the natural frequency in the linear vibration of shallow spherical shells. It may be further employed to solve for nonshallow shells. However, employing this method is based on the specific assumption that the natural frequency is the same in all

the directions. Thus, a larger research effort would be required in solving the problems in which different frequencies are assumed in different displacement directions.

## APPENDIX A

## DERIVATION OF STRAIN-DISPLACEMENT RELATIONS

In this appendix, the theory of elasticity [7, 12] is employed to derive the strain-displacement relations for the homogeneous spherical shell.

Firstly, the infinitesimal distance of an undeflected state of the spherical shell has the form [7]:

$$ds^2 = (R+z)^2 d\phi^2 + (R+z)^2 \sin^2\phi d\theta^2 + dz^2,$$

or $$ds^2 = g_{\phi\phi} d\phi^2 + g_{\theta\theta} d\theta^2 + g_{zz} dz^2, \qquad \text{(A1)}$$

where, $g_{\phi\phi} = (R+z)^2$, $g_{\theta\theta} = (R+z)^2 \sin^2\phi$, $g_{zz} = 1$. (A2)

Let $P_0$ and $P_1$ be two neighboring points in an unstrained state. After deformation, $P_o$ and $P_1$ take the positions as $P_0'$ and $P_1'$, respectively. We assume the coordinates of the points $P_0$ and $P$ are $\alpha$ and $\alpha + d\alpha$ respectively, where $\alpha$ represents the coordinates, $\phi$, $\theta$ or $z$. The coordinates of the points $P_0'$ and $P_1'$ will then be denoted by $\alpha + \xi$ and $\alpha + \xi + d\alpha + d\xi$, where $\xi$ is the coordinate change.

Hence, the infinitesimal distance is deflected in the following state:

$$ds'^2 = (R+z+\xi_z)^2 (d\phi + d\xi_\phi)^2 + (R+z+\xi_z)^2 \sin^2(\phi+\xi_\phi)(d\theta + d\xi_\theta)^2 + (dz + d\xi_z)^2$$

where $U_\phi = (R+z)\xi_\phi$, $U_\theta = (R+z)\sin\phi\xi_\theta$, $U_z = \xi_z$. (A3)

By taking the axisymmetric (torsionless) simplifications , i.e. $U_\theta = 0$, we get,

$\xi_\theta = 0$, $d\xi_\theta = 0$ , and independence with $\theta$.

Taking the first order differential approximation [7], we have,

$$d\xi_\phi = \frac{\partial \xi_\phi}{\partial \phi} d\phi + \frac{\partial \xi_\phi}{\partial \theta} d\theta + \frac{\partial \xi_\phi}{\partial z} dz = \frac{\partial \xi_\phi}{\partial \phi} d\phi + \frac{\partial \xi_\phi}{\partial z} dz,$$

$$d\xi_\theta = \frac{\partial \xi_\theta}{\partial \phi} d\phi + \frac{\partial \xi_\theta}{\partial \theta} d\theta + \frac{\partial \xi_\theta}{\partial z} dz = 0, \tag{A4}$$

$$d\xi_z = \frac{\partial \xi_z}{\partial \phi} d\phi + \frac{\partial \xi_z}{\partial \theta} d\theta + \frac{\partial \xi_z}{\partial z} dz = \frac{\partial \xi_z}{\partial \phi} d\phi + \frac{\partial \xi_z}{\partial z} dz .$$

In order to have the approximation be consistent with linear elasticity theory, the following assumptions are further taken,

$$\xi_i^2 = 0 \text{ or } d\xi_i^2 = 0 \quad \text{where } i = \phi \text{ or } z,$$

$$\text{and} \quad \sin(\phi + \xi_\phi) = \sin\phi\cos\xi_\phi + \cos\phi\sin\xi_\phi \approx \sin\phi + \cos\phi\xi_\phi . \tag{A5}$$

Therefore, (A3) becomes,

$$\begin{aligned} ds'^2 &= [(R+z)^2 + 2(R+z)\xi_z][d\phi^2 + 2d\phi d\xi_\phi] \\ &\quad + [(R+z)^2 + 2(R+z)\xi_z][\sin^2\phi + 2\sin\phi\cos\phi\xi_\phi]d\theta^2 \\ &\quad + [dz^2 + 2dzd\xi_z] \\ &= [(R+z)^2 + 2(R+z)\xi_z][d\phi^2 + 2d\phi(\frac{\partial \xi_\phi}{\partial \phi}d\phi + \frac{\partial \xi_\phi}{\partial z}dz)] \\ &\quad + [(R+z)^2 + 2(R+z)\xi_z][\sin^2\phi + 2\sin\phi\cos\phi\xi_\phi]d\theta^2 \\ &\quad + [dz^2 + 2dz(\frac{\partial \xi_z}{\partial \phi}d\phi + \frac{\partial \xi_z}{\partial z}dz)] \end{aligned}$$

$$\text{or,} \quad ds'^2 = G_{\phi\phi}d\phi^2 + G_{\theta\theta}d\theta^2 + G_{zz}dz^2 + G_{\phi z}d\phi dz , \tag{A6}$$

where,

$$G_{\phi\phi} = [(R+z)^2 + 2(R+z)\xi_z][1 + 2\frac{\partial \xi_\phi}{\partial \phi}] \approx (R+z)^2 + 2(R+z)^2\frac{\partial \xi_\phi}{\partial \phi} + 2(R+z)\xi_z ,$$

$$G_{\theta\theta} \approx [(R+z)^2 + 2(R+z)\xi_z]\sin^2\phi + 2(R+z)^2\sin\phi\cos\phi\xi_\phi , \tag{A7}$$

$$G_{zz} = 1 + 2\frac{\partial \xi_z}{\partial z},$$

$$G_{\phi z} = 2(R+z)^2 \frac{\partial \xi_\phi}{\partial z} + 2\frac{\partial \xi_z}{\partial \phi}.$$

From [12], we have the following formulas,

Normal strains (Linear case): $e_{ii} = \frac{1}{2}\frac{G_{ii} - g_{ii}}{g_{ii}}$ where $i = \phi, \theta, z$, (A8a)

Shear strain (Linear case): $e_{ij} = \frac{1}{2}\frac{G_{ij}}{\sqrt{g_{ii} g_{jj}}}$ where $i, j = \phi, \theta$ or $z$. (A8b)

From (A6), since $G_{\phi\theta} = G_{\theta z} = 0$, we get,

$$e_{\phi\theta} = 0, \quad e_{\theta z} = 0. \tag{A9}$$

Substituting (A2) and (A7) with (A3) into (A8) yields,

$$e_{\phi\phi} = \frac{1}{2}\frac{G_{\phi\phi} - g_{\phi\phi}}{g_{\phi\phi}} = \frac{1}{2}\left[\frac{2(R+z)^2 \frac{\partial}{\partial \phi}\left(\frac{U_\phi}{R+z}\right) + 2(R+z)U_z}{(R+z)^2}\right] = \frac{1}{(R+z)}\left[\frac{\partial U_\phi}{\partial \phi} + U_z\right],$$

$$e_{\theta\theta} = \frac{1}{2}\frac{G_{\theta\theta} - g_{\theta\theta}}{g_{\theta\theta}} = \frac{1}{2}\left[\frac{2(R+z)^2 \sin\phi\cos\phi \frac{U_\phi}{(R+z)} + 2(R+z)U_z \sin^2\phi}{(R+z)^2 \sin^2\phi}\right]$$

$$= \frac{1}{(R+z)}[U_\phi \cot\phi + U_z],$$

$$e_{zz} = \frac{1}{2}\frac{G_{zz} - g_{zz}}{g_{zz}} = \frac{1}{2}\left(2\frac{\partial U_z}{\partial z}\right) = \frac{\partial U_z}{\partial z},$$

$$e_{\phi z} = \frac{1}{2}\frac{G_{\phi z}}{\sqrt{g_{\phi\phi} g_{zz}}} = \frac{1}{2}\left[\frac{2(R+z)^2 \frac{\partial}{\partial z}\left(\frac{U_\phi}{R+z}\right) + 2\frac{\partial U_z}{\partial \phi}}{(R+z)}\right] = \frac{\partial U_\phi}{\partial z} - \frac{U_\phi}{R+z} + \frac{1}{(R+z)}\frac{\partial U_z}{\partial \phi}.$$

(A10)

Employing the thin shell assumption the following is taken as,

$$(R+z) = R(1+\frac{z}{R}) \approx R. \tag{A11}$$

Assuming the shell to be shallow gives,

$$\sin\phi \approx \phi, \quad \cot\phi \approx \frac{1}{\phi}, \quad R\phi = r, \quad \frac{1}{R}\frac{\partial}{\partial\phi} \approx \frac{\partial}{\partial r}. \tag{A12}$$

By taking the axisymmetric (torsionless) assumptions, the displacement form is,

$$\begin{aligned} &U_\phi(\phi,z,t) \rightarrow U_r(r,z,t) = u(r,t) + z\beta(r,t), \\ &U_\theta(\phi,z,t) \rightarrow U_\theta(r,z,t) = 0, \\ &U_z(\phi,z,t) \rightarrow U_z(r,z,t) = w(r,t). \end{aligned} \tag{A13}$$

Substituting (A13) with (A11) and (A12) into (A10), the strain – displacement (linear) relations become,

$$\begin{aligned} &e_{rr} = \frac{\partial U_r}{\partial r} + \frac{U_z}{R} = \frac{\partial u}{\partial r} + \frac{w}{R} + z\frac{\partial\beta}{\partial r}, && e_{\theta\theta} = \frac{U_r}{r} + \frac{U_z}{R} = \frac{u}{r} + \frac{w}{R} + z\frac{\beta}{r}, \\ &e_{rz} = \frac{\partial U_r}{\partial z} - \frac{U_r}{R} + \frac{\partial U_z}{\partial r} \approx \frac{\partial w}{\partial r} + \beta, && e_{zz} = \frac{\partial U_z}{\partial z} = \frac{\partial w}{\partial z} = 0, \end{aligned} \tag{A14}$$

where, from [1, 2], $\frac{U_r}{R} \approx 0$.

From [1], the strain-displacement relations for the sandwich case are,

$$e_{rr}^{(1)} = \frac{\partial U_r^{(1)}}{\partial r} + \frac{U_z^{(1)}}{R} = \frac{\partial u}{\partial r} + \frac{w}{R} + z_1\frac{\partial\beta}{\partial r}, \qquad e_{\theta\theta}^{(1)} = \frac{U_r^{(1)}}{r} + \frac{U_z^{(1)}}{R} = \frac{u}{r} + \frac{w}{R} + z_1\frac{\beta}{r},$$

$$e_{rz}^{(1)} = \frac{\partial U_r^{(1)}}{\partial z_1} - \frac{U_r^{(1)}}{R} + \frac{\partial U_z^{(1)}}{\partial r} \approx \frac{\partial w}{\partial r} + \beta,$$

$$e_{rr}^{(2)} = \frac{\partial U_r^{(2)}}{\partial r} + \frac{U_z^{(2)}}{R} = \frac{\partial u}{\partial r} + \frac{w}{R} - h_1\frac{\partial\beta}{\partial r}, \qquad e_{\theta\theta}^{(2)} = \frac{U_r^{(2)}}{r} + \frac{U_z^{(2)}}{R} = \frac{u}{r} + \frac{w}{R} - h_1\frac{\beta}{r},$$

$$e_{rr}^{(3)} = \frac{\partial U_r^{(3)}}{\partial r} + \frac{U_z^{(3)}}{R} = \frac{\partial u}{\partial r} + \frac{w}{R} + h_1 \frac{\partial \beta}{\partial r}, \qquad e_{\theta\theta}^{(3)} = \frac{U_r^{(3)}}{r} + \frac{U_z^{(3)}}{R} = \frac{u}{r} + \frac{w}{R} + h_1 \frac{\beta}{r},$$

$e_{rz}^{(2)} = e_{rz}^{(3)} = 0$ (membrane face layers assumption).

(A15)

## APPENDIX B

## NONLINEAR STRESS-STRAIN-DISPLACEMENT RELATIONS

In this appendix, the nonlinear theory of elasticity [2, 3, 4, 5] is employed to derive the stress-strain-displacement relations for the homogeneous spherical shell. Assuming a shallow shell leads to the following nonlinear stress components [2]:

$$\sigma_{rr}^{*} = \sigma_{rr}(1+e_{rr}) + \sigma_{r\theta}(\frac{1}{2}e_{r\theta} - \omega_{z}) + \sigma_{rz}(\frac{1}{2}e_{rz} + \omega_{\theta}),$$

$$\sigma_{r\theta}^{*} = \sigma_{rr}(\frac{1}{2}e_{r\theta} + \omega_{z}) + \sigma_{r\theta}(1+e_{\theta\theta}) + \sigma_{rz}(\frac{1}{2}e_{\theta z} - \omega_{r}),$$

$$\sigma_{rz}^{*} = \sigma_{rr}(\frac{1}{2}e_{rz} - \omega_{\theta}) + \sigma_{r\theta}(\frac{1}{2}e_{\theta z} + \omega_{r}) + \sigma_{rz}(1+e_{zz}), \qquad \text{(B1)}$$

$$\sigma_{\theta\theta}^{*} = \sigma_{r\theta}(\frac{1}{2}e_{r\theta} + \omega_{z}) + \sigma_{\theta\theta}(1+e_{\theta\theta}) + \sigma_{\theta z}(\frac{1}{2}e_{\theta z} - \omega_{r}),$$

$$\sigma_{\theta z}^{*} = \sigma_{r\theta}(\frac{1}{2}e_{rz} - \omega_{\theta}) + \sigma_{\theta\theta}(\frac{1}{2}e_{\theta z} + \omega_{r}) + \sigma_{\theta z}(1+e_{zz}),$$

$$\sigma_{zz}^{*} = \sigma_{rz}(\frac{1}{2}e_{rz} - \omega_{\theta}) + \sigma_{\theta z}(\frac{1}{2}e_{\theta z} + \omega_{r}) + \sigma_{zz}(1+e_{zz}),$$

where, the superscript $*$ represents the nonlinear stress components, and $\omega$ is the rotation.

In the simplified nonlinear case, often referred to as the case of small rotations as in [3], we omit the effects of the linear strains on the nonlinear stresses and on the nonlinear strain terms in (B1). Thus, the nonlinear stresses based on the simplified nonlinear theory are formulated as follows:

$$\sigma_{rr}^{*} = \sigma_{rr} - \sigma_{r\theta}\omega_{z} + \sigma_{rz}\omega_{\theta}, \qquad \sigma_{r\theta}^{*} = \sigma_{rr}\omega_{z} + \sigma_{r\theta} - \sigma_{rz}\omega_{r},$$

$$\sigma_{rz}^{*} = -\sigma_{rr}\omega_{\theta} + \sigma_{r\theta}\omega_{r} + \sigma_{rz}, \qquad \sigma_{\theta\theta}^{*} = \sigma_{r\theta}\omega_{z} + \sigma_{\theta\theta} - \sigma_{\theta z}\omega_{r}, \qquad \text{(B2)}$$

$$\sigma_{\theta z}^{*} = -\sigma_{r\theta}\omega_{\theta} + \sigma_{\theta\theta}\omega_{r} + \sigma_{\theta z}, \qquad \sigma_{zz}^{*} = -\sigma_{rz}\omega_{\theta} + \sigma_{\theta z}\omega_{r} + \sigma_{zz}.$$

To further simplify the problem [2, 4, 5], the angle of rotation $\omega_z$ about an axis normal to the middle surface is assumed to be negligible, since it is usually much smaller than the surface rotations $\omega_r$ and $\omega_\theta$. Furthermore, the axisymmetric (torsionless) assumption yields $\omega_r = 0$. Therefore, the final nonlinear stress components become:

$$\sigma_{rr}^* = \sigma_{rr} + \sigma_{rz}\omega_\theta \approx \sigma_{rr} \quad (\text{assume } \sigma_{rz}\omega_\theta = 0 \text{ from [2]}),$$

$$\sigma_{\theta\theta}^* = \sigma_{\theta\theta},$$

$$\sigma_{rz}^* = \sigma_{rz} - \sigma_{rr}\omega_\theta,$$

$$\sigma_{r\theta}^* = \sigma_{r\theta} = 0 \quad (\text{from Equation (2.12c)}), \tag{B3}$$

$$\sigma_{\theta z}^* = -\sigma_{r\theta}\omega_\theta + \sigma_{\theta z} = 0 \quad (\text{from Equation (2.12c)}),$$

$$\sigma_{zz}^* = -\sigma_{rz}\omega_\theta + \sigma_{zz} = 0 \quad (\text{from [2]}),$$

where, $\omega_\theta = \frac{1}{2}(\beta - \frac{\partial w}{\partial r})$.

From [2, 3], we have the following nonlinear strain components,

$$e_{rr}^* = e_{rr} + \frac{1}{2}[e_{rr}^2 + (\frac{1}{2}e_{r\theta} + \omega_z)^2 + (\frac{1}{2}e_{rz} - \omega_\theta)^2],$$

$$e_{r\theta}^* = e_{r\theta} + e_{rr}(\frac{1}{2}e_{r\theta} - \omega_z) + e_{\theta\theta}(\frac{1}{2}e_{r\theta} + \omega_z) + (\frac{1}{2}e_{rz} - \omega_\theta)(\frac{1}{2}e_{\theta z} + \omega_r),$$

$$e_{rz}^* = e_{rz} + e_{zz}(\frac{1}{2}e_{rz} - \omega_\theta) + e_{rr}(\frac{1}{2}e_{rz} + \omega_\theta) + (\frac{1}{2}e_{\theta z} - \omega_r)(\frac{1}{2}e_{r\theta} + \omega_z), \tag{B4}$$

$$e_{\theta\theta}^* = e_{\theta\theta} + \frac{1}{2}[e_{\theta\theta}^2 + (\frac{1}{2}e_{\theta z} + \omega_r)^2 + (\frac{1}{2}e_{r\theta} - \omega_z)^2],$$

$$e_{\theta z}^* = e_{\theta z} + e_{\theta\theta}(\frac{1}{2}e_{\theta z} - \omega_r) + e_{zz}(\frac{1}{2}e_{\theta z} + \omega_r) + (\frac{1}{2}e_{r\theta} - \omega_z)(\frac{1}{2}e_{rz} + \omega_\theta),$$

$$e_{zz}^* = e_{zz} + \frac{1}{2}[e_{zz}^2 + (\frac{1}{2}e_{rz} + \omega_\theta)^2 + (\frac{1}{2}e_{\theta z} - \omega_r)^2],$$

where, the superscript $*$ represents the nonlinear strain.

The simplified nonlinear assumptions stated before yield,

$$e_{rr}^{*} = e_{rr} + \frac{1}{2}\omega_{\theta}{}^{2} = \frac{\partial u}{\partial r} + \frac{w}{R} + z\frac{\partial \beta}{\partial r} + \frac{1}{2}\omega_{\theta}^{2} \quad (\text{from Equation (2.9)}),$$

$$e_{\theta\theta}^{*} = e_{\theta\theta} = \frac{u}{r} + \frac{w}{R} + z\frac{\beta}{r} \quad (\text{from Equation (2.9)}),$$

$$e_{rz}^{*} = e_{rz} = \frac{\partial w}{\partial r} + \beta \quad (\text{from Equation (2.9)}), \tag{B5}$$

$$e_{r\theta}^{*} = e_{r\theta} = 0, \quad (\text{from Equation (2.12c)}),$$

$$e_{\theta z}^{*} = e_{\theta z} = 0, \quad (\text{from Equation (2.12c)}),$$

$$e_{zz}^{*} = e_{zz} + \frac{1}{2}\omega_{\theta}{}^{2} = 0, \quad (\text{from [2]}),$$

where, $\omega_{\theta} = \frac{1}{2}(\beta - \frac{\partial w}{\partial r})$.

It should be noted that for the presentation in Chapter 3, the superscripts $*$, which represents the nonlinear terms, have been omitted.

## REFERENCES


1. Koplik, B., and Yu, Y. Y., "Axisymmetric Vibrations of Homogeneous and Sandwich Shallow Spherical Caps," *Journal of Applied Mechanics*, Trans. ASME, Vol. 89, Series E, Sept. 1967, pp. 667-673.

2. Grossman, P. L., Koplik, B., and Yu, Y. Y., "Nonlinear Vibrations of Shallow Spherical Shells," *Journal of Applied Mechanics*, Trans. ASME, Vol. 91, Series E, Sept. 1969, pp. 451-458.

3. Novozhilov, V. V., *Theory of Elasticity,* Pergamon Press, New York, 1961.

4. Yu, Y. Y., "Generalized Hamilton's Principle and Variational Equation of Motion in Nonlinear Elasticity Theory, with Application to Plate Theory," *Journal of the Acoustical Society of America*, vol. 36, 1964, pp. 111-120.

5. Yu, Y. Y., "Application of Variational Equation of Motion to the Nonlinear Vibration Analysis of Homogeneous and Layered Plates and Shells," *Journal of Applied Mechanics*, vol. 30, No. 1, Trans. ASME, vol. 85, Series E., Mar. 1963, pp. 79-86.

6. Xu, C. and Chia, C. Y., "Non-Linear Vibration and Buckling Analysis of Laminated Shallow Spherical Shells with Holes," *Composites Science & Technology*, Vol. 54, n1, 1995, pp. 67-74.

7. Soedel, W., *Vibrations of Shells and Plates*, Marcel Dekker Inc. New York, 1993.

8. Kraus, H., *Thin Elastic Shells*, Wiley, New York, 1967.

9. Leissa, A. W., *Vibrations of Shells*, NASA SP-288, U.S. Government Printing Office, Washington, D.C., 1973.

10. Leissa, A. W., *Vibrations of Plates*, NASA SP-160, U.S. Government Printing Office, Washington, D.C., 1969.

11. Wang, C. T., *Applied Elasticity*, McGraw-Hill Book Company, New York, 1953.

12. Sokolnikoff, I.S., *Mathematical Theory of Elasticity*, McGraw-Hill, 1956.

13. Burden, R. L. & Faires, J D., *Numerical Analysis*, International Thomson Publishing, 1993.

14. Kockler, N., *Numerical Methods and Scientific Computing*, Oxford Science Publications, 1994.

15. Action, F.S., *Numerical Methods that Work*, Harper & Row, New York, 1970.

16. Soare, M. V., *Application of Finite Difference Equations to Shell Analysis*, Oxford, New York, Pergamon Press, 1967.

17. Street, R. L., *The Analysis and Solution of Partial Differential Equations*, Monterey, California, Brooks/Cole Pub. Co., 1973.

18. Ugural, A. C., *Stresses in Plates and Shells*, WCB McGraw-Hill, 1999.